


# DAM BREACH ANALYSIS AND FLOOD INUNDATION MAPPING THE CASE OF KOGA DAM, ABAY BASIN, ETHIOPIA

**BEWKET DAGNE TEGEGNE**

**MASTER OF SCIENCE**

**ADDIS ABABA SCIENCE AND TECHNOLOGY UNIVERSITY**

**FEBRUARY, 2020**




# DAM BREACH ANALYSIS AND FLOOD INUNDATION MAPPING THE CASE OF KOGA DAM, ABAY BASIN, ETHIOPIA

**BY**

**BEWKET DAGNE TEGEGNE**

**A Thesis Submitted to**

**The Department of Civil Engineering for the Partial Fulfillment of the**

**Requirements for the Degree of Master of Science in Civil Engineering (Hydraulic Engineering)**

**ADDIS ABABA SCIENCE AND TECHNOLOGY UNIVERSITY**

**FEBURARY, 2020**

## DECLARATION

I hereby declare that this thesis entitled "**Dam Breach Analysis and Flood Inundation Map the Case of Koga Dam, Abay Basin, Ethiopia**" was composed by myself, with the guidance of my advisor, that the work contained herein is my own except where explicitly stated Otherwise in the text and that this work has not been submitted, in whole or in part, for any Other degree or professional qualification. Parts of this work have been published in [state previous publication].

Name: Signature, Date:

Bewket Dagne ---------- ----------

## CERTIFICATION

This is to certify that the thesis prepared by BEWKET DAGNE TEGEGNE entitled: "**Dam Breach Analysis and Flood Inundation Map the Case of Koga Dam, Abay Basin, Ethiopia**" and submitted in fulfillment of the requirements for the Degree of Master of Science complies with the regulations of the University and meets the accepted standards with respect to originality and quality.

Singed by Examining Board:

| | | |
|---|---|---|
| External Examiner: | Signature, | Date: |
| DR TILAHUN DERIB | _____ | _____ |
| Internal Examiner: | Signature, | Date: |
| DR BROOK ABATE | _____ | _____ |
| Chair person | | |
| _____ | _____ | _____ |
| Thesis Advisor: | Signature | Date: |
| Dr. FITSUM TESFAYE (PhD) | _____ | Feburary 2020 |

## DEDICATION

This thesis is dedicated to my respectful wife Addis Yigezaw and my kids Natnium and Maraki Bewket.

## ABSTRACT

Unsteady-flow simulation of the dam break is performed using HEC-RAS and results are mapped using the RAS mapping. Inundation mapping of water surface profile, Velocity and depth results from dam failure models and provides a preliminary assessment of the flood hazard and provides insight for emergency preparedness. The Unsteady process is for gathering and preparing data, creating an unsteady-flow model in HEC-RAS, entry of dam breach parameters, performing a dam failure analysis, and mapping of the flood progression. Break parameters prediction, the understanding of dam break mechanics, peak outflow prediction were shown as the essential for the dam break analysis and flood mapping. The results show that dam break is a complicated and comprehensive process involving lots of principles. Koga Dam break due to overtopping elongates the time period of high water surface level, which increases the duration of risk. The design Probable Maximum Flood (PMF) is 570 $m^3$/sec statically estimated and PMF also estimated in HEC-HMS model after calibration and validation is 537$m^3$/sec. The calibration result of HEC-HMS model is the Nash-Sutcliffe Efficiency criteria for the calibration N=0.543 coefficient of determination ($r^2$) of 0.7334 daily based. Validation result is the Nash-Sutcliffe Efficiency N=0.6 and coefficient of determination ($r^2$)=0.8.The result of the simulation under overtopping failure showed that the inundated area surrounding Koga River downstream of the dam is about 10.2 $km^2$ with maximum flood depth is 16 m, water surface velocity ranges from 0.00 to 11 m/s. Most of floodplain areas varied from middle to high flood hazard level, and only few areas had very high level of flood hazard especially on river side. Whereas under piping failure inundated area is 9.1 $km^2$ with maximum flood depth is 13 m, water surface velocity ranges from 0.00 to 6 m/s. This flood affect the downstream town $Wetit\ \ Abay$ town settlement near Koga river and irrigation canal also affected. Dam break has a greater impact on the downstream location where is closer to the dam is high flood depth in accordance with the comparison of the hydrographs at different downstream locations. The structural flood control measurement to be recommended is to construct flood dike and flood gate. The non-structural measurement one is to improve watershed management and socialization of flood awareness.



**KEY WORDS**:Dam Breach Analysis, Flood Inundation Map, HEC- RAS, HEC Geo RAS, HEC-HMS, HEC Geo HMS, Koga Dam, PMF.

## ACKNOWLEDGEMENT

First of all I would like to give my deepest gratitude to my advisor Dr. Fitsum Tesfaye for his continuous supports and advices; My work and providing me with all the necessary materials for the successful completion of my research. I admire his initiation and commitment to assist others, and I wish him success and prosperity throughout his life. I am motivation to work this paper that give an assignment on sediment mechanics course and his unlimited sharing of knowledge on HEC RAS software. I would like to extend my gratitude to the ERA for the financial support. MOWIE providing me with the necessary data of Koga River flow and land use land cover data and soil map data without delaying. And also I would like to thanks NMA that give the necessary metrological data for this thesis. My respectful gratitude to Amedemariam helps me the whole journey of this work.

Finally, I would like to thank my family for providing me the basic necessities in life to recognize the importance of education, and realize my academic goals, and all others who have been the reasons for all achievements I deserved from the early stage of my studies till now.

# Contents

**DECLARATION** ..... ii

**CERTIFICATION** ..... iii

**DEDICATION** ..... iv

**ABSTRACT** ..... v

**ACKNOWLEDGEMENT** ..... vi

**LIST OF FIGURES** ..... x

**LIST OF TABLES** ..... xii

**LIST OF ABBREVIATIONS** ..... xiii

1. INTRODUCTION ..... 1

1.1 Background of the Study ..... 1

1.2 Statement of the Problem ..... 2

1.3 Objective of the Study ..... 3

1.4 Research Question ..... 4

1.5 Significance of the Study ..... 4

1.6 Scope of the Study ..... 4

2. LITERATUR REVIEW ..... 5

2.7.1. General ..... 5

2.7.2. General Approaches to Dam Break Analysis ..... 6

2.7.3. Dam Failure Hazard Classification ..... 7

2.7.4. Inundation Mapping ..... 8

2.7.5. Dam break failure ..... 9

**2.5.1. Overtopping Failure** ..... 9

**2.5.2. Piping Failure** ..... 11

2.7.6. Dam Break Analysis Tools ..... 13

2.6.1. Breach Characteristics Prediction Tools ..... 13

2.6.2. **Parametric Models** ..... 14

2.7.7. Previous Study ..... 15

**2.7.1. Hydrological Modeling for Rainfall Runoff Modeling** ..... 16

**2.7.1. Soil moisture accounting (SMA ) and HEC-HMS** ..... 17

**2.7.2. Hydrological Model Simulation** ..... 17

**2.7.3. Probable Maximum Precipitation** ..... 18

3. MATERIALS AND METHODS ..... 19
3.1. Description of the Study Area ..... 19
3.1.1. **Location of Koga Dam** ..... 19
3.1.2. **Climate** ..... 20
3.1.3. **Soil Type of the Catchment** ..... 21
3.1.4. **Topography of the Koga Watershed** ..... 23
3.1.5. **Land Use** ..... 24
3.1.6. **Koga Dam Features and Appurtenances Paramteres** ..... 25
3.2. Data Collection and Availability ..... 25
3.2.1. **Hydro Meteorological Data Availability** ..... 26
3.2.2. **Meteorological Data** ..... 26
3.2.3. **Rainfall** ..... 27
3.2.4. **Hydrological Data** ..... 27
3.3. Data Analysis ..... 27
**3.3.1. Infilling Missing Data** ..... 27
**3.3.2. Data Quality Analysis** ..... 28
3.4. Tools Used for Analysis ..... 28
3.5. Conceptual Frame work of the Study ..... 29
3.6. Time of Concentration ..... 30
3.7. Probable Maximum Flood (PMF) Derivation of Koga Dam ..... 31
**3.7.1. Adjustment of Mean and Standard Deviation of Rain Fall** ..... 36
**3.7.2. Fitting Distribution Test** ..... 37
**3.7.3. Estimation of PMP for Different Return Period of Koga Dam** ..... 38
**3.7.4. Base flow** ..... 43
3.8. Model Selection ..... 44
**3.8.1. HEC-GEOHMS** ..... 44
**3.8.2. Model Selection and Brief Description of the HEC HMS** ..... 46
**3.8.3. ARC GIS Software** ..... 51
**3.8.4. HEC-GeoRAS** ..... 53
**3.8.5. Hydraulic Modeling with HEC-RAS** ..... 55
3.9. Routing the Inflow Flood through the Reservoir ..... 64
3.10. Dam Breach-Parameters and Breach Modeling ..... 65

**3.10.1. Breach Parameters** ..... 66
**3.10.2. Modeling the Rivers and Structures in HEC-RAS** ..... 70
3.11. Flood Inundation and Hazard Mapping ..... 71
4. RESULTS AND DISCUSSIONS ..... 73
4.1. Double Mass Curve Analysis Result for Homogeneity test ..... 73
4.2. Calibration and Validation of HEC HMS Model ..... 74
4.3. Probable maximum flood of Koga dam ..... 76
4.4. Dam Breach Modeling ..... 78
**4.4.1. Breach Modeling in Koga Dam by Overtopping** ..... 80
**4.4.2. Breach Modeling in Koga Dam in Piping(Sunny Day Failure)** ..... 81
**4.4.3. Computation Time Step** ..... 81
**4.4.4. Koga Dam breaches Parameters Result under PMF Event Overtopping Modes** ..... 83
**4.4.5. Koga Dam Breaches Parameters Result Under Piping Modes** ..... 89
4.5. Flood inundation ..... 94
4.6. Flood Hazard Analysis ..... 96
**4.6.1. Flood Hazard Dam Failure in Overtopping** ..... 96
**4.6.2. Flood Hazard Dam Failure in Piping** ..... 100
5. CONCULSION AND RECOMMENDATION ..... 105
5.1. Conclusion ..... 105
5.2. Recommendation ..... 107
6. REFERENCES ..... 108
7. ANNEX ..... 113

# LIST OF FIGURES

Figure 2: 1: Breach process for an overtopping HEC RAS manual ..... 10
Figure 2: 2: Breach process for piping HEC RAS Manual ..... 12
Figure 2: 3:Simulated and observed hydrograph for calibration period daily time scale (1997-2008) . 18
Figure 3. 1: Location of the Study Area Generated by Arc GIS software from DEM ..... 19
Figure 3. 2: Mean monthly rainfall of the study area ..... 20
Figure 3. 3: Soil coverage of Koga watershed generated by Arc GIS ..... 22
Figure 3. 4: The Longitudinal Profile of the River ..... 23
Figure 3. 5: Land Use Land Cover of Koga Watershed Generated By Arc GIS ..... 24
Figure 3. 6: Conceptual Formwork of the Study. ..... 29
Figure 3. 7: Unit hydrograph of koga watershed using Synder's and SCS method ..... 35
Figure 3. 8: Model schematization ..... 48
Figure 3. 9: Contour Map of the Study area generated from DEM. ..... 52
Figure 3. 10: HEC Geo RAS Preprocessing in Geometric data. ..... 54
Figure 3. 11: Geometric Map of the River ..... 56
Figure 3. 12: Representation of Terms in the Energy Equation HEC-RAS Hydraulic reference manual ..... 58
Figure 3. 13: The river cross section manning roughness property ..... 60
Figure 3. 14: Flow sub-division at a given cross-section in HEC-RAS Hydraulic reference manual ... 62
Figure 3. 15: Cross section for fully dynamic routing through a reservoir (Source: Using HEC-RAS for Dam Break Studies, TD-39, USACE HEC, 2014) ..... 64
Figure 3. 16: HEC-RAS modeling approach for level pool routing (Source: Using HEC-RAS for Dam Break Studies, TD-39, USACE HEC, 2014) ..... 65
Figure 3. 17: Description of Breach parameters HEC RAS hydraulic references manual 2016. ..... 66
Figure 3. 18: Koga dam breach geometry according to Froehlich (2008) ..... 71
Figure 3. 19: Flood Hazard categories ..... 72
Figure 4. 1: Double mass plot of Meshenti versus other stations: DM plot of Adet versus other stations ..... 73
Figure 4. 2: Double mass plot of Tilli versus other stations: DM Sekela versus other stations. ..... 73
Figure 4. 3: Double mass plot of Finotselam versus other Stations. DM plot of Dangela versus other stations. ..... 74
Figure 4. 4: Double mass plot of Enjebara versus other stations. ..... 74
Figure 4. 5: HEC HMS Calibration observed vs simulation result ..... 76
Figure 4. 6: PMF Hydrograph of Koga Dam by CSC Method ..... 77

Figure 4. 7: Using HEC HMS estimated PMF ..... 78
Figure 4. 8: cross sectional geometry and river ..... 79
Figure 4. 9: PMF of the study area ..... 80
Figure 4. 10: Koga dam schematic diagram of overtopping ..... 80
Figure 4. 11: Dam failure under piping schematic diagram ..... 81
Figure 4. 12: Breach progression in time ..... 82
Figure 4. 13: Overtopping of dam and depth of overtopping ..... 83
Figure 4. 14: Stage and flow hydrograph und overtopping failures. ..... 84
Figure 4. 15: General overtopping profile plot. ..... 85
Figure 4. 16: Velocity mapping ..... 86
Figure 4. 17: Depth of flood mapping ..... 88
Figure 4. 18: Stage and outflow hydrograph under piping failures. ..... 90
Figure 4. 19: Cross-sectional depth of flood ..... 91
Figure 4. 20: Velocity of flood ..... 92
Figure 4. 21: Flood Depth of breach ..... 93
Figure 4. 22: Affected infrastructure due to flooding ..... 94
Figure 4. 23: Flooding area Dam failure due to overtopping. ..... 95
Figure 4. 24: Flood inundation boundary of Dam failure of piping ..... 95
Figure 4. 25: Flood Hazard Classification in overtopping Failures. ..... 97
Figure 4. 26: Flood hazard at various location in piping failures ..... 98
Figure 4. 27: Flood Hazard Classification in Piping Failures. ..... 101
Figure 4. 28: Flood Hazard piping Failure at various locations. ..... 102
Annex Figure 7. 1: Flood mapping area by overtopping. ..... 114
Annex Figure 7. 2: Intake Tower and Spillway of the Koga Dam ..... 115
Annex Figure 7. 3: Flood mapping area by overtopping. ..... 116
Annex Figure 7. 4: Koga Dam crest ..... 117
Annex Figure 7. 5: Adjustment of mean of annual series for maximum observed rainfall (Hershfield, 1961b) ..... 133
Annex Figure 7. 6: Adjustment of Standard deviation of annual series for maximum observed rainfall (Hershfield, 1961b) ..... 134
Annex Figure 7. 7: overtopping Failure at various distance flood hydrograph. ..... 137
Annex Figure 7. 8: piping Failure at various distance flood hydrograph ..... 137

# LIST OF TABLES

Table 2. 1: Results of Goodness of Fit Test ..... 18
Table 3. 1: Soil Coverage of Koga Catchment ..... 21
Table 3. 2: Dam and appurtenances structures parameters ..... 25
Table 3. 3: Nearest Meteorological station UTM Coordinate. ..... 26
Table 3.4: The classification of dam for the recommendation of Spillway design flood ..... 31
Table 3. 5: Koga Dam sites catchment characteristics and values of Snyder's parameters ..... 34
Table 3. 6: unit hydrograph ordinates ..... 35
Table 3. 7: Ratio of the basic Dimensionless hydrograph of the Snyder's ..... 36
Table 3. 8: Maximum aerial precipitation of the study area parameter ..... 36
Table 3. 9: Calculation of PMP different return period values for Koga dam catchments by Hershfield method ..... 37
Table 3. 10: Frequency factors for various periods for various return periods ..... 39
Table 3. 11: Point and Aerial Rainfall ..... 40
Table 3. 12: Temporal distribution of areal rainfall ..... 40
Table 3. 13: Temporal distribution of rainfall Per Adimasu method ..... 41
Table 3. 14: Rainfall Incremental ..... 41
Table 3. 15: Excess rainfall ..... 42
Table 3. 16: Put excesses Rainfall in Reverse Critical Sequencing ..... 43
Table 3. 17 : Base flow separated by constant slope line constraints ..... 43
Table 3. 18: SMA parameters ..... 50
Table 3. 19: Values for the Computation of the Roughness Coefficient, n (CHOW, 1988) ..... 61
Table 3. 20: Computation of manning's n for Koga River ..... 61
Table 3. 21:Manning's Roughness Coefficient (CHOW, 1988) ..... 62
Table 3. 22: Cb values ..... 69
Table 3. 23: Simplified Flood Depth and Velocity Severity Grid Symbolization Categories ..... 72
Table 4. 1: PMF of Koga Dam ..... 77
Table 4. 2: Koga Dam breach parameters for overtopping failure ..... 83
Table 4. 3: Koga Dam breach parameters for piping failure ..... 89
Table 4. 4: overtopping Flood hazards at various location in flood plain ..... 99
Table 4. 5: piping Flood hazards at various location ..... 103
Annex Table 7. 1: station annual maximum precipitation ..... 113
Annex Table 7. 2: Probability Fitting a Distribution Kolmogorov _Simonov test ..... 118
Annex Table 7. 3: Probability Fitting a Distribution test by X-square test ..... 118
Annex Table 7. 4: Dimensional unit hydrograph ..... 119
Annex Table 7. 5: percent of accumulated rainfall and duration ..... 121
Annex Table 7. 6: Unit Hydrograph for Koga dam site catchment based on CSC Method ..... 122
Annex Table 7. 7: Weighted maximum precipitation ..... 124
Annex Table 7. 8: Monthly rainfall of different station ..... 125
Annex Table 7. 9: Aerial maximum precipitation of study area. ..... 136

## LIST OF ABBREVIATIONS

- BC Boundary condition
- DEM Digital Elevation Model
- DMC Double mass curve
- ERA Ethiopian Road Authority
- HEC GeoRAs Hydrologic Engineering Center's Geospatial River Analysis System
- HEC GeoHMS Hydrologic Engineering Center's Geospatial Hydrology modeling System
- HEC HMS Hydrology engineering center Hydrology modeling System
- HEC RAS Hydraulic Engineering center River Analysis System
- Hrs Hours
- IC Initial Condition
- ICOLD International committee on large dams
- m/s Meter Per Second
- $m^3/s$ Meter cubic per second
- MoWIE Minster of water irrigation and energy
- NMA National metrology Agency
- PMF Probable Maximum Flood
- PMP Probable maximum precipitation
- PPN Precipitation
- RF Rainfall
- **SMA** Soil Moisture Accounting
- TIN Triangular Irregular Networks
- UH Unit hydrograph
- USACE United states Army Corps of Engineers
- USDA United states Department of Agriculture
- UTM Universal Transverse Mercator
- WSEL water surface elevation level
- WWDSE Water Works Design and Supervision Enterprise

# 1. INTRODUCTION

## 1.1 Background of the Study

Dams are an important part of the nation's infrastructure, providing flood control, water supply, irrigation, hydropower, navigation, and recreation benefits. Despite their many beneficial uses and value, dams also present risks to property and life due to their potential to fail and cause catastrophic flooding. To mitigate these risks, dam owners and regulators carefully analyze and inspect dams to identify potential failure modes and protect against them. Since no program for preventing failure can ever be certain, and because the potential for loadings exceeding design limits can never be eliminated, another essential part of risk mitigation is simulating potential failures and planning for them (Tony,2010).

All dams, regardless of their design or construction, have increased forces applied to them during extreme events which increase the potential risk of failure (Ahmad Asnaashari, 2014). Dam provides many benefits for our society, but floods resulting from the failure of constructed dams have also produced some of the most devastating disasters of the last two centuries. Simulation of dam break events and the resulting floods are crucial to characterizing and reducing threats due to potential dam failures. Development of effective emergency action plans requires accurate prediction of inundation levels and the time of flood wave arrival at a given location. There are more than 79,000 dams listed in the National Inventory of Dams (NID) for the United States and territories. According to the U.S. Geological Survey, more than 7,700 of these dams are categorized as major dams. Major dams include dams 15.24 meter or more in height, dams with normal storage capacity of 6.17 million cubic meter or more, and dams with a maximum storage capacity of 30.84 million cubic meter or more (USGS, 2005a).

Dam breach analysis is used to determine the ultimate discharge from a hypothetical breach of a dam under extreme events. The outcome is a breach hydrograph from dam failure with a flood wave immediately downstream of the dam, which is routed throughout the river system to determine the flood arrival time, peak flow, and the depth of flow at downstream locations mapping of inundation areas.

Dam break pre-event analysis is vital to predict the dam breach parameters, outflow magnitude and its downstream nature of propagation (Yared, 2015). The dam breach modeling and analysis of Koga dam that are found in the upper Abay basin (Tana Basin). There seems to be a danger of flooding hazard to the downstream infrastructure and community, if the dams fail. There is a town i.e. *Wetit Abay*, irrigation scheme, and social infrastructures downstream of the dams including the Addis Ababa to Bahir Dar main road and Bridge that could be at risk. The potential consequences of a dam failure should be understood for Koga dams. It is important to understand the concerns associated with existing and future downstream developments, especially the risk associated with loss of life and property if a dam fails. In dams under planning stage, one can use the dam breach inundation information for classifying the dam (and its hazard class) and this classification can then be used to robustly estimate spillway discharge capacity, seismic parameters, and others. Moreover, this information is essential for early warning, preparedness and emergency action planning related to dam failure. A number of causes can trigger dam break such as extreme hydrologic events, seismic activity, operational errors, spillway gates dysfunction, excessive seepage and other hydraulic activities. When a dam breaches, the uncontrolled release of water from the reservoir causes downstream inundation and ultimately causes loss of life and property. Therefore, this study is to illustrate the extent and severity of failure of the dams under hydraulic and hydrological triggers. The scope of the study is limited to the estimation of dam break flooding as the flood propagates to downstream areas through Koga River and tributaries of the Koga River and map the resulting flood downstream of the dams.

## 1.2 Statement of the Problem

So many dams have been constructed in the world, many of them failed because of different consequences. The failures resulted to flooding of land and communities located downstream of the dam with a consequent risk of loss of human life, damage to structures, economic losses to businesses, farms and horticultural industries erosion, deposition of sediment over an area up to perhaps a kilometre long, several hundred metres wide failure of utility services, including roads, bridges and pipework located in the path of the flood and distraction of homes. Dam breach modeling and inundation mapping is useful for many purposes. Some of the uses are: to identify the possible causes of dam failure, to simulate the breaching

process so that design parameters can be reviewed, to map the area that shall be flooded, to alert concerned bodies to take a precaution on dam safety plans. In Ethiopia, in contrary to the development of dams, such pre event analysis is not being studied by designers or researchers vastly.

The Dam type is embankment dam this type of dam is different failure scenario i.e. overtopping (Hydraulic failures from the uncontrolled flow of water over the dam), piping (Seepage occurs through the earthen embankment), sliding and Erosion of downstream toe of the earth slope caused by misdirected spillway outlet discharge of the embankment of the dam.

However, it often poses the hazard potential that affect the downstream settlement and irrigation project. The need of this study pre event dam break analysis is therefore aimed to model the possible breaching process of the embankment dam and to delineate the area that would be flooded out due to the hazardous wave front should have work. The peoples in the dam break flood risks area are found in the existing towns: *Wetit Abay*, and in the newly Koga irrigation project at the downstream area. The downstream area is at natural flooding risk by the River Abay, which has a tendency to change its course very often in addition to a dam failure occurrence. Also used to alert populations and properties at risk and used to estimate warning time for people. Koga dam stores 83.1 million cubic meter of water to irrigate 7,000 hectare of land. Koga dam is classified under intermediate hazard dam (Koga dam design report, 2003). Perhaps, if the dam fails there are towns and wide irrigation lands that may leads to loss of life and property. Therefore, dam breach analysis and inundation mapping aimed to study the possible breaching process of Koga embankment dam by delineating the flooding hazard wave areas.

## 1.3 Objective of the Study

### 1.3.1. General Objectives

The general objective of this study is to analysis dam breach process and to map flood inundation areas of Koga embankment dam.

### 1.3.2. Specific Objectives

The specific objectives of this study are,

- To predict the dam break peak outflows Hydrograph produced at Koga dam
- To identify the dam break modeling scenario in piping and overtopping
- To identify the flood mapping area at the downstream

## 1.4 Research Question

After completion of Koga dam break simulation, the following main questions would be answered:

1. How much flow would be released to downstream region for each scenario if the Koga dam were to breach?
2. Which downstream areas are more prone to dam break flood?
3. How long would it take a dam break flood to arrive at each key settlement on the route?

## 1.5 Significance of the Study

An attempt is made to predict the Koga dam break flood and identify possible flood hazard zones at downstream region. A preliminary flood inundation map was developed for identified flood hazard zones. Hence, direct model outputs together with inundation map are assumed to assist the dam owner (MoWIE) to plan existing irrigation land use and for future expansion, to use proposed flood mitigation tools (structures) to protect loss of life and property, and in developing a detailed emergency action plans (EAP) to mitigate flood damage.

## 1.6 Scope of the Study

This thesis covers determination of dam breach parameters and catastrophic outflow hydrograph. Different scenarios of inflow, mode of failure and initial breach size will be analyzed and the one giving a worst condition shall be selected for further downstream routing and flooding. The scope of the study is limited to the estimation of dam break flooding as the flood propagates to downstream areas through Koga River and tributaries of the Koga River and map the resulting flood downstream of the dams.

# 2. LITERATUR REVIEW

## 2.7.1. General

Guidelines for dam breach analysis defines, dam is a man-made barrier, together with appurtenant structures, constructed above the natural surface of the ground for the purpose of impounding water. Dams are an important part of this nation's infrastructure, providing flood control, water supply, irrigation, hydropower, navigation, and recreation benefits. Despite their many beneficial uses and value, dams also present risks to property and life due to their potential to fail and cause catastrophic flooding (Tony L. Wahl, 2010). Dam failure can cause loss of life, property damage, cultural and historic losses, environmental losses as well as social impacts (Wayne et al, 1999).

Sever loss of life and property were recorded in many countries due to failure of large dams and their examples will be presented in next section. A large dam has a height of not less than 15 m or stores more than three million cubic meters of water in the reservoir (Zhangdong et al, 2012).

Dams are of numerous types, and type classification is sometimes less clearly defined. An initial broad classification into two generic groups can be made in terms of the principal construction material employed (Novak, 2007): The term "dam failure" suggests a single event; a quickly rising super flood of fast flowing water presumably varying in scale (depending on the volume of water released) and in human impact (depending on the size of the downstream population) but otherwise of similar character wherever it may occur. In fact, of course, dam failure floods can be quite different depending on both environmental conditions and mode of failure, and these differences are likely to be of great significance in terms of defining appropriate emergency responses. In effect, different failure modes and different environments present quite different planning problems .Ideally, of course, the plans which are drawn up must create a capacity for effective response regardless of environment or the precise nature of the flood which occurs. Given the existence of a plan or "family" of plans for each below dam area for which evacuation operations may be needed, the environmental issue is necessarily built in to the planning problem on a case-by-case basis. Variation by failure mode presents more serious complications (CSAE, 2013).

Historically, many of the early dams were small, in-channel structures built by locals with little or no engineering background. Griffin (1974) suggests that dam safety for early dams was less of a concern because the areas around early dams were less densely populated and, therefore, few people were directly affected by the dams, these dams were generally small in relation to modern dams, and the dams were generally built by cultures who took pride in their work ( Pierce,2010). Loss of life sometimes results from dam failure. Loss of life is likely if a dam fails without warning and the failure produces flooding that destroys residential structures (Wayne et al, 1999).

However, modern dam-safety analysis has been an evolving science since the failure of Teton dam (USA) in 1976, there has been a significant evolution in the understanding of floods, dams and other critical infrastructures on which modern society and people's wellbeing rely. Regardless of the reason of failure, the event of a dam failure is quite a disaster, even catastrophic in the absence of pre-event measures in place. However, until very recently, dams and reservoir safety had focused almost exclusively on the structure or the civil works and this, with an eminently determinist approach. In this respect, risks were controlled through the respect of certain rules and practices sanctioned by experience, as well as by checking safety factors that were understood as conservative measures of prudence (SNCLD, 2013).

### 2.7.2. General Approaches to Dam Break Analysis

Breaching of a dam is a time–dependent and non–linear phenomenon. Water-soil interaction together with often non-homogeneous and specific material properties for each structure leads to the difficulty of accurately modeling the processes involved in breach development. Hydrodynamics, sediment transport mechanics, and geotechnical aspects are all present in the breach formation and their accurate modeling is very important for the accurate prediction of breach outflow. The development of effective emergency action plans and the design of early warning systems heavily rely on these prediction results (Zagonjolli, M. 2007)

Dam break analyses provide information on the consequences of a possible dam failure for risk estimation and rescue planning purposes. Guideline for dam breach analysis (Colorado

dam safety office, 2010) suggests to all dam safety engineers to follow the four critical approaches listed below:

1. Breach parameter estimation (breach size (shape) and time of failure)
2. Breach peak discharge and breach hydrograph estimation
3. Breach flood routing, and
4. Estimation of the hydraulic conditions at critical locations.

(Tony L. Wahl, 2010). Further categorized the above said procedures for dam break analysis in to two major tasks:

1. The prediction of the reservoir outflow hydrograph and
2. The routing of that hydrograph through the downstream valley to determine dam failure consequences (i.e. inundated regions).

Pandya and Jitaji (2013) viewed these two key tasks in two basic perspectives for dam break analysis procedures to be followed.

**The first perspective** is to answer the basic question that whether or not, a given dam will fail. This basically refers to the strength parameter of materials of dam section and this perspective basically deals with simulation of breaching process of dam section. Various parameters relating to dam failure like breach characteristics, time of formation etc. are estimated by this approach.

**The second perspective** is to assume a given dam failure and study the resulting consequences in the downstream area. This includes assuming breach geometry based on the guidelines provided by various research agencies. This approach helps in preparation of emergency action planning for a possible failure of dam. The final basic product of such analysis is inundation details of downstream area owing to the flood generated due to the failure of dam. Hence, it is realized that this (the second) perspective fits for the case study Koga dam.

### 2.7.3. Dam Failure Hazard Classification

A dam hazard classification is the placement of a dam into one of three/or four categories based on the hazard potential derived from an evaluation of the probable incremental adverse

consequences due to failure or improper operation of the dam. Characterization of the threat to public safety (people at risk) that a dam poses establishes the hazard classification of the dam and the associated standard of care to which the dam is held. “People at risk" is defined as the number of people in the dam failure floodplain prior to the issuance of any flood or dam failure warnings (Wayne, et’al, 1999).

The hazard classification also triggers the requirement to prepare an emergency action plan, requiring preparation of inundation maps which accurately predict dam breach flood depths and arrival times (flood warning time) at critical locations. Adverse effects of a dam failure can be classified in to four categories (SNCLD, 2013).

**Damage to people**: in principle, apart from loss of life, damage to people could also consider other aspects such as people injured with different degrees of gravity.

However, due to the difficulty of quantification of wounded numbers, quantitative analysis usually focuses only on the first aspect.

**Direct economic damage**: damage caused directly by the impact of the flood and is the most visible type. It includes the cost associated with the damage suffered by the dam itself.

**Indirect economic damage**: damage happened after the event as a result of the interruption of the economy and other activities in the area.

**Other damages**: these are related to environmental damage, social disturbing, loss of reputation, damages to historical or cultural heritage, etc. However, all of these aspects are difficult to quantify and so are usually treated in a qualitative way. FEMA guidelines (US Dep LS,2013) recommends a three-step rating system that defines low hazard, significant-hazard and high-hazard potential classifications depending on the potential for loss of life, economic loss, and environmental damage resulting from a hypothetical dam failure.

### 2.7.4. Inundation Mapping

One of the preemptive measures is to prepare potential inundation map and to prepare a detailed emergency action plan before the occurrence of an actual dam failure. The inundation map provides a description of the areal extent of flooding which would be produced by the dam break. The inundation map will help in identification of areas under risk, the location

where population is concentrated, locations that are hard to evacuate or where there are not any high grounds to seek shelter etc. It also identifies zones of high velocity flow and depicts inundation for representative cross-sections of the channel. This information is standard outputs from HEC-RAS program flood routing model and inundation map may be developed utilizing cross-section and flood height data in conjunction with Digital Elevation Model (DEM) or Digital Terrain Model (MGS Engineering, 2007).

Inundation mapping can be accomplished in the GIS using HEC-GeoRAS. GIS information is exported from HEC-RAS and read into the GIS with GeoRAS. The geo-referenced cross sections are imported and water surface elevations attached to the cross sections are used to create a continuous water surface. The water surface is then compared with the terrain model and the floodplain is identified where the water surface is higher than the terrain. The HEC-GeoRAS has an ability to produce inundation maps for flood extent and depth (HEC GeoRAS reference manual).

## 2.7.5. Dam break failure

### 2.5.1. Overtopping Failure

An overtopping failure of an earthen dam a head cut erosion process will first start on the downstream side of the dam embankment Figure 2.1A.While water is going over the dam crest the dam crest acts like a broad crested weir. The head cut will erode back towards the center of the dam and widen over time figure B. As the head cut begins to cut into the dam crest the weir crest length will become shorter and the appropriate weir coefficient will trend towards a sharp crested weir value figure C. The time for breach initiation used in HEC RAS is shortly after what is depicted in figure C. when the head cut reaches the upstream side of the dam crest, a mass failure of the upstream crest may occur, and the hydraulic control section will act very much like a sharp crested weir Figure D. The head cut will continue to erode upstream through the dam embankment, as well as erode down through the dam and widen at the same time figure E During this process, the appropriate weir coefficient will begin to trend back towards a broad crested weir coefficient. As the downward cut reaches the natural river bed elevation, and the breach is more in a widening phase, the appropriate weir coefficient is more in the range of a broad –crested weir value.

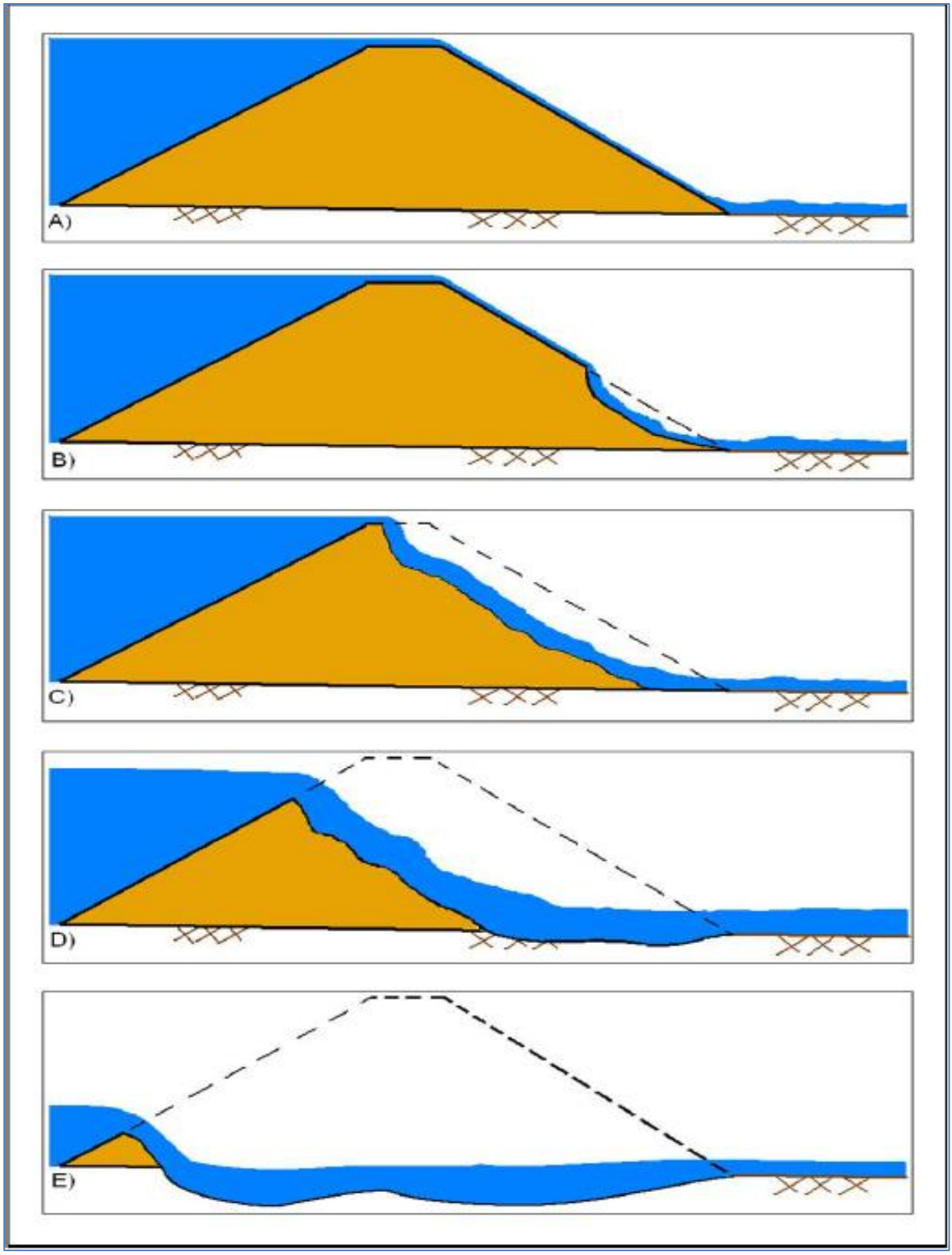



**Figure 2: 1**: Breach process for an overtopping HEC RAS manual

### 2.5.2. Piping Failure

A general description of piping failure Figure 2.2 is as follows. Water is seepage through the dam at a significant enough rate, such that it is internally eroding material and transporting it out of the dam. As the material is eroded, a larger hole is formed thus able to carry more water and erode more material figure A. The movement of water through the dam during this process is modeled as a pressurized orifice type of flow. During the piping flow process, erosion and head cutting will begin to occur on the downstream side of the dam figure 6B as a result of flow the existing the pipe. As the piping hole grows larger, material above the hole will begin to slough off and fall into the moving water figure C. The head cutting and material sloughing processes will continue to move back towards the upstream side of the dam, while the piping hole continue to grow simultaneously figure D,. If the piping hole is large enough, the weight of the material above the hole may be too great to maintain and a mass caving of material will occur. Thus will result in a large rise in the outflow through the breach and will accelerate the breaching process. Also at this point, the hydraulics of the flow transitions from a pressure /orifice type flow to an open air weir type flow. The head cutting and erosion process then continues back through the dam, as well as downward figure 6E. Additionally, the breach will be widening. Depending on the volume of water behind the dam, the breach may continue to cut down and widen until the natural channel bed is reached. Then the breach will go into a widening phase.

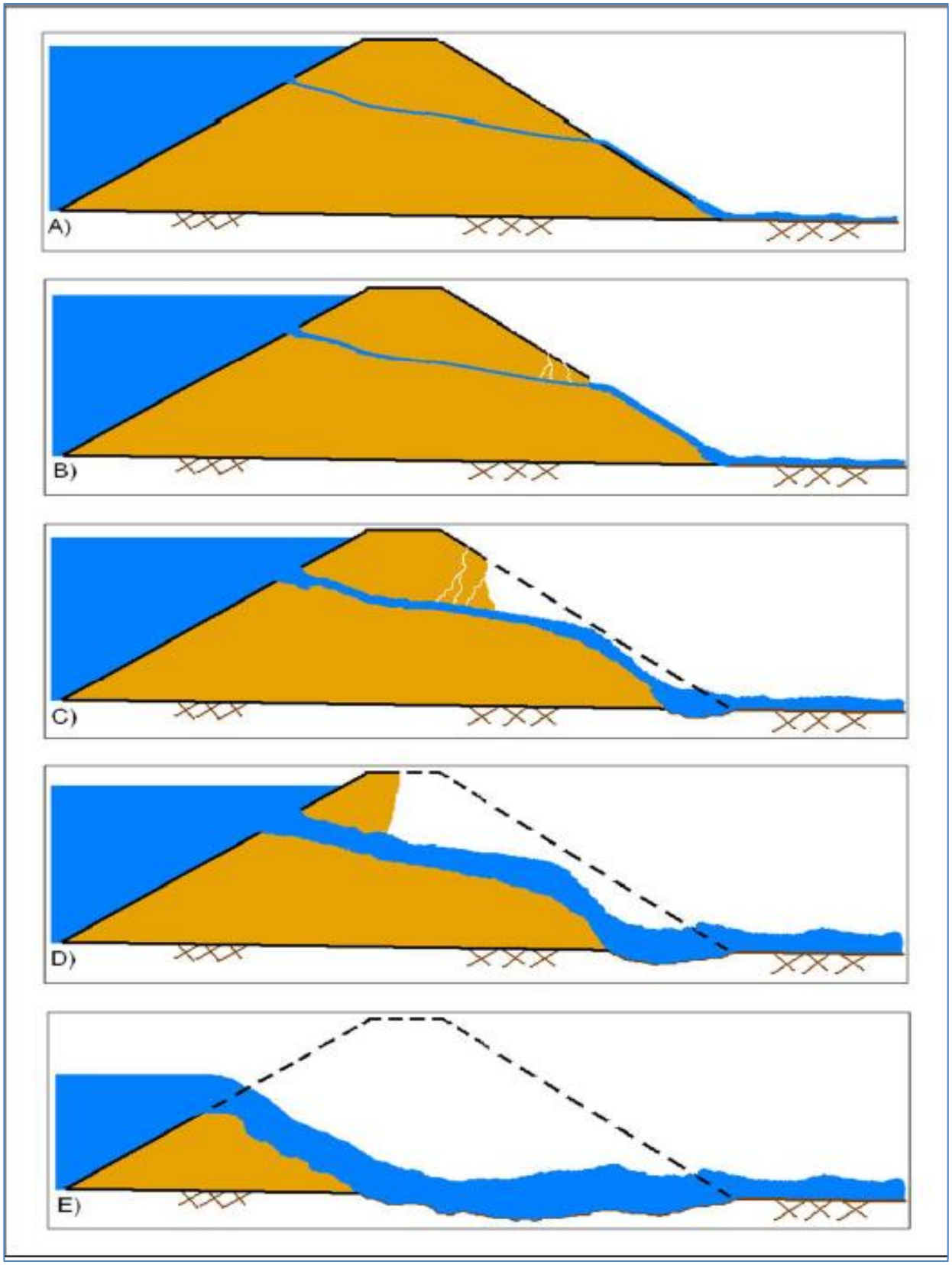



Figure 2: 2: Breach process for piping HEC RAS Manual

## 2.7.6. Dam Break Analysis Tools

Guideline for dam breach analysis suggests the following four critical approaches

As to accomplish dam break analysis study:

1. Breach parameter estimation (breach size (shape) and time of failure)
2. Breach peak discharge and breach hydrograph estimation
3. Breach flood routing, and
4. Estimation of the hydraulic conditions at critical locations.

These procedures can be further categorized in to two main tasks as:

1. The prediction of the reservoir outflow hydrograph and
2. The routing of that hydrograph through the downstream valley to determine dam failure consequences (i.e. inundated regions).

### 2.6.1. Breach Characteristics Prediction Tools

Breach characteristics can be estimated in several ways. However, there are three viable methods that are used to estimate breach characteristics (Michael, 2010).

1. **Comparative Analysis**: -perhaps the simplest approach to dam breach characteristics estimation is comparative analysis. This method compares a given dam of interest with those in a database of well documented dam failure case histories. In this method, a given dam geometry, height, slope angles, and reservoir areas and volumes are compared with a list of similar sized dams that have failed. Dam breach characteristics reported from the failure case histories of similarly configured dams are then directly applied to the dam being analyzed. Due to lack of failed dam record of similar size and type in Ethiopia, this method is not selected for case study dam break analysis.
2. **Empirical equations**: -these are relations developed from historical dam failures that correlate breach size and development time with dam and reservoir characteristics.The empirical approaches rely on statistical analysis of data obtained from documented failures. In this work, regression/empirical equations are used to estimate breach characteristics for use with HEC-RAS model and most widely used empirical equations
3. **Physical based computer models**:-these are computer based-programs that model the physical breaching process using sediment transport (erosion) equation, soil mechanics, and principles of hydraulics. A physically-based model (also referred to as a “process” or

"causal" model) utilizes generally accepted relationships based on physical principles to establish the framework of a model. The model then attempts to solve those relationships for a given input. This is a relatively simple concept, but it can become very complex when the input is changing with time. In the case of dam breach analysis, both the input and physical constraints are changing with time as the dam erodes and the reservoir evacuates.

Although several physically-based models have been reported as being in the development stage for research purposes, the National Weather Service's BREACH program (NWS BREACH or BREACH) is currently the only widely available model.

BREACH predicts the development of a breach and the resulting outflow using an erosion model based on principles of hydraulics, sediment transport and soil mechanics. It was initially developed in 1987, but has had several upgrades in 1988, 1991, and 2005. The model takes into account several components of a dam and reservoir that are not considered in the empirical methods, such as area versus elevation, dam dimensions, soil properties of the dam, and tail water effects downstream. It is relatively simple to run and is widely used within the United States. Unfortunately, BREACH is no longer supported by the National Weather Service and significant advances in the understanding of the complex mechanics of a dam failure have not been incorporated. Also, the model has only been calibrated with a very limited number of cases. It is deduced that, physically based method has clear limitations. Furthermore, this method suffer from extreme data demands, (e.g. area versus elevation, dam dimensions, soil properties of the dam, tail water effects downstream…etc.). Due to stated limitations and high demand for input data, this method mostly is not practically feasible for limited time and finance. Hence, this method is not selected in this work.

### 2.6.2. **Parametric Models**

Hydrologic and hydraulic models are the two widely used parametric (numerical) models used to predict dam breach hydrographs based on breach parameters provided by the modeler.

**Hydrologic models**: commonly used hydrologic models for dam break analysis are:

HEC-HMS and HEC-1. In the absence of significant backwater effects, the hydrologic routing models offer the advantages of simplicity, ease of use and computational efficiency. However, during downstream flood routing, backwater effect is expected for realistic flood routing.

Furthermore, the hydrologic models do not provide useful information on hydraulic conditions (i.e. water surface elevations, flow velocities). These and other critical requirements limit use of hydrologic model for dam break analysis. Hence, due to these limitations, hydrologic model is not selected by the Author.

**Hydraulic models**: hydraulic models are broadly classified into steady flow and unsteady flow models. In unsteady flow, time dependent changes in flow rate are analyzed explicitly as a variable, while steady flow analysis models neglect time all together. Steady flow analysis can determine a water surface elevation and flow velocity at a given cross section for a given flow using Manning's equation under the assumption of gradually varied flow conditions.

### 2.7.7. Previous Study

The unsteady flow simulation in HEC-RAS software uses the same hydraulic calculations (cros section properties, bridges, gated structures, etc.). HEC-RAS can be used to model both overtopping as well as piping failure breaches for earth dams. The resulting flood wave is routed downstream using the unsteady flow equations. Dams are modeled with HEC-RAS by using inline structure editor. The inline structure editor used to put embankment and defined overflow spillway and weirs with gated openings. Koga embankment dam breach failure is simulated for piping failure scenario. After unsteady flow simulation of the breach, HEC-RAS model give output of peak dam breach flood which is 3071 $m^3/s$ on inline structure. Generally, Koga river have moderately meander this irregular surface make the peak discharge, the velocities as well as maximum water surface are decreased as the flood travel to the downstream. For more detail the Piping failure event, including the maximum water levels all breach simulation outputs for selected cross-sections Accordingly, the maximum water velocities is approximately 0.1-42 m/s immediately downstream of the dam with water depth 0.32 - 35 meter. These velocity and water depth profiles are very high during flood the highest peak shows during breach time on dam body) this may harm peoples at downstream of the river. For more visualization, velocities for left bank side, at center of channel and at right side of bank (Adane A, 2017).

### 2.7.1. Hydrological Modeling for Rainfall Runoff Modeling

HBV model is used to simulate the flow in order to check the precipitation data or the simulated flow with the observed flow. Different parameters were used to carry out the calibration process also it allows for multiple parameter calibration at the same time. Eight parameters were selected for calibration (Adnan A, 2017).

HEC-HMS rainfall-runoff model is among the most applicable ones. Rainfall-runoff models are used to estimate peak discharge using rainfall data as input. Their use can be favorable when longer precipitation records are available than runoff, or when precipitation can be more reliably estimated from surrounding stations (Wilson et al., 2011).

The unit hydrograph approach is based on the assumption that the shape of the hydrograph resulting from a rainfall event of a specified duration and large enough to exceed the infiltration capacity of the catchment will always be the same .As such the flood hydrographs resulting from rainfall events of varying intensities can be derived by scaling of the unit hydrograph. However, the unit hydrograph has to be defined for each catchment separately, where possible from rainfall and runoff observations. Alternatively, empirical formulas can be used to derive the unit hydrograph from physiographic catchment data for ungauged catchments. However, the use of the formulas is only recommended for catchments in the regions for which they were developed. No estimation methods for the unit hydrograph of natural catchments in Norway are known and standard unit hydrographs of natural catchments are used in practice. For small catchments with observed rainfall and flood events, on the other hand, the unit hydrograph approach is a very useful method (Boyum et al., 1997) and can be applied even when only a few flood observations are available. However, both hydrograph observations and recording rain gauge data are needed (Pilgrim & Cordery (1993).

Selection of a rainfall-runoff model is a compromise between model complexity and available input data. For this purpose, first by considering observed events, HEC-HMS model was optimized and calibrated (Coonrad. J and Bui.C, 2011).

### 2.7.1. Soil moisture accounting (SMA ) and HEC-HMS

SMA, a loss model within the HEC HMS software suite was designed to compute runoff discharge on a continuous time base. This model was successfully applied for long term rainfall-runoff modeling and reference is made to the work of Fleming (2002) Fleming and Neary (2004)

A number of methods can be used to transform excess precipitation into surface runoff i.e. SCS unit hydrograph, Clark unit hydrograph, Later , two other sources ,ground water storage in 2 zones are routed in to a set of linear reservoirs and then used to calculate base flow contributions (Feldman,2000).

## 2.7.2. Hydrological Model Simulation

HBV model is used to simulate the flow in order to check the precipitation data or the simulated flow with the observed flow. Different parameters were used to carry out the calibration process also it allows for multiple parameter calibration at the same time. Eight parameters were selected for calibration.

The HBV- model is calibrated and validate for the observed period of 25 years (1990-2015) for the Koga catchment and the best-fit parameters sets are selected. Model calibration involves determination of model parameters that gives the best possible correspondence between observed and simulated discharge from a catchment.

HBV Model calibrates either manual or computer based. To identify the optimum parameter set; the manual calibration is functional for this model. Based on this, several runs were made to select the most optimum parameter set in order to match the observed discharge with simulate discharge. The result of each run was evaluated after final calibration result of RVE (relative volume error< 5%) 0.35 and R2 (Nash and Sutcliffe coefficient) 0.786 as shown Figure below.

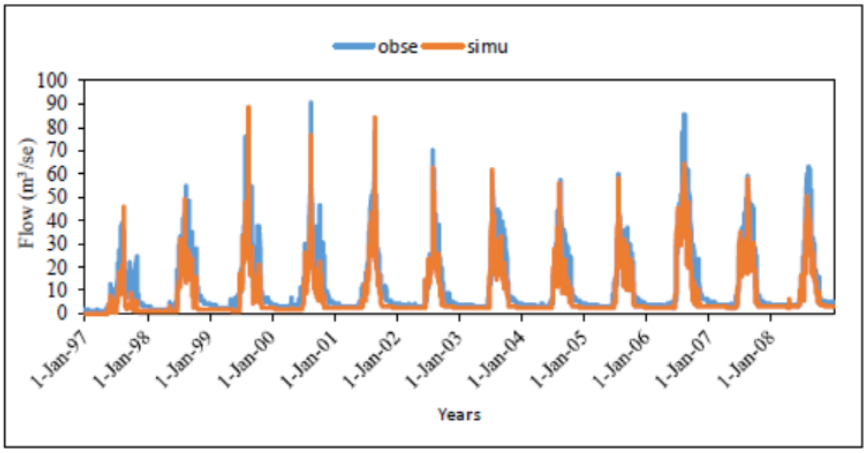



Figure 2: 3:Simulated and observed hydrograph for calibration period daily time scale (1997-2008)

### 2.7.3. Probable Maximum Precipitation

Computation of Easy Fit software helps to determine the best fit distribution. So the Easy Fit software approve or select Log Pearson type III as the best fit for the time series data. Because, it was selected based on the minimum error as shown table below. The detail description of the candidate probability distributions goodness of fit details and summary results were given in the appendix III.

Table 2. 1: Results of Goodness of Fit Test

| S.No | Distributions | Kolmogorov sminov | | Anderson Darling | | Chi-Squared | |
|---|---|---|---|---|---|---|---|
| | | Static | Rank | Static | Rank | Static | Rank |
| 3 | Log -Pearson III | 0.11953 | 1 | 0.21977 | 2 | 0.03131 | 1 |
| 2 | Gumbel Max | 0.11958 | 2 | 0.21914 | 1 | 0.03339 | 2 |
| 1 | Gumbel Extreme value | 0.12292 | 4 | 0.22622 | 3 | 0.03546 | 3 |
| 4 | Normal | 0.12074 | 3 | 0.51778 | 4 | 0.43258 | 4 |

# 3. MATERIALS AND METHODS

## 3.1. Description of the Study Area

### 3.1.1. Location of Koga Dam

The Koga dam and irrigation development project is found in the upper Abay basin in Amhara Regional State in the West Gojjam Zone. Dam site is located at 560Km from Addis Ababa. The watershed lies between the coordinates $11^0 24' 62''$N latitudes to $11^o 58' 56''$ and $37^0 08' 97''$E longitudes to $37^0$ 59 ' 45''and covers an estimated area of 209 $km^2$.

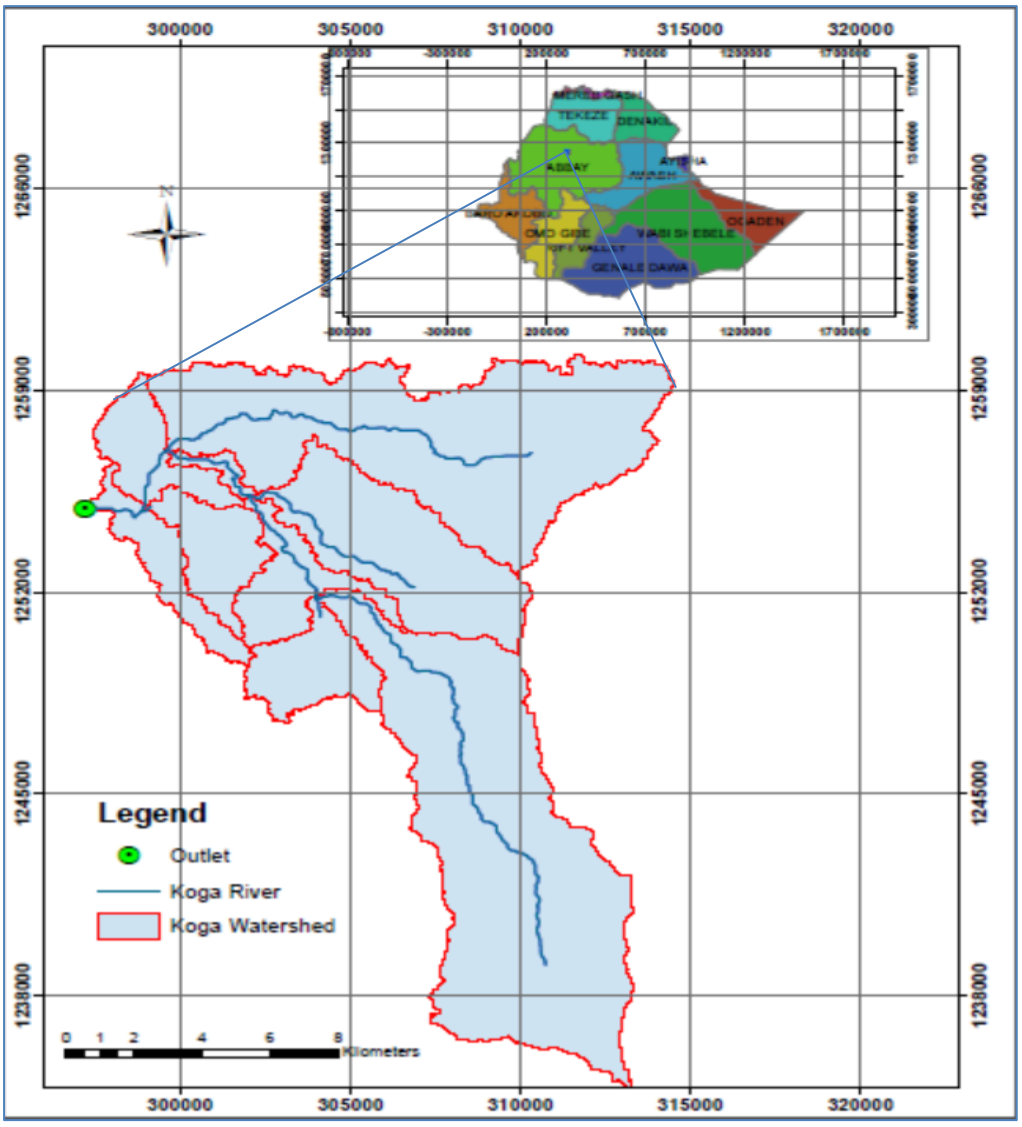



Figure 3. 1: Location of the Study Area Generated by Arc GIS software from DEM

### 3.1.2. **Climate**

The rainfall distribution over the area is unimodal .The rains usually begins in May and increase gradually in frequency to reach a maximum in July or August. Rainfall declines rapidly after a peaking the cessation of the rains is much more abrupt compared to its onset shown on Figure 3.2 below. The average daytime temperature of the study area was found to be $24^0$ C. Mean maximum temperature varies from $30.1^0$ C in April to 24.3 $^0$C in July and August. Mean minimum temperature varies from 8.9 $^0$C in January to $15.5^0$C in May. The highest mean temperatures are always between March and May. The mean monthly relative humidity (RH) is the 58.4%; RH values are highest during the humid rainy seasons75% from July to August and lowest during March 42.9%. The variability of relative humidity was also lowest during the wet season. Mean monthly sunshine hour varies from a low value of 4.4 h/d during the month of August (rainy season) to as high as 9.9 h/d during the month of December (National Mereology Agency).

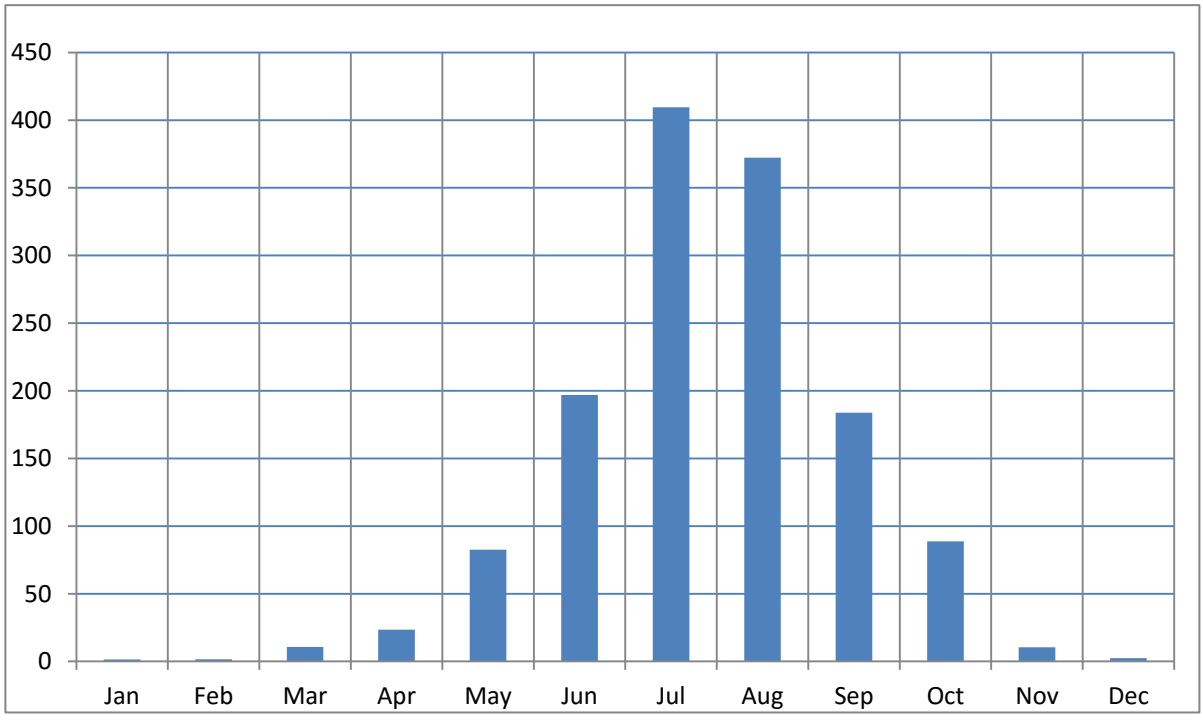



Figure 3. 2: Mean monthly rainfall of the study area

### 3.1.3. **Soil Type of the Catchment**

Koga catchment is predominately covered by chromic vertisols (36.94%) and followed by Dystric gleysols (23.47%). Pellic vertisols, eutric cambisols, chromic vertisols, dystric fluvisols, dystric nitisols, eutric cambisols, orthic acrisols, orthis solonchaks and leptosols are other soils that cover the rest of the catchment shown on figure 3.3 below. Almost all soil type of Koga catchment is classified under hydrological soil type B. According to drainage manual of Ethiopian Road Authority, "soil Group B" has the character of Silt loam, or loam soil types, where known for moderately low runoff potential due to moderate infiltration rates. These soils primarily consist of moderately deep to deep, moderately well to well drained soils with moderately fine to moderately coarse textures (ERA,2013).The soil type of the Koga watershed is shown below Table 3.1.

Table 3. 1: Soil Coverage of Koga Catchment

| S.no | Soil type | Hydrological soil group | Area (km2 ) | Percent of coverage |
|---|---|---|---|---|
| 1 | Chromic Cambisols | B | 11.447 | 5.63% |
| 2 | Chromic Luvisols | B | 8.778 | 4.32% |
| 3 | Chromic Vertisols | B | 75.085 | 36.94% |
| 4 | Dystric Gleysols | B | 47.704 | 23.47% |
| 5 | Eutric Nitisols | B | 12.011 | 5.91% |
| 6 | Leptosols | D | 0.100 | 0.05% |
| 7 | No data | D | 5.234 | 2.58% |
| 8 | Pellic vertisols | D | 42.88017 | 21.10% |
| | | | 203.2384 | 100.00% |

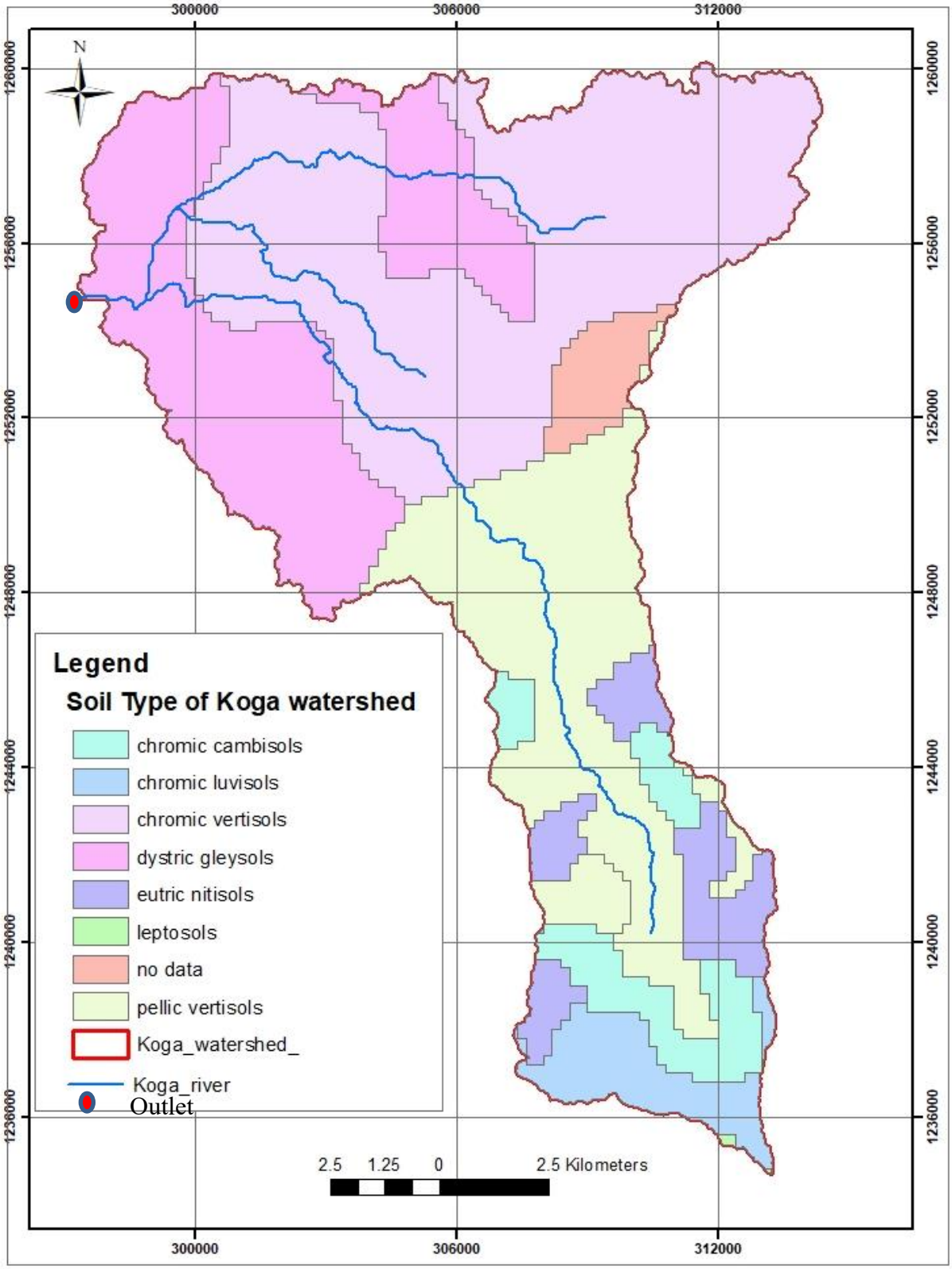



Figure 3. 3: Soil coverage of Koga watershed generated by Arc GIS

### 3.1.4. **Topography of the Koga Watershed**

On the basis of topographic maps and digital elevation model DEM; topography of the study area was found to be steep slope at the upstream with slope ranging between 0 to 10%. The downstream of the watershed is almost flat. The majority of the study area lies within slope ranges of 0-2% with topographic features of uplands followed by flat plain and low lying depression. Here the longitudinal profile of the river is shown below Figure 3.4.

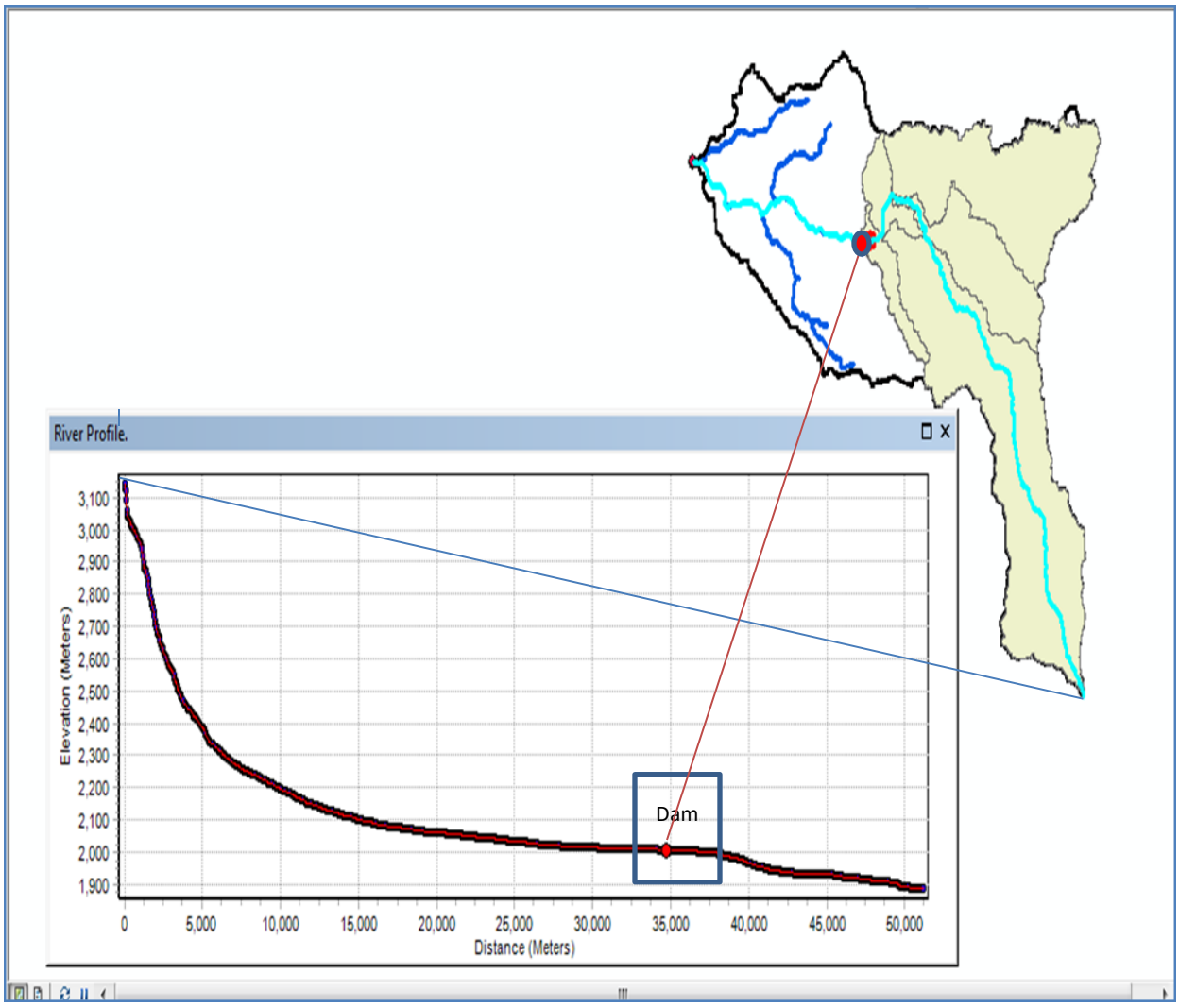



Figure 3. 4: The Longitudinal Profile of the River

### 3.1.5. **Land Use**

According to Ethio GIS Land use of the area is dominated by traditional rain fed substance farming on individuals holding and traditional grazing on communal lands. The overall farming system is strongly oriented towards grain production and is dependent on use of oxen for land preparation. The population generally keeps a number of livestock for production of milk by products and as transferable assets. Crop residue and extensive grazing in the low lying areas are the major contribution to livestock feed resources. In the upper watershed 60% of the land area is under intensive cultivation shown on Figure 3.5 below.

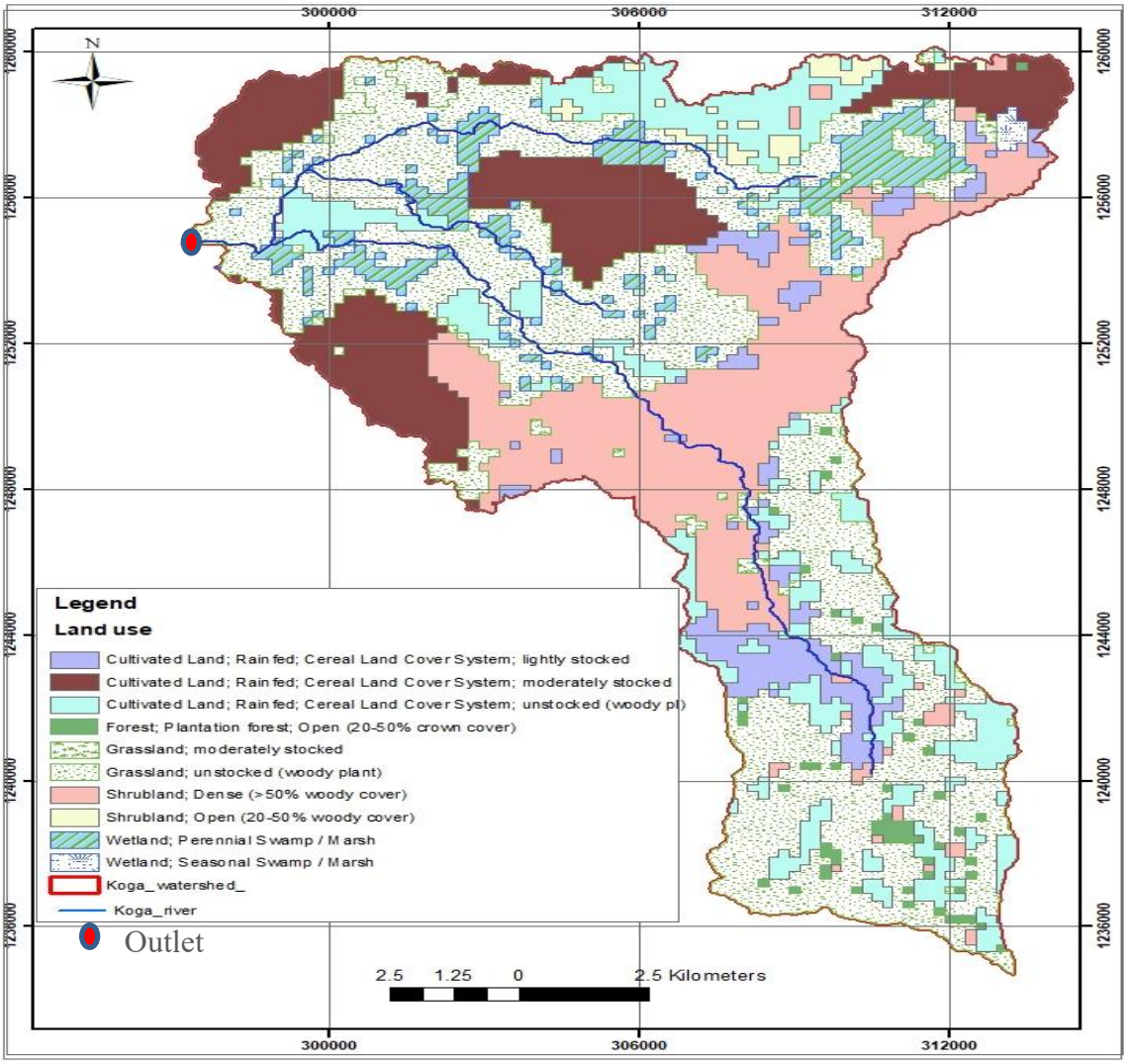



Figure 3. 5: Land Use Land Cover of Koga Watershed Generated By Arc GIS

### 3.1.6. **Koga Dam Features and Appurtenances Paramteres**

Table 3. 2: Dam and appurtenances structures parameters

| | |
|---|---|
| **Reservoir** | Impounded Volume 83.1 $Mm^3$ water and Impounded Area of the reservoir 1,750 ha |
| **Main Dam** | Type is Earth fill with clay core and zoned filters with rip rap facing protection. |
| | The dam axis is Length is 1,730 m |
| | The dam height Maximum Height: 21m |
| **Spillway** | Spillway Capacity:336 $m^3/s$ with and<br>crest length of 21.5 m<br>Chute + Basin length of 108 m. |
| **Outlet Structure** | Irrigation Outlet Split Horseshoe culvert with capacity to pass 9.1 $m^3/s$ irrigation releases in the top half. |
| | Bottom Outlet Split Horseshoe culvert with capacity to pass 31 $m^3/s$ emergency drawdown releases in the bottom half. |
| | Compensation Releases Provision has been made for environmental releases to match the existing dry season flows in the Koga River. |
| **Saddle Dam** | Type: Earth fill with clay core and zoned filters with rip rap facing protection. |
| | Length:1,162 m |
| | Maximum Height: 9 m |
| **Access Road** | Length:6.3km |
| | Number of Structures125 drop structures. 6 Cross drainage structures |
| **Irrigated Area** | Number of Command Areas 12 |
| | Net irrigated area: 7004ha |
| | Irrigation Method: Furrow |
| | Cropping: winter and summer |
| **Main Canal (all lined)** | Length: 19.7 km |
| | Capacity: 9.1 $m^3/sec$ |
| | Operation: 24hrs |

## 3.2. Data Collection and Availability

The main data that are used for this study are:

- Hydrological data, and Meteorological data
- Land use map, Soil map
- STRM of 12.5mx12.5m resolution
- Topographic map 50,000

### 3.2.1. **Hydro Meteorological Data Availability**

For the study towards the development of the breach of Koga Dam structures on the Koga River, The data on meteorological and hydrometric data become relevant with respect to the estimation of PMP, PMF, breach parameters and flood inundation mapping in the Koga dam project. Therefore, the necessary climatic data (like Rainfall, Temperature, humidity, sunshine, Wind Speed etc. data) from the National Meteorological Agency from 1986 to 2017 years of record and hydrometric data (i.e. flow data of the Koga River), Soil map and land use land cover map from Ministry of Water, Irrigation and Energy were collected for this analysis.

### 3.2.2. **Meteorological Data**

The available raw data from the time horizon 1986 to 20017 for 13 identified stations in the nearest study area were collected from NMA. The obtained data of those stations were found with certain data gaps that are existed around the study area and out of these about 9 stations were found with significant record length. The stations location all climate data records presented in Table 3.3.

Table 3. 3: Nearest Meteorological station UTM Coordinate.

| S No | Station Name | Easting | Northing |
|---|---|---|---|
| 1 | Meshenti | 312855 | 1268938 |
| 2 | Adet | 335342 | 1245644 |
| 3 | Askuna | 290462 | 1198199 |
| 4 | Sekela | 339723 | 1207152 |
| 5 | Dangla | 264317 | 1245284 |
| 6 | Enjibara | 274141 | 1211217 |
| 7 | Finoteselam | 309849 | 1181720 |
| 8 | Tilili | 283828 | 1200194 |
| 9 | Zege | 316222 | 1293063 |
| 10 | Dekeistifanose | 313875 | 1316529 |
| 11 | Denbecha | 334493 | 1165744 |
| 12 | Merawi | 298729 | 1262271 |

| S No | Station Name | Easting | Northing |
|---|---|---|---|
| 13 | Bahirdar | 318332 | 1284833 |

#### 3.2.3. Rainfall

The rainfall requires critical analysis for this study, and the upstream for appreciating and developing floods; either as a full hydrograph or in the form of flood peak rate, expected at different exceedance probability levels (return periods) and PMF is required maximum precipitation of the station.

#### 3.2.4. Hydrological Data

The river flows data time series preferably on daily or fortnightly time resolution levels, forms the forerunner for establishing water resources availability. The flow data has to be analyzed in a different form as discharge (flow rates instead of flow volumes) with respect to flood analysis.

## 3.3. Data Analysis

The data was screened, missing data was filled, the maximum probable precipitation and flood with a reasonable return period was computed, and various literatures was revised so.

### 3.3.1. Infilling Missing Data

Missing data are often found in time series and are sometimes very challenging to estimate their values. Missing data in the hydro meteorological data were filled using various approaches that were found relevant to the specific situations.

For this reason all missing daily values of stations used in this analysis should be estimated. Infilling daily rainfall and flow data is challenging because daily records do not show often-strong correlation with nearby stations and/or altitude. To fill the missing data, bi- and multivariate regression using the hydrological statistics software tool kit Hydro-gnomon; version 4.1.0 (N.T. University of Athens, ITIA research team, 2012) and direct infilling from the closest station for daily missing values were carried out. Hydro-gnomon is capable of infilling missing values based on a number of infilling options like applying different regression equations for each month, extrapolation to the past and future, randomly seeding

values and so on. In some cases, stations that are involved in this study have no records for the same period. In such cases, the long-term monthly average values were used.

### 3.3.2. Data Quality Analysis

The double mass curve technique was employed using Hydrognomon for homogeneity check of all stations. Hydro gnomon is capable of performing many of the statistical procedures in hydrology. It is such a powerful tool for double mass curve analysis. In addition to plotting the double mass curve, it is capable of automatically correcting the homogeneity of the time series with respect to a user selected reference station. The sample results for some selected stations are shown in the following Fig (4.1-4.3).

## 3.4. Tools Used for Analysis

The models used in the whole course of the study are:

- Digital Elevation Model (DEM) with 12.5mx12.5m resolution
- Arc GIS 10.3
- HEC-RAS 5.0.7
- HEC-Geo RAS 10.3
- Auto CAD 2007
- Global Mapper 19
- Google Earth and online data extraction web-page
- MS Excel
- Hydro gnomon software 4.1
- HEC Geo-HMS
- HEC HMS
- Topographic map 50,000 scale

In selecting these materials and models among alternative ones, different aspects were considered as discussed in detail on subsequent section.

## 3.5. Conceptual Frame work of the Study

The Conceptual framework of the dam breach and flood inundation is shown in Figure below in short diagram of the thesis procedure. The Available should have collected i.e. DEM, Hydro metrology data, Dam parameter, Land use land cover and insert in HEC Geo RAS. PMF also estimated from catchment characteristics and maximum precipitation. Based on those data process HEC RAS or HEC- Geo RAS model and estimate the flood mapping i.e. flood depth, flood velocity map and flood water surface profile.

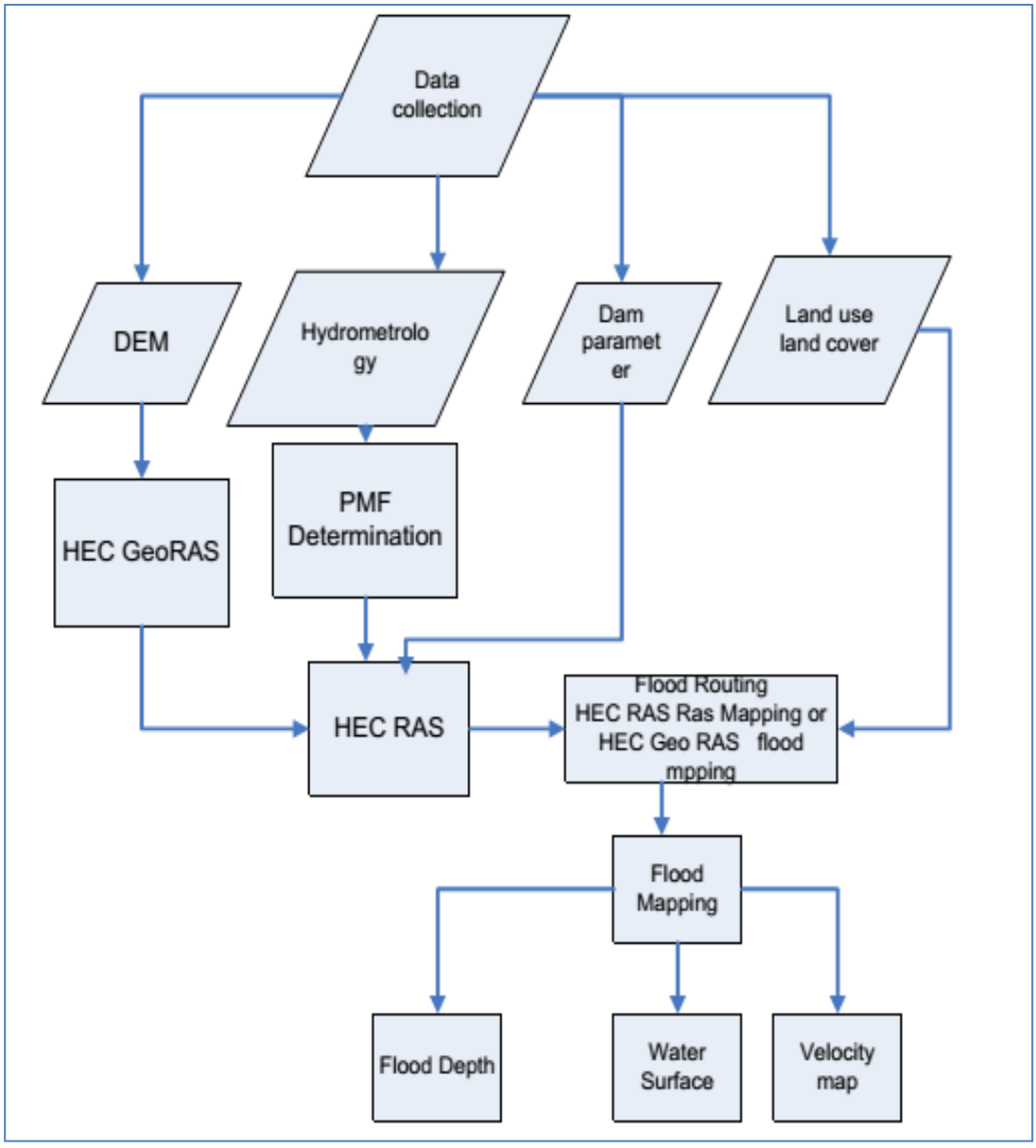



Figure 3. 6: Conceptual Formwork of the Study.

## 3.6. Time of Concentration

The time of concentration, Tc, is an index of lag frequently used to define a catchment's response time. Time of concentration is the time taken for runoff to travel from the hydraulically most remote point of the catchment to the point of outlet.

The time of concentration was computed considering part of the flow as sheet/shallow flow and the remaining as channel flow. Therefore partitioning the time of concentration is unlikely to improve the result of the discharge estimation. However, we have assumed 250 m as sheet, 500m as shallow flow and the rest of the total length as the channel flow. Therefore, for this section sheet and shallow Tc, which are designated as $Tc_1$ and $Tc_2$ are calculated using **Manning's kinematic** solution (Overton and Meadows 1976) otherwise the $Tc_3$ for channel flow will be calculated **using Kirpich formula** as described below. Tc was computed as total sum of the Tc's, generally the following procedures have been adopted:

1) For Sheet flow, natural range, length = 250m. From ERA manual (2013) .The formula adopted for calculation of $Tc_1$ is described below :

$$Tc_1 = [0.091\ (nL)^{0.8} / (P)^{0.5}S^{0.4}] \text{---------- ( 3. 1)}$$

Where:

$Tc_1$ =travel time, hr.

P= 24-hour rainfall, mm

S = slope of hydraulic grade line (land slope), m/m

L =flow length, m

n =Manning's roughness coefficient from table

2) For Shallow concentrated flow, unpaved from Equation below

$$V = 4.9178\ (s)^{0.5} \text{---------- (3. 2)}$$

Where:

S=Slope of Shallow flow

V= Velocity of flow Shallow (m/sec)

From Equation above:

$$Tc_2 = L/ (3600V) \text{ ---------- (3. 3 )}$$

Where:

$T_{c2}$ = travel time, hr.

L = flow length, m

V = average velocity, m/s

3600 = conversion factor from seconds to hours

3) Finally for Channel flow, one of the most used empirical equation to calculate time of concentration is the Kirpich equation (1940), given by:

$$Tc3 = \frac{0.0195\left[\frac{L}{S^{0.5}}\right]^{0.77}}{60} \quad \text{---------- (3. 4)}$$

**Where:**

$Tc_3$= time of concentration (hr)

L = the length of the catchment's along the longest river channel (m)

S = the overall catchment's slope in m/m = ΔH/L

ΔH = the difference in elevation between the most remote point and the outlet point

$Tc_{total} = Tc_1+Tc_2+Tc_3$

## 3.7. Probable Maximum Flood (PMF) Derivation of Koga Dam

Probable Maximum Flood (PMF): This is the flood resulting from the most severe combination of critical meteorological and hydrological conditions that rare reasonably possible in the region. The PMF is computed by using the Probable Maximum Storm (PMS) which is an estimate of the physical upper limit to storm rainfall over the catchment. This is obtained from the studies of all the storms that have occurred over the region and maximizing them for the most critical atmospheric conditions.

Recommended Spillway Design Flood (USACE) classified in to four groups see Table 3.4 below.

Table 3.4: The classification of dam for the recommendation of Spillway design flood

| Hazard | Hazard Definition | Reservoir design flood | |
|---|---|---|---|
| Low | No loss life & Minimal | Small Dam | 50-100 return period |

| | | | |
|---|---|---|---|
| | economic loss | Medium Dam | 100 ARI - 0.5 PMF |
| | | Large Dam | 0.5-1.0 PMF |
| Significant | Few lives lost-small number of habitable structures Appreciable economic loss | Small Dam | 100 ARI - 0.5 PMF |
| | | Medium Dam | 0.5-1.0 PMF |
| | | Large Dam | PMF |
| High | More than a few lives lost , Extensive economic loss (community, industry, agriculture) | Small Dam | 0.5-1.0 PMF |
| | | Medium Dam | PMF |
| | | Large Dam | PMF |

Recommended Spillway design flood (After US Army Corps of Engineers)

- Small dam Storage capacity 0.62-1.23 MCM with height 7.6-12.2m
- Medium dam capacity 1.23-61.5 MCM with height 12.2-30.5m
- Large capacity >61.5 MCM with height >30.5m

The rainfall and runoff data recorded in the study area are adequate but determine unit hydrographs for catchment it is necessary to determine a unit hydrograph for Dam site synthetically. Synthetic unit hydrograph methods usually relate time base to catchment, which is in turn, is related to the timing response characteristic of catchment, including catchment shape, length and slope.

Among several known methods of unit hydrographs, the one developed by Snyder (1938) is most commonly used. The method is derived from drainage basins in the Appalachian mountain regions in the United States ranging in area from 25km$^2$ to 25,000km$^2$. The synthetic unit hydrograph of Snyder is based on relationships found between three characteristics of standard unit hydrograph and descriptors of basin morphology. The hydrograph characteristics are the effective rainfall duration, (tr), the peak direct runoff rate (qp), and basin lag time (tp).

The standard unit hydrograph is associated with specific effective rainfall duration, tr, defined by equation 3.6 with basin lag time (hr.), tp. the peak discharge (m$^3$/sec), qp and basin period (hr.) as shown in equation (3. 6)

$$Tp = 5.5Tr$$ ---------- (3. 5)

$$Tp = C1Ct(LLc)\text{^}0.3$$ ---------- (3. 6)

$$qp = C2Cp/Tp$$ ---------- (3. 7)

$$Tb = 5.56/qp$$ ---------- (3. 8)

$$Ct = (1 + 0.33S^{-0.1})$$ ---------- (3. 9)

$$Tpr = tp - (tr - tR)$$ ---------- (3. 10)

TR = 2 ---------- (3. 11)

$T_r = T_p // 5.5$ ---------- (3.12)

QP = qp*A, QP ---------- (3. 13)

Where:

L = the length of the main stream in kilometers from the outlet to the upstream divide.

$L_c$ = the distance in kilometers from the outlet to a point on the stream near the centroid of the watershed area

Ct = is a coefficient derived from gauged watersheds in the same region and represents variations in watersheds slopes and storage characteristics.

S = the slope of main stream

It was though Snyder and some investigators observed a range for:

$C_p$ was also found to vary in the range of 0.31 to 0.93 by some investigators, though in the studies conducted by Snyder it was 0.56 to 0.69 and C1 is between 0.5 and 1

qp = the peak discharge per unit area in $m^3/s/sq.km$ and

Qp= peak discharge of the standard unit hydrograph in $m^3/sec$

A = the basin area in $km^2$, and $C_2$ =2.75 adopted.

Generally the catchment characteristics such as L, Lc, Area, slope and derived values for Snyder's method for catchment of Dam sites are given in Table 3.5 below:

Table 3. 5: Koga Dam sites catchment characteristics and values of Snyder's parameters

| basin name | | Koga |
|---|---|---|
| Catchment characteristics | | Dimension |
| Area ($km^2$) | delineated | 203.25 |
| Length (km) | delineated | 27 |
| Centroid distance (km) | delineated | 13.5 |
| Max. Elevation ( m a s l) | delineated | 2279 |
| Min. elevation (m a s l) | delineated | 2001 |
| Elevation difference (m) | Max. El-Min El | 276 |
| Av, slope, S (m/m) | (Max. el-Min El)/Longest path | 0.010 |
| $C_t$ | 1.62 | 1.62 |
| $C_p$ | 0.61 | 0.61 |
| $T_c$ (hr) calculated | 1/3000*(longest path)/(slope^0.77) | 5.03 |
| $T_p$ (hr) = $C_1C_t(LL_c)^{0.3}$ | | 7.13 |
| tr (hr) = tp/5.5 | | 1.30 |
| TR (adopted) | 2 | 2 |
| $T_{pr}$ (adj) = $t_p-(t_r-t_R)/4$ (hr) | | 7.31 |
| $q_p$ = 2.78Cp/Tpr (cumec/sq.km) | | 0.228 |
| Qp = $q_p$xA($m^3$/sec) | | 46.40 |
| $T_b$= 5.56/qp(hr) | | 24.35 |
| W50 = $2.14(qp)^{-1.08}$ (hr),width at 50% of peak discharge | | 10.55 |
| W75 =$1.22(qp)^{-1.08}$ (hr), width at 75% of peak discharge | | 6.01 |

**Snyder** developed a dimensionless hydrograph that has its ordinate values expressed as the dimensionless ratio, Ti/tp and qi/qp, where Qi is the discharge at any time Ti and $Q_P$ is peak discharge at time Tp as shown Table 3.7. Below For a given catchment, once the value of Tp is defined, the unit hydrograph can be constructed; 2-hrs unit hydrograph developed based on Snyder's parameters is described in Table 3.8.The Snyder's and SCS method unit hydrograph was developed based on the above parameter. $C_2$ = 1.62. As $C_t$, $C_p$ is a coefficient derived from gauged watersheds in the area, and represents the effects of retention and storage.

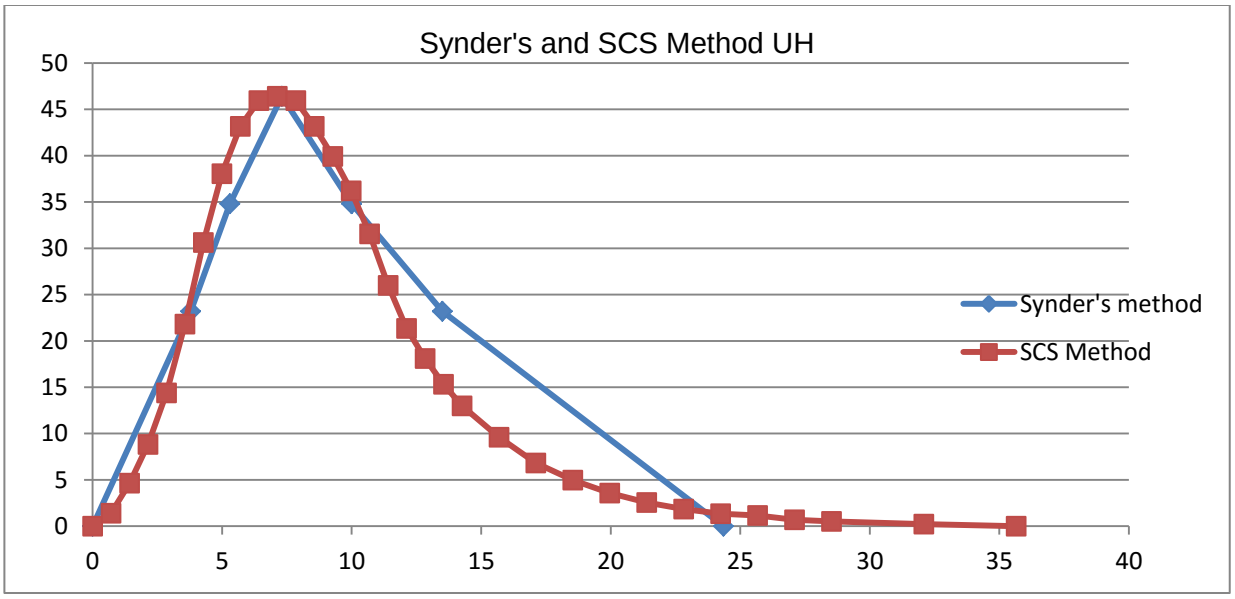



Figure 3. 7: Unit hydrograph of koga watershed using Synder's and SCS method

Table 3. 6: unit hydrograph ordinates

| | | UH ordinates | |
|---|---|---|---|
| | | Time | Disharge |
| Tpr | 7.31 | 0 | 0 |
| qpr | 0.228 | 3.8 | 23.20 |
| Qp` | 46.40 | 5.3 | 34.80 |
| W75 | 6.01 | 7.31 | 46.40 |
| W50 | 10.55 | 10 | 34.80 |
| Tb | 24.35 | 13.5 | 23.20 |
| | | 24.35 | 0 |

Table 3. 7: Ratio of the basic Dimensionless hydrograph of the Snyder's

| Ti/Tp | Qi/qp | Ti/Tp | Qi/qp | Ti/Tp | Qi/qp |
|---|---|---|---|---|---|
| 0 | 0 | 1.2 | 0.93 | 2.6 | 0.107 |
| 0.1 | 0.03 | 1.3 | 0.86 | 2.8 | 0.077 |
| 0.2 | 0.1 | 1.4 | 0.78 | 3 | 0.055 |
| 0.3 | 0.19 | 1.5 | 0.68 | 3.2 | 0.04 |
| 0.4 | 0.31 | 1.6 | 0.56 | 3.4 | 0.029 |
| 0.5 | 0.47 | 1.7 | 0.46 | 3.6 | 0.025 |
| 0.6 | 0.66 | 1.8 | 0.39 | 3.8 | 0.015 |
| 0.7 | 0.82 | 1.9 | 0.33 | 4 | 0.011 |
| 0.8 | 0.93 | 2 | 0.28 | 4.5 | 0.011 |
| 0.9 | 0.99 | 2.2 | 0.207 | 5 | 0.0 |
| 1 | 1 | 2.4 | 0.147 | | |
| 1.1 | 0.99 | | | | |

The nearest Meteorological station in the Koga Dam are Bahir Dar , Meshenti and Skela From those station Collection of daily maximum rainfall and estimated weighted aerial precipitation (calculated its mean and standard deviation) and find catchment characteristics of the study site, like catchment area, longest path of channel, maximum elevation, minimum elevation, mean slope, and centroid of the channel as shown Table 3.8.

Table 3. 8: Maximum aerial precipitation of the study area parameter

| | |
|---|---|
| Mean (n) | 59.9 |
| Mean (n-m) | 61.9 |
| SD (n) | 14.1 |
| SD(n-m) | 13.9 |
| CV (n) | 0.2 |
| CV(n-m) | 0.2 |

### 3.7.1. Adjustment of Mean and Standard Deviation of Rain Fall

Now adjustments to the values of mean and standard deviation of rainfall which appropriately represent the project catchment area are, therefore, proposed to be made from such a series of curve (Ref: WMO No.332, 1986). Similarly corrections for the sample size i.e., length of the series have also been proposed. Thus, using the envelope values of the frequency factors so found and necessary corrections to the mean and the standard deviation for sample size (i.e. no. of observations), adjustment of mean and δ for maximum observed event and adjustment for fixed observational interval (i.e. conversion of 1- day RF to 24 hrs RF values), point maximum precipitation (PMP) depths can be found.

The PMP for large catchment areas: the point rainfall has to be converted to the corresponding areal rainfall value before its application to the concerned river basin. The area reduction factor (Fr) is introduced to account for the spatial variability of point rainfall over the catchment. It has been possible to relate maximum point rainfall in a storm with aerial extent and duration. The relationship adopted for the reduction factor is based on the relationship developed for east African condition (Fiddes, 1996) as expressed below:

$Fr = 1 - 0.02D^{-0.33}A^{0.5}$ ---------- (3. 14)

Where

D = duration in hours (in our case D=24hrs)

A = drainage area in sq.km

Table 3. 9: Calculation of PMP different return period values for Koga dam catchments by Hershfield method

| Station Name | Mean | Slandered deviation | Coefficient of variant | Conversion of 1-day RF to 24 hr. RF value | Adjusted Mean | Adjusted Slandered deviation | area reduction factor (Fr) |
|---|---|---|---|---|---|---|---|
| Koga Dam | 77.2 | 14.2 | 0.2 | 1.13 | 90.7 | 18.3 | 0.9 |

Average PMP value for project catchments, has been calculated as per procedure of standardized mean and tendered deviation given in WMO 332 and based on maximum RF values and for appropriate station, taking into account relevant adjustment factors.

### 3.7.2. Fitting Distribution Test

Fitting Distribution is used for rain fall to know distribution of flow in the catchment. As the distributions are many and very long steps for each distribution, the team recently need different free and simple software like Hydro gnomon 4- Version 4.1.0.26 march 30th, 2012 and U.S. Army corps of Hydrologic Engineering center Statistical software package (HEC-SSP).

Arranged the available maximum rainfall, in the form of software considered, then select the best fitness distribution through the graphically fitness or X-square test acceptance and

Kolmogorov Smirnov test in case of Hydro gnomon 4. Procedures of in case of Hydro gnomon 4 selection annual maximum rainfall and New projects created from file and save it with project name; adjust time zone and unit measurement of selected data Enter the data through procedure of Edit insert record to enter the beginning year of record, and also insert multi records to enter the total number of data continued copy the data from spread sheet and past it.

In Hydrology pythia-statistical analyses, continued in statistic Test (select X-square test or Kolmogorov Smirnov test) to select the best fitness.

A probability distribution is a function representing the probability of occurrence of a random variable. By fitting a distribution to a set of hydrologic data, a great deal of the probabilistic information in the sample can be compactly summarized in the function and its associated parameters. Fitting distributions can be accomplished by the method of moments or the method of maximum likelihood the best fit distribution is Gumbel EV1 by Kolmogorov smirnove test (see annex Table 7.1 and 7.2)

### 3.7.3. Estimation of PMP for Different Return Period of Koga Dam

However there is not necessary to developed the PMP value through the procedure we can gate the intermediates value of return periods like, 25, 50, 100, 500 and 1000 and PMF years.

The statistical approach suggested by Hershfield (1961) can be used to estimate PMP and rainfall of different return periods.

The procedure developed by Hershfield (1961) and later modified (1965) is based on the general flood frequency equation Chow (1961):

$$X_T = X_{av} \pm \sigma K$$ ---------- (3. 15)

Where: $X_T$ is the event (magnitude) at return period of T years

$X_{av}$ the mean of the sample data

$\sigma$ the standard deviation and

K the frequency factor, which depends upon the frequency distribution representing the sample series.

If the maximum observed rainfall, $X_m$ is substituted for $X_t$ and $K_m$ for K. then

$X_m = X_n + \delta * K_m$ ---------- (3. 16)

Where $X_{m=}$ is the event (magnitude) at return period of T years

$X_n$ = the mean of the maximum sample data

$\delta$ =The standard deviation and

$K_{m=}$ the frequency factor, which depends upon the frequency distribution representing the sample series.

For distributing the areal PMP value, the approach to different return period flood adopted on Frequency factor ($K_T$) for Gumble's distribution is best fit.

$$KT = -\langle \frac{\sqrt{6}}{\pi} * \left[0.5772 + \ln(\ln(\frac{T}{T-1})\right] \rangle$$ ---------- (3. 17)

Where, T is the return period in years.

Table 3. 10: Frequency factors for various periods for various return periods

| Return period | 25YRS | 50 YRS | 100 YRS | 200YRS | 500 YRS | 1000 YRS | 2000 YRS | 5000YRS | 10000 YRS | PMP |
|---|---|---|---|---|---|---|---|---|---|---|
| Frequency factor . $KT = -\langle \frac{\sqrt{6}}{\pi} * \left[0.5772 + \ln(\ln(\frac{T}{T-1})\right] \rangle$ | 2.0 | 2.6 | 3.1 | 3.7 | 4.4 | 4.94 | 5.5 | 6.2 | 6.7 | 15 |

Temporal distributed of Areal rainfall of different return period in to 24 hours by one, two or less hours' time steps. The point PMP for large catchment areas: the point rainfall has to be converted to the corresponding areal rainfall value before its application to the concerned river basin. The area reduction factor (Fr) is introduced to account for the spatial variability of point rainfall over the catchment shown on Table 3.11.

Table 3. 11: Point and Aerial Rainfall

| Return period | Depth of PRF(mm) | Depth of RF(cm) | Areal RF(mm) | Areal RF(cm) |
|---|---|---|---|---|
| 25 | 128.12 | 12.8 | 115.32 | 11.53 |
| 50 | 138.16 | 13.8 | 124.36 | 12.44 |
| 100 | 148.13 | 14.8 | 133.33 | 13.33 |
| 200 | 158.06 | 15.8 | 142.27 | 14.23 |
| 500 | 171.16 | 17.1 | 154.06 | 15.41 |
| 1000 | 181.06 | 18.1 | 162.98 | 16.30 |
| 2000 | 190.97 | 19.1 | 171.89 | 17.19 |
| 5000 | 204.05 | 20.4 | 183.66 | 18.37 |
| 10000 | 213.95 | 21.4 | 192.57 | 19.26 |
| PMP | 365.20 | 36.5 | 328.72 | 32.87 |

Average point PMP value for dam catchments, calculated as per procedure given in WMO 332 and based on maximum RF values represented stations, taking into account relevant adjustment factors of mean and standard deviation, has been estimated (see Table 3.11). Probability maximum rainfall of different return periods for the catchment after applying areal correction factor has been estimated as value for dam's catchment. Statistical parameters of 1-day maximum RF and calculation of hydrograph of different return period from equation 3.16 above for stations for Dams catchment:

The temporal distribution of areal rainfall is Prepared from Table 3.12. The study area temporal distribution of rainfall per Adimasu method is shown below Table 3.13.For 24 hours rainfall various return periods 100% multiplied by aerial reduction factor of rainfall depth that already got in Table 3.11 column 4.

Table 3. 12: Temporal distribution of areal rainfall

| % of rainfall and duration | | | |
|---|---|---|---|
| Duration (%) | Accumulated RF (%) | Duration (%) | Accumulated RF (%) |
| **0** | **0** | 54.2 | 45.8 |
| 2.1 | 1.91 | 56.3 | 47.71 |
| 4.2 | 2.67 | 58.3 | 49.62 |
| 6.3 | 4.27 | 60.4 | 51.53 |
| 8.3 | 5.73 | 62.5 | 53.44 |
| 10.4 | 7.18 | 64.6 | 55.34 |
| 12.5 | 8.63 | 66.7 | 57.25 |
| 14.6 | 10.08 | 68.8 | 59.16 |
| 16.7 | 11.53 | 70.8 | 61.07 |
| 18.8 | 12.98 | 72.9 | 63.74 |

| | | | |
|---|---|---|---|
| 20.8 | 15.27 | 75 | 66.41 |
| 22.9 | 17 | 77.1 | 69.08 |
| 25 | 18.87 | 79.2 | 71.76 |
| 27.1 | 20.74 | 81.3 | 74.43 |
| 29.2 | 22.61 | 83.3 | 77.1 |
| 31.3 | 24.48 | 85.4 | 79.77 |
| 33.3 | 26.35 | 87.5 | 82.44 |
| 35.4 | 28.22 | 89.6 | 85.11 |
| 37.5 | 30.09 | 91.7 | 87.79 |
| 39.6 | 31.96 | 93.8 | 90.46 |
| 41.7 | 33.83 | 95.8 | 93.13 |
| 43.8 | 35.7 | 97.9 | 95.8 |
| 45.8 | 37.57 | 100 | 100 |
| 47.9 | 39.44 | | |
| 50 | 41.31 | | |
| 52.1 | 43.18 | | |

Table 3. 13: Temporal distribution of rainfall Per Adimasu method

| Time (hrs.) | Accumulated RF (cm) for different return period | | | | | | | | | |
|---|---|---|---|---|---|---|---|---|---|---|
| | 25 | 50 | 100 | 200 | 500 | 1000 | 2000 | 5000 | 10000 | PMP |
| 0 | 0.00 | 0.00 | 0.00 | 0.00 | 0.00 | 0.00 | 0.00 | 0.00 | 0.00 | 0.00 |
| 2 | 0.66 | 0.71 | 0.76 | 0.81 | 0.88 | 0.93 | 0.98 | 1.05 | 1.10 | 1.88 |
| 4 | 1.33 | 1.43 | 1.54 | 1.64 | 1.78 | 1.88 | 1.98 | 2.12 | 2.22 | 3.79 |
| 6 | 2.18 | 2.35 | 2.52 | 2.68 | 2.91 | 3.08 | 3.24 | 3.47 | 3.63 | 6.20 |
| 8 | 3.04 | 3.28 | 3.51 | 3.75 | 4.06 | 4.29 | 4.53 | 4.84 | 5.07 | 8.66 |
| 10 | 3.90 | 4.21 | 4.51 | 4.81 | 5.21 | 5.51 | 5.81 | 6.21 | 6.51 | 11.12 |
| 12 | 4.76 | 5.14 | 5.51 | 5.88 | 6.36 | 6.73 | 7.10 | 7.59 | 7.96 | 13.58 |
| 14 | 5.72 | 6.17 | 6.62 | 7.06 | 7.64 | 8.09 | 8.53 | 9.11 | 9.56 | 16.31 |
| 16 | 6.60 | 7.12 | 7.63 | 8.15 | 8.82 | 9.33 | 9.84 | 10.52 | 11.03 | 18.82 |
| 18 | 7.66 | 8.26 | 8.85 | 9.45 | 10.23 | 10.82 | 11.42 | 12.20 | 12.79 | 21.83 |
| 20 | 8.89 | 9.59 | 10.28 | 10.97 | 11.88 | 12.57 | 13.25 | 14.16 | 14.85 | 25.34 |
| 22 | 10.12 | 10.92 | 11.70 | 12.49 | 13.52 | 14.31 | 15.09 | 16.12 | 16.91 | 28.86 |
| 24 | 11.53 | 12.44 | 13.33 | 14.23 | 15.41 | 16.30 | 17.19 | 18.37 | 19.26 | 32.87 |

The rainfall incremental was calculated from Table 3.13: Temporal distribution of rainfall Per Adimasu method. The calculation was done for each return period 24 hours rainfall depth minus the previous rainfall depth i.e for 25 years returen periods 11.53-10.14=1.41.

Table 3. 14: Rainfall Incremental

| Time (hrs.) | Accumulated RF (cm) for different return period | | | | | | | | | |
|---|---|---|---|---|---|---|---|---|---|---|
| | 25 | 50 | 100 | 200 | 500 | 1000 | 2000 | 5000 | 10000 | PMP |
| 0 | 0.00 | 0.00 | 0.00 | 0.00 | 0.00 | 0.00 | 0.00 | 0.00 | 0.00 | 0.00 |

| | | | | | | | | | | |
|---|---|---|---|---|---|---|---|---|---|---|
| 2 | 0.66 | 0.71 | 0.76 | 0.81 | 0.88 | 0.93 | 0.98 | 1.05 | 1.10 | 1.88 |
| 4 | 0.67 | 0.72 | 0.77 | 0.83 | 0.89 | 0.95 | 1.00 | 1.07 | 1.12 | 1.91 |
| 6 | 0.85 | 0.91 | 0.98 | 1.04 | 1.13 | 1.20 | 1.26 | 1.35 | 1.41 | 2.41 |
| 8 | 0.86 | 0.93 | 1.00 | 1.06 | 1.15 | 1.22 | 1.29 | 1.37 | 1.44 | 2.46 |
| 10 | 0.86 | 0.93 | 1.00 | 1.06 | 1.15 | 1.22 | 1.29 | 1.37 | 1.44 | 2.46 |
| 12 | 0.86 | 0.93 | 1.00 | 1.06 | 1.15 | 1.22 | 1.29 | 1.37 | 1.44 | 2.46 |
| 14 | 0.96 | 1.03 | 1.11 | 1.18 | 1.28 | 1.35 | 1.43 | 1.53 | 1.60 | 2.73 |
| 16 | 0.88 | 0.95 | 1.02 | 1.09 | 1.18 | 1.24 | 1.31 | 1.40 | 1.47 | 2.51 |
| 18 | 1.06 | 1.14 | 1.22 | 1.30 | 1.41 | 1.49 | 1.57 | 1.68 | 1.76 | 3.01 |
| 20 | 1.23 | 1.33 | 1.42 | 1.52 | 1.65 | 1.74 | 1.84 | 1.96 | 2.06 | 3.51 |
| 22 | 1.23 | 1.33 | 1.42 | 1.52 | 1.65 | 1.74 | 1.84 | 1.96 | 2.06 | 3.51 |
| 24 | 1.41 | 1.52 | 1.63 | 1.74 | 1.88 | 1.99 | 2.10 | 2.24 | 2.35 | 4.01 |

**Infiltration lose**

After obtaining the design rainfall hyetograph, its ordinates are reduced by deducting for infiltration losses. Commonly, the initial loss and infiltration index values are derived on the basis of available hydrologic records, and minimum values are selected on the assumption that the basin would be saturated at time of occurrence of design storm, resulting in very low lose rate. Where sufficient data is not available, it is recommended that loss rate or Phi index of the Lose rate or infiltration rat 3mm/hrs. The excess rainfall was calculated as rainfall depth at various duration subtracted infiltration rate i.e 6mm/2hrs.

Table 3. 15: Excess rainfall

| Time (hrs.) | Accumulated RF (cm) for different return period | | | | | | | | | |
|---|---|---|---|---|---|---|---|---|---|---|
| | 25 | 50 | 100 | 200 | 500 | 1000 | 2000 | 5000 | 10000 | PMP |
| 0 | 0.00 | 0.00 | 0.00 | 0.00 | 0.00 | 0.00 | 0.00 | 0.00 | 0.00 | 0.00 |
| 2 | 0.06 | 0.11 | 0.16 | 0.21 | 0.28 | 0.33 | 0.38 | 0.45 | 0.50 | 1.28 |
| 4 | 0.07 | 0.12 | 0.17 | 0.23 | 0.29 | 0.35 | 0.40 | 0.47 | 0.52 | 1.31 |
| 6 | 0.25 | 0.31 | 0.38 | 0.44 | 0.53 | 0.60 | 0.66 | 0.75 | 0.81 | 1.81 |
| 8 | 0.26 | 0.33 | 0.40 | 0.46 | 0.55 | 0.62 | 0.69 | 0.77 | 0.84 | 1.86 |
| 10 | 0.26 | 0.33 | 0.40 | 0.46 | 0.55 | 0.62 | 0.69 | 0.77 | 0.84 | 1.86 |
| 12 | 0.26 | 0.33 | 0.40 | 0.46 | 0.55 | 0.62 | 0.69 | 0.77 | 0.84 | 1.86 |
| 14 | 0.36 | 0.43 | 0.51 | 0.58 | 0.68 | 0.75 | 0.83 | 0.93 | 1.00 | 2.13 |
| 16 | 0.28 | 0.35 | 0.42 | 0.49 | 0.58 | 0.64 | 0.71 | 0.80 | 0.87 | 1.91 |
| 18 | 0.46 | 0.54 | 0.62 | 0.70 | 0.81 | 0.89 | 0.97 | 1.08 | 1.16 | 2.41 |
| 20 | 0.63 | 0.73 | 0.82 | 0.92 | 1.05 | 1.14 | 1.24 | 1.36 | 1.46 | 2.91 |
| 22 | 0.63 | 0.73 | 0.82 | 0.92 | 1.05 | 1.14 | 1.24 | 1.36 | 1.46 | 2.91 |
| 24 | 0.81 | 0.92 | 1.03 | 1.14 | 1.28 | 1.39 | 1.50 | 1.64 | 1.75 | 3.41 |

The water available to runoff after interception, depression storage and infiltration has been satisfied. Effective rain fall excess hyetograph is then placed against the ordinates of unit hydrograph in the order of magnitude and the sequence is then reversed to get the critical sequence for adoption in the estimation of design flood.

Table 3. 16: Put excesses Rainfall in Reverse Critical Sequencing

| Time (hrs.) | Accumulated RF (cm) for different return period | | | | | | | | | |
|---|---|---|---|---|---|---|---|---|---|---|
| | 25 | 50 | 100 | 200 | 500 | 1000 | 2000 | 5000 | 10000 | PMP |
| 0 | 0.00 | 0.00 | 0.00 | 0.00 | 0.00 | 0.00 | 0.00 | 0.00 | 0.00 | 0.00 |
| 2 | 0.07 | 0.12 | 0.17 | 0.23 | 0.29 | 0.35 | 0.40 | 0.47 | 0.52 | 1.31 |
| 4 | 0.26 | 0.33 | 0.40 | 0.46 | 0.55 | 0.62 | 0.69 | 0.77 | 0.84 | 1.86 |
| 6 | 0.26 | 0.33 | 0.40 | 0.46 | 0.55 | 0.62 | 0.69 | 0.77 | 0.84 | 1.86 |
| 8 | 0.28 | 0.35 | 0.42 | 0.49 | 0.58 | 0.64 | 0.71 | 0.80 | 0.87 | 1.91 |
| 10 | 0.63 | 0.73 | 0.82 | 0.92 | 1.05 | 1.14 | 1.24 | 1.36 | 1.46 | 2.91 |
| 12 | 0.81 | 0.92 | 1.03 | 1.14 | 1.28 | 1.39 | 1.50 | 1.64 | 1.75 | 3.41 |
| 14 | 0.63 | 0.73 | 0.82 | 0.92 | 1.05 | 1.14 | 1.24 | 1.36 | 1.46 | 2.91 |
| 16 | 0.46 | 0.54 | 0.62 | 0.70 | 0.81 | 0.89 | 0.97 | 1.08 | 1.16 | 2.41 |
| 18 | 0.36 | 0.43 | 0.51 | 0.58 | 0.68 | 0.75 | 0.83 | 0.93 | 1.00 | 2.13 |
| 20 | 0.26 | 0.33 | 0.40 | 0.46 | 0.55 | 0.62 | 0.69 | 0.77 | 0.84 | 1.86 |
| 22 | 0.25 | 0.31 | 0.38 | 0.44 | 0.53 | 0.60 | 0.66 | 0.75 | 0.81 | 1.81 |
| 24 | 0.06 | 0.11 | 0.16 | 0.21 | 0.28 | 0.33 | 0.38 | 0.45 | 0.50 | 1.28 |

### 3.7.4. Base flow

Base flow is added to direct runoff hydrograph to obtain flood hydrograph. It is seen from the hydrological series. Therefore, the base flow separated by graphical with constant slope method or designer can need different software's to separate base flow from measured stream flow.

Base flow is the portion of the stream discharge that is derived from natural storage (e.g., groundwater outflow and the draining of large lakes and swamps or other source outside the net rainfall that creates surface runoff).

Table 3. 17 : Base flow separated by constant slope line constraints

| Jan | Feb | Mar | Apr | May | Jun | Jul | Aug | Sep | Oct | Nov | Dec | Average |
|---|---|---|---|---|---|---|---|---|---|---|---|---|
| 1.7 | 1.8 | 3.7 | 5.5 | 6.15 | 8.38 | 16 | 23 | 17.8 | 12.1 | 7.8 | 2.5 | 8.87 |

For application of Unit Hydrograph approach, main data requirement are rainfall data for corresponding return period rainfall and UH for the basin. UH developed has been used for estimation of any return period flood. Since rainfall can have a minimum limit of zero with upper limit depends on its return period K value. The PMF of Koga river is shown at result Table 4.20.

## 3.8. Model Selection

A 12.5 meter resolution DEM and 1:50,000 topographic map of the study area is available. These data were imported to Arc GIS for preprocessing of the necessary inputs to HEC-RAS model. The analysis in Arc GIS basically involves the use of HEC-Geo RAS extension to extract geometric data which ultimately be fed to HEC-RAS for dam break modeling. Moreover, the built-in RAS Mapper in HEC-RAS software or HEC-Geo RAS tool in Arc GIS can then be used for post-processing of HECRAS unsteady flow simulation outputs to undertake flood inundation mapping.

In addition to topographical data, land use map and hydrological data of the area (i.e. Probable Maximum Flood (PMF) inflow hydrograph at the upstream end of Koga dam reservoir .HEC-RAS has a very easy to use graphical users‟ interface (GUI) and this provides a highly efficient file management, data entry and editing, hydraulic analyses, and tabulation and graphical displays of input and output data.

### 3.8.1. HEC-GEOHMS

The Geospatial Hydrologic Modeling Extension (HEC-GEOHMS) has been developed as a geospatial hydrology tool kit for hydrologists and engineers with limited GIS experience. HEC-GEOHMS uses Arc-GIS and the Spatial Analyst extension to develop a number of hydrologic modeling inputs for the Hydrologic Engineering Center's Hydrologic Modeling System, HEC-HMS. ARC-GIS and its Spatial Analyst extension are available from the Environmental Systems Research Institute, Inc (ESRI). The program allows users to visualize spatial information, document watershed characteristics, perform spatial analysis, and delineate sub basins and streams. Working with HEC-GEOHMS through its interfaces, menus, tools, buttons, and context-sensitive online help allows the user to expediently create hydrologic inputs for HEC-HMS.

**(a) Data Management**

The USGS digital elevation model (DEM) contains terrain cells of surface elevations at a spacing of 30 meters in both the horizontal and vertical direction. This DEM data was used to generate the stream network and sub basin areas within the watershed. All data layers were projected to the Adinidian Northern hemisphere Plane coordinate system.

**(b) Terrain Pre-processing**

Before hydrologic modeling with HEC-HMS was possible, the terrain model is used to derive eight datasets described in proceeding sections. These processes were performed using HEC-Geo-HMS in Arc-Map. The steps involved delineation of the Koga River, its tributaries, watershed, and watershed properties (i.e. runoff curve number, time of concentration). With the DEM and GIS tools, the watershed properties were extracted using automated procedures (USACE 2009).

The spacing of elevations in the DEM was not sufficient for the stream centerline; therefore the DEM was modified to be consistent with the input vector stream network. This DEM reconditioning increases the degree of agreement between stream networks delineated from the DEM and input vector stream network shape file. If the reconditioning process was not applied, the path of the Koga River would be too crude .Meaning is that the reach lengths generated in Arc-Map would not represent site conditions. This is mainly due to the precision of elevation data along the stream in the initial DEM. By manually detailing, or burning in the stream network, a distinct stream profile was created and a new DEM was created. If a cell is surrounded by higher elevations, the water is trapped and cannot flow out of the sink.

After the terrain pre-processing, the reconditioned DEM is the starting point for delineating sub basins and river reaches. The first five of the eight datasets are grid layers that represent:

- Flow Direction, defines the direction of steepest descent for each terrain cell
- Flow Accumulation, determines the number of cells upstream draining to a given cell (upstream drainage area can be calculated by multiplying the flow accumulation value (number of cells) by the grid cell area (12.5m x 12.5m)

- ❖ Stream Definition, the generation of a stream defined by the number of Flow Accumulation cells
- ❖ Stream Segmentation, divides the grid of streams into segments, these are sections of the stream that connect two joining streams (junction), junction and an outlet, or junction and the drainage divide.
- ❖ Catchment Delineation, creates a grid layer that delineates a sub basin for each stream segment After the terrain processing is completed, the first watershed project was defined by identifying the downstream outlet area. The catchment polygons were either merged or subdivided until the area of the sub basins were comparable to the drainage area size Next, it was possible to extract physical characteristics of the streams and sub basins. These characteristics included computed length of the river segments, upstream and downstream elevations of the reach and the slope of the river segments. Basin slope uses the slope grid to determine the average slope for the sub basin. Longest flow path creates a polyline that stores the upstream and downstream elevations and slope between endpoints. The Basin Centroid, Centroid Elevation, and Centroidal Flow Path are hydrologic elements easily performed in GIS.

### 3.8.2. Model Selection and Brief Description of the HEC HMS

The criteria of Cunderlik and Simonovic (2007) used for selecting the hydrological model. Therefore, HEC –HMS model was selected for this study due to the following reasons.

- Its model structure is simple but flexible such that a catchment can be sub-divided into different elevation and vegetation zones,
- It is not data intensive and most of the data needed were readily available (available of input data).
- The required model outputs are important to the project and therefore to be estimated by the model.
- Recent studies demonstrate it has been widely used world-wide.
- Hydrologic processes that need to be modeled estimate the desired project outputs adequately.
- It is open source software and belongs to public domain

The model selected for this purpose was HEC-HMS, version 4.1 (USACE, 2013). It is a comprehensive catchment model that could simulate a number of hydrological variables with a single model setup. HEC-HMS is composed of many hydrological models, soil erosion and sedimentation and hydraulic routing models to simulate hydrological systems in a variety of applications ranging from event based storm runoff analysis to long term continuous predictions and forecasting, lumped and distributed, empirical and conceptual models to simulate the whole surface and upper sub-surface hydrological processes of a given hydrological system. The software provides a user friendly graphical user interface to input variables/parameters and query both graphical and table outputs. Moreover, it has an automatic parameter estimation routine using a user selected parameterization algorithm that could assist manual calibration. For detailed description of the model, the model technical reference manual is available (HEC-HMS technical reference manual, 2002).

The method used for the simulation of runoff volume in this analysis was the Soil Moisture Accounting (SMA) loss methods. This method accounts the losses in vegetation, surface and subsurface and movement of rainfall as it travels from the atmosphere to the water bodies continuously. It requires a continuous daily precipitation and daily/monthly evapotranspiration data together with optimized model parameters to compute basin runoff and other variables. The parameters of the model should be estimated through calibration process.

Direct runoff was computed using Clark unit hydrograph. It is a linear reservoir model that represents two critical processes i.e translation and attenuation, as the excess precipitation transforms into runoff. Storage Coefficient and Time of Concentration are the parameters needed by the model. The storage coefficient was estimated through calibration whereas the time of concentration was estimated using the USDA approach using the physical features of the catchment in ArcGIS environment using Hec-GeoHMS.

Since base flow plays a significant role in perennial rivers, especially for the upstream catchment, it was also included in the model. For this purpose, linear reservoir method, which is normally used in combination with SMA loss model with two ground water zones, was used. Its parameters have been estimated through calibration.

Finally, the computed runoff was routed using Muskingum-Cunge wave method. The method is well suited for rivers that experience overbank and backwater flow effects as in the case of in the study area i.e Koga River. The model uses physical parameters (geometry of the river and manning's coefficients) that were estimated from the geographic information of the river.

#### 3.8.2.1. Model set-up

**Model Configuration and Assumptions**

The Koga River catchment was divided in to manageable sub-catchments based on the gauge station and Major tributaries locations and similarity in hydro-physiographic features. observed data available at the upstream and downstream the catchment so that the calibration are to be conducted in the gauge station, to calibrate the model at the gauge station of the catchment, where daily flow records are available, and incorporate the hydrological processes as best as possible, measure some of the physical model parameters and take tangible assumptions.

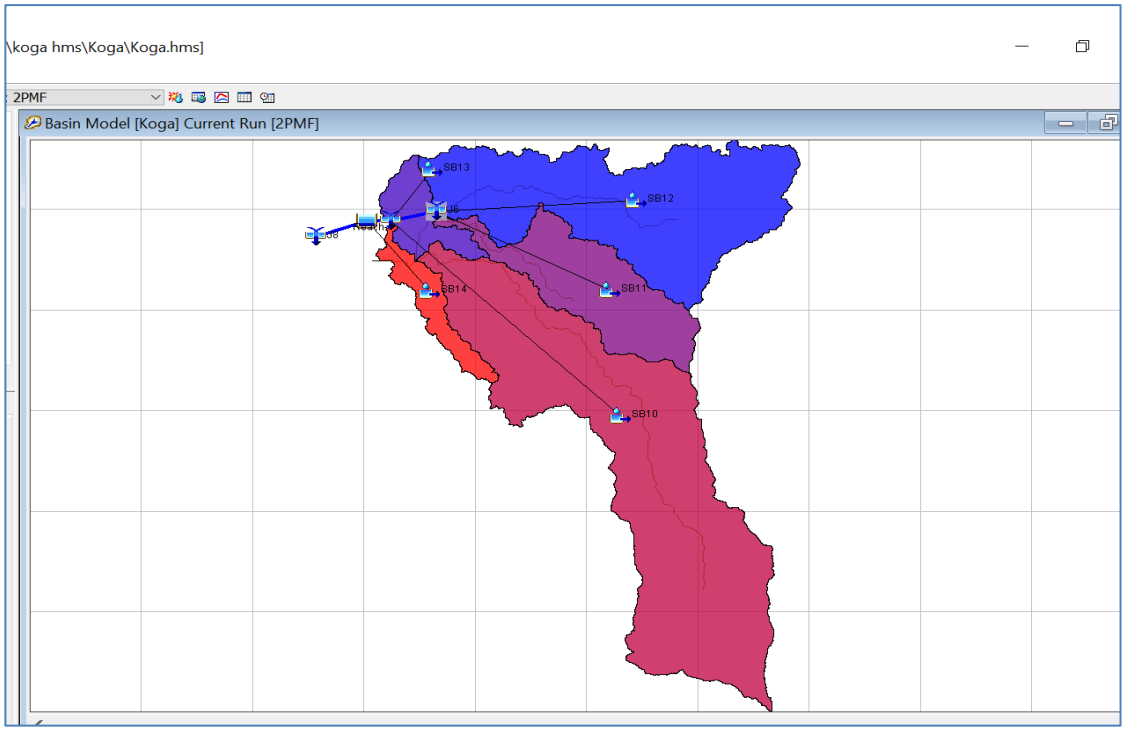



Figure 3. 8: Model schematization

**Loss determination**

The term loss refers to the amount of rainfall infiltrated into the soil. HEC-HMS supports the most common methods for calculating losses–such as initial/constant, SCS Curve No., gridded SCS Curve No., and the Green Ampts, and provides a moisture depletion option for simulations over extended periods of time. In this paper for gage weight method the soil moisture accounting loss method is chosen because it has been used for long term simulations and also it is consider more atmosphere, surface and ground zone model that has been used successfully in many studies throughout the US (USACE, 2003).

**Transform method**

Continuous hydrologic models account for the soil moisture balance in the catchment over a long term period. Different hydrologic physical processes such as: interception, surface depression storage, infiltration, soil storage, percolation, and groundwater storage should be considered in continuous hydrologic modeling. In this paper, the Hydrologic Modeling System (HMS) model was used for continuous hydrologic simulation of the Koga watershed

Runoff transformations convert excess precipitation on a sub-basin to direct runoff at the sub-basin outlet. Again, HEC-HMS allows runoff transformation determinations using lumped or linear distributed approaches. Similarly, the Clark's Unit Hydrograph model for direct runoff computation was chosen because of not only due to simplicity and minimum data requirements but also it gives a good performance than the other modules. In addition, it is suitable for conceptual models to transform rainfall to runoff process. The surface runoff calculations were performed using Clark Unit Hydrograph method which requires time of concentration to be computed from HEC GeoHMS for implementation.

The time of concentration is defined as the length of time the runoff spent from the furthest point till it reaches the out let. The time of concentration can be approximated from the relation. A sub-basin element conceptually represents infiltration, surface runoff, and subsurface processes interacting together. The actual infiltration calculations are performed by a loss method contained within the sub-basin. All of the possible loss methods in HEC-HMS conserve mass. That is, the sum of infiltration and precipitation left on the surface will always be equal to total incoming precipitation. The model calibration and validation performance evaluation equation is described below.

The Coefficient of Determination ($r^2$) is given as;

$$r^2 = \left( \frac{\sum_{i=1}^{n} (O_i - \bar{O})(P_i - \bar{P})}{\sqrt{\sum_{i=1}^{n} (O_i - \bar{O})^2} \sqrt{\sum_{i=1}^{n} (P_i - \bar{P})^2}} \right)^2$$

Where,

- $O_i$ = Observed flow
- $P_i$= Predicted flow
- $\bar{O}$ Long term mean observed flow
- $\bar{P}$= Long term mean predicted flow
- $r^2$= Coefficient of determination (0 to 1)

The Nash Sutcliffe efficiency (E) is given as;

$$E = 1 - \frac{\sum_{i=1}^{n} (O_i - P_i)^2}{\sum_{i=1}^{n} (O_i - \bar{O})^2}$$

Where,

- $O_i$ = Observed flow
- $P_i$= Predicted flow
- $\bar{O}$= Long term mean observed flow
- $E$= Nash Sutcliffe Efficiency (-∞ to 1)

Table 3. 18: SMA parameters

| Layers | Parameters (unit) |
|---|---|
| Canopy interception storage | ▪ Storage capacity (in); |
| Surface depression storages | ▪ Storage capacity (in); |
| | ▪ Soil infiltration max. rate (in/hr); |
| Soil profile storage | ▪ Storage capacity (in);<br>▪ Tension zone capacity (in); |
| | ▪ Percolation max. rate (in/hr); |
| Groundwater layer-1 storage | ▪ Storage capacity (in); |
| | ▪ Percolation max. rate (in/hr); |
| | ▪ Storage coefficient (hr); |
| Groundwater layer-2 storage | ▪ Storage capacity (in); |
| | ▪ Percolation max. rate (in/hr); |
| | ▪ Storage coefficient (hr); |

### 3.8.3. ARC GIS Software

The Geographical Information System, GIS is a system capable of capturing, storing, analyzing and displaying geographically referenced information. GIS is currently well known for its diverse applications both in the social and physical development of a society. In the water resources development it has vast use such as generating elevation contours using satellite data, geo-referencing maps with known reference coordinates, delineating catchment area of a specific point of interest (outlet), producing maps and so on. GIS works these and other functions integrated with different extensions. For such specific studies it can be used to extract cross-sectional data of stream and adjacent plains export to other models and also to prepare different flood maps after the necessary hydraulic analysis is conducted in other model and results have been imported. The Digital elevation model is changed to contour on Analysis tool using Surface changed to Contour map 20 meter interval shown below Figure 3.9.

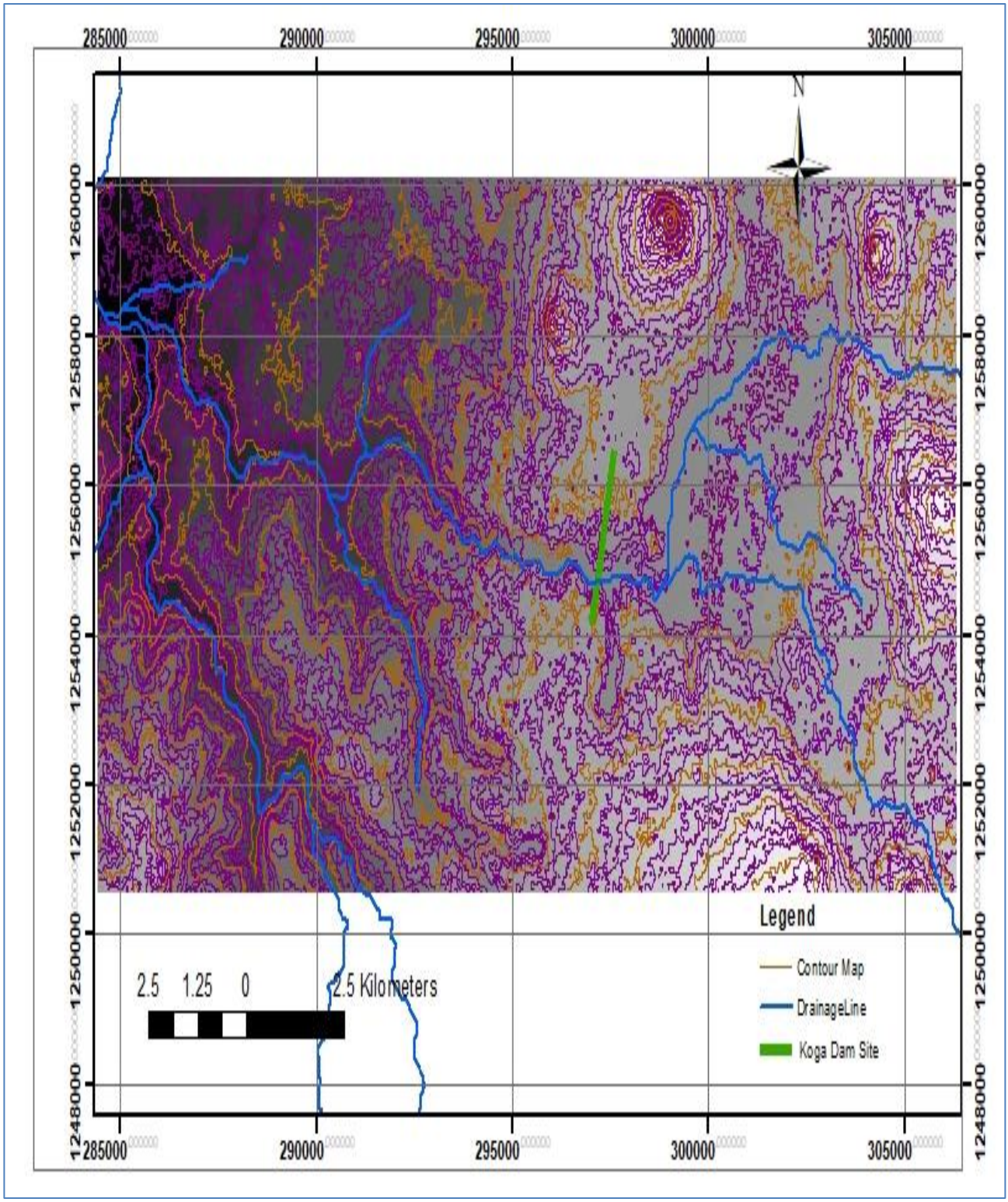



Figure 3. 9: Contour Map of the Study area generated from DEM.

### 3.8.4. HEC-GeoRAS

HEC-Geo RAS is an Arc GIS extension developed by the HEC. This model contains a set of tools specifically designed to process geospatial data to support hydraulic model development and analysis of water surface profile results. It assists in creating data sets in GIS to extract information essential for hydraulic modeling (Cameron T. Ackerman).

After steady or unsteady flow simulation, HEC-RAS results can be exported for processing in the GIS by Geo RAS. The user can read the HEC-RAS results into the HEC-Geo RAS and perform the flood inundation mapping (Brunner, 2006).

HEC-Geo RAS is an extension developed by the USACE for use with Arc GIS. It consists of a set of tools and procedures for extracting primarily topographic data within the GIS platform and for importing directly into a HEC-RAS geometric file. HEC-Geo RAS allows for a quick and seamless conversion of contour or DEM data into a cross-section format that can then be used by HEC-RAS to facilitate the calculation of water surface elevations (USAE HEC CPD-83, 2011).

#### 3.8.4.1. Geometric Data

A good starting point for estimating maximum cross section spacing are two empirically derived equations by Dr Danny Fread (Fread ,1993) and P.G. Samuels (Samuels, 1989). These two equations represent very different methods for coming up with spacing. Samuels' equation implies that smaller streams and steeper steams will require tighter cross section spacing. In general, Samuels' equation was derived for typical flood studies in which the modeler is developing a steady state model for typical floodplain study of the two year through 100 year events. For Dam break flood studies, Samuels' equation may be too strict in that it requires much tighter cross section spacing than needed. Samuels' equation is as follows:

$$\Delta X \leq \frac{0.15\,D}{S0} \quad \text{---------- 3. 18}$$

Where.

$\Delta X$= the cross section spacing distance (feet)

D =the average main channel bankfull depth (feet)

S0 = the bed slope (feet /feet)

Geometric data such as river route, banks, cross sections, and flow paths were extracted from DEM using HEC-Geo RAS and then these data were imported into HEC-RAS (see figure 3.10). In addition to these data, reach lengths between cross-sections, contraction and expansion coefficients, and other relevant data were also imported Figure 3.10. The river reach considered in this analysis starts just upstream of the Koga reservoirs to confluence of wetit Abay.

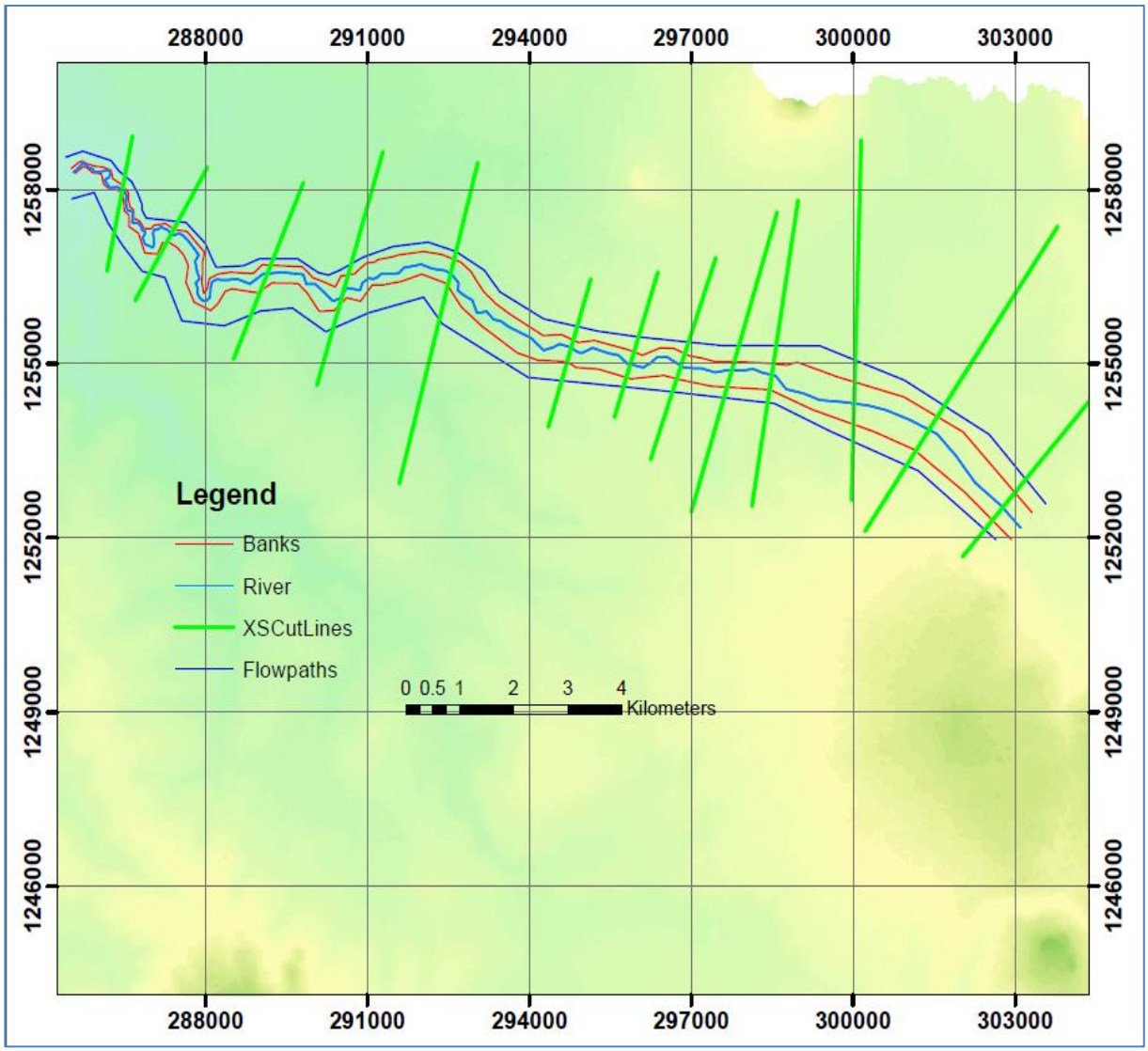



Figure 3. 10: HEC Geo RAS Preprocessing in Geometric data.

#### 3.8.4.2. Boundary and Initial Conditions

For unsteady flow analysis, upstream boundary conditions are typically flow hydrographs; design hydrograph of particular return period, or PMF hydrograph (for hydrologically induced failures), or a constant inflow which in this case is taken as base flow (for sunny day failure analyses). At the upstream end of Koga dam reservoir, PMF inflow hydrograph of the catchment from Koga dam. Downstream boundary conditions can be set to normal depth, a rating curve, a known water surface elevation, or critical depth. Here, the downstream boundary conditions are input as a normal depth with friction slope of 0.001. The use of this value as a downstream boundary condition is reasonable since the reach below the last cross section is very flat (downstream of confluence of Wetit Abay).

Initial conditions were set to as the base flow of the PMF i.e. 8.87 $m^3/s$ for Koga River dam inflow. The fact the dams are designed to handle the PMF event, it means that the dams would never get overtopped theoretically and thus would not get breached hydrologic ally. The PMF of Koga Dam estimation of a is going to be to 570 $m^3/s$ using PMP event occurs, the upstream Koka Dam would not be able to pass the PMF safely and thus breaches). On the other hand, there are three numbers of major tributaries that could counterbalance the attenuation significantly.

Therefore, in order to simulate hydrologically induced failure, the design PMF inflow hydrograph of the respective dams were scaled by 2 times so that the dams would get overtopped. The scaled PMF magnitude is the breach the Koga Dam.

### 3.8.5. Hydraulic Modeling with HEC-RAS

HEC-RAS 5.0.7 was used for the breach analysis and inundation modeling. This software is used to simulate a one-dimensional (1D) unsteady flow routing integrating complex channels and structures under dynamic hydrologic conditions. HEC-RAS has the capability of modeling dam breach events under a wide range of scenarios.

Basically, the software has four 1D river analysis components: steady flow water surface computations; unsteady flow simulation; sediment transport computations; and water quality analysis. HEC-RAS also has quite a number of options, such as mixed flow regime analysis, allowing analysis of both sub- and supercritical flow regimes in a single computer run, culvert

and bridge routines allowing for multiple openings of different types and sizes, quasi 2-D velocity distributions, and 3D visualization of the river channel system.

The stream flow profile follows the basic physical laws: principle of conservation of mass and principle of conservation of momentum. These laws are expressed mathematically and referred as continuity and momentum equations.

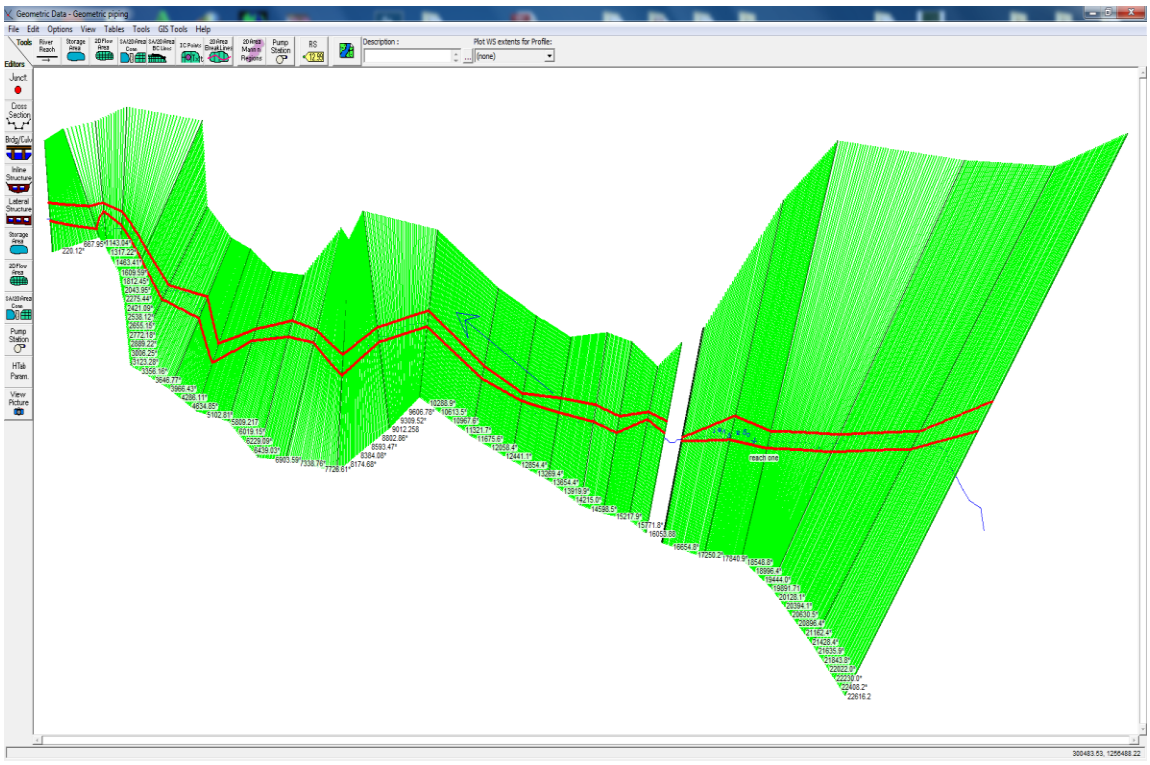


Figure 3. 11: Geometric Map of the River

**Steady flow water surface computation**: this component computes water-surface profiles and energy grade lines in 1-D for a steady and gradually-varied flow. It can handle a single reach, and full network of channels or streams. This component can model subcritical, supercritical, and mixed flow regimes' water surface profiles.

The flow computations are based on basic physical laws: principle of conservation of mass (continuity equation) and principle of conservation of momentum (momentum equation).Energy losses are evaluated by Manning's equation and contraction/expansion (coefficient multiplied by the change in velocity head). The momentum equation is utilized in situations where the water surface profile is rapidly varied.

**Unsteady Flow Simulation**: this component models 1D unsteady flow through a single or full network of channels or streams. The unsteady flow component was developed primarily for subcritical flow regime calculations.

Basic equations used in HEC-RAS algorithm to solve steady state water surface profiles are briefly presented below.

**Energy equation**

Water surface profiles are computed from one cross section to the next by solving the Energy equation with an iterative procedure called the standard step method. The Energy equation is written as;

$$Y_2 + Z_1 + \frac{\alpha_1 V_1}{2g} = Y_1 + Z_1 + \frac{\alpha_1 V_1}{2g} + he \text{----------} \quad (3.\ 19)$$

Where:

Y1, Y2 = depth of water at cross sections

Z1, Z2 = elevation of the main channel inverts

V1, V2 = average velocities (total discharge/total flow area)

α1, α2= velocity weighting coefficients

g = gravitational acceleration

he = energy head loss

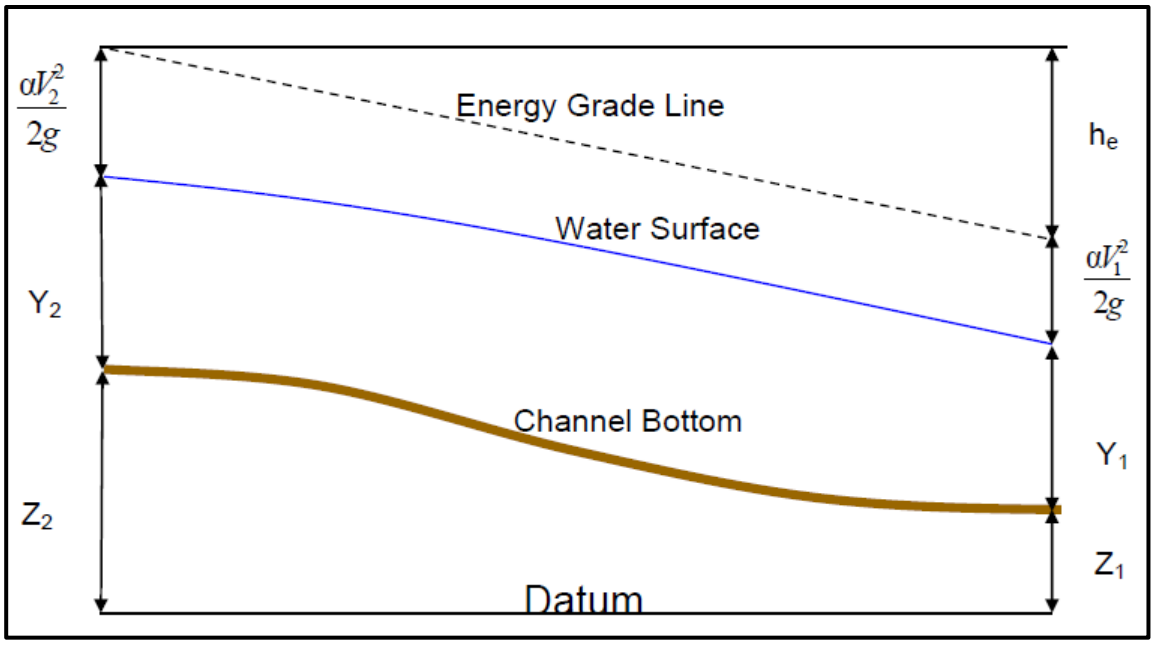



Figure 3. 12: Representation of Terms in the Energy Equation HEC-RAS Hydraulic reference manual

The energy head loss between two cross sections is a contribution of friction losses and contraction/expansion losses. The energy head loss is written as follows (Equation 3.21)

$$\mathbf{h_e = L\bar{S}_f + C\left|\frac{\alpha_2 V_2^{\,2}}{2g} - \frac{\alpha_1 V_1^{\,2}}{2g}\right|} \quad \text{---------- (3. 20)}$$

Where:

L= discharge weighted reach length

$\bar{S}_f$= representative friction slope between two sections

C= expansion or contraction loss coefficient

$V_1$, V2 = average velocity (m/s)

g = gravitational acceleration ($m/s^2$)

The weighted reach length, L, is calculated as follows (Equation 3.22):

$$\mathbf{L = \frac{L_{lob}Q_{lob} + L_{ch}\bar{Q}_{ch} + L_{rob}\bar{Q}_{rob}}{\bar{Q}_{lob} + \bar{Q}_{ch} + \bar{Q}_{rob}}} \quad \text{---------- (3. 21 )}$$

Where:

$L_{lob}$, $L_{ch}$,$L_{rob}$ = cross section reach lengths specified for flow in the left overbank, main channel, and right over bank, respectively

$\bar{Q}_{lob}, \bar{Q}_{ch}, \bar{Q}_{rob}$= arithmetic average of the flows between sections for the left overbank, main channel, and right over bank, respectively.

### 3.8.4.3. Manning's Roughness Coefficient

Selection of an appropriate value for manning's n is very significant to the accuracy of the computed water surface elevations. The value of manning's n is highly variable and depends on a number of factors including: surface roughness; vegetation; channel irregularities; channel alignment; scour and deposition; obstructions; size and shape of the channel; stage and discharge; seasonal changes; temperature, and suspended material and bed load. It's difficult to assign a specific representative friction slope value even for small areas. Especially when we come to natural channels it's possible to find a wide range of land use land cover types within small reaches. It is because of this fact that some dam breach analysis studies are focused on sensitivity analysis of the peak breaching flood upon increasing or decreasing the manning coefficient. Manning's n values were estimated as Chow's (1988).

Different values are added to no considering surface irregularities, variation in shape and size of channel cross-sections, channel obstructions, vegetation cover and flow conditions and meandering of the river to get a final 'n' representing the channel. Cowan's formula is given as;

$$\mathbf{n} = (\mathbf{n0} + \mathbf{n1} + \mathbf{n2} + \mathbf{n3} + \mathbf{n4})\ \mathbf{m5}$$

Proper values of no to n4 and m5 are selected from Table 3.20 and a value of 0.04 has been obtained using the above equation.

In these study, manning's n-value is selected based on catchment characteristics. To provide numerical stability to the hydraulic model Manning's n-values were based on published values for similar conditions, and on engineering judgment and experience with help of Koga dam design documents.



Figure 3. 13: The river cross section manning roughness property

Table 3. 19: Values for the Computation of the Roughness Coefficient, n (CHOW, 1988)

| | Channel conditions | | Values |
|---|---|---|---|
| materials involved | Earth | no | 0.020 |
| | Rock cut | | 0.025 |
| | Fine gravel | | 0.024 |
| | Coarse gravel | | 0.028 |
| Degree of irregularity | Smoth | n1 | 0.000 |
| | Minor | | 0.005 |
| | Moderate | | 0.010 |
| | Severe | | 0.020 |
| Variations of channel cross section | Gradual | n2 | 0.000 |
| | Alternating occasionally | | 0.005 |
| | Alternating frequently | | 0.01-0.005 |
| Relative effect of Obstruction | Negligible | n3 | 0.000 |
| | Minor | | 0.01-0.015 |
| | Appreciable | | 0.02-0.03 |
| | Severe | | 0.04-0.060 |
| Vegetation | Low | n4 | 0.005-0.01 |
| | Medium | | 0.01-0.025 |
| | High | | 0.025-0.05 |
| | Very high | | 0.05-0.1 |
| Degree of meandering | Minor | m5 | 1.000 |
| | Appreciable | | 1.150 |
| | Severe | | 1.300 |

Table 3. 20: Computation of manning's n for Koga River

| | Channel conditions | | Values |
|---|---|---|---|
| Materials involved | Earth | no | 0.020 |
| Degree of irregularity | Minor | n1 | 0.005 |
| Varations of channel cross section | Alternating occasionally | n2 | 0.005 |
| Relative effect of Obstruction | Negligible | n3 | 0.000 |
| Vegetation | Medium | n4 | 0.011 |
| Degree of meandering | Minor | m5 | 1.000 |
| Overall manning's n | | | 0.04 |

The computed manning's coefficient is selected as above also the computed value in the design document is almost similar for further analysis the result is selected.

Table 3. 21:Manning's Roughness Coefficient (CHOW, 1988)

| Type of channel and descrption | Minimum | Normal | Maximum |
|---|---|---|---|
| Flood plains | | | |
| | A pasture ,no brush | | |
| 1 short grass | 0.025 | 0.03 | 0.035 |
| 2 High grass | 0.03 | 0.035 | 0.05 |
| | b, Cultivated areas | | |
| 1 No crop | 0.02 | 0.03 | 0.04 |
| 2. Mature row crops | 0.025 | 0.035 | 0.045 |
| 3.mature field crps | 0.03 | 0.04 | 0.05 |
| | c Brush | | |
| 1. scatered brush ,heavy weeds | 0.035 | 0.05 | 0.07 |
| 2.Light brush and trees in winter | 0.035 | 0.05 | 0.06 |
| 3. Light brush and trees in summer | 0.04 | 0.06 | 0.08 |
| 4. Medium to dense brush in winter | 0.045 | 0.07 | 0.11 |
| 5. Medium to brush in summer | 0.07 | 0.1 | 0.16 |

The cross sectional flow has to be subdivided into units of uniform velocity distribution then the total conveyance and velocity coefficient for each unit can then be calculated. In HEC-RAS, the flow in the overbank areas is subdivided using the input cross section Manning's value break points (i.e. locations where 'n' values change) as the basis for subdivision see figure 3.15 below. Then, conveyance is estimated within each subdivision using the following form of Manning's equation (Equation 3.23 and 3.24): The values of manning's n values used for the flood plain is 0.08 and 0.04 for the main river channel.

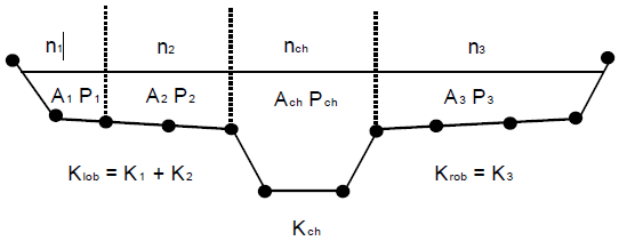



Figure 3. 14: Flow sub-division at a given cross-section in HEC-RAS Hydraulic reference manual

$Q = K S_f^{½}$ ---------- (3. 22)

Where:

$K = 1/n\ A\ R^{2/3}$ ---------- **(** 3. 23)

K = Conveyance for subdivision

n = Manning's roughness coefficient for subdivision

A = flow area for subdivision ($m^2$)

R = hydraulic radius for subdivision (m)

Q = discharge for the subdivision ($m^3/s$)

The velocity coefficient α is computed using Equation (3.26):

$$\alpha = \frac{(A_t)^2\left[\frac{K_{lob}^3}{A_{lob}^2}+\frac{K_{ch}^3}{A_{ch}^2}+\frac{K_{rob}^3}{A_{rob}^2}\right]}{K_t^3}$$ ---------- **(** 3. 24)

$A_t$ = total flow area of cross section

$A_{lob}$, $A_{ch}$, $A_{rob}$ = flow areas of left overbank, main channel and right over bank, respectively

$K_t$ = total conveyance of cross section (sum of left overbank, main channel and right overbank conveyances)

$K_{lob}$, $K_{ch}$, $K_{rob}$= Conveyance of left overbank, main channel and right over bank, respectively.

The HEC-RAS program sums up all the incremental conveyances in the overbanks to get a conveyance for the left over bank and the right overbank. The main channel conveyance is normally computed as a single conveyance element. The total conveyance for the cross section is obtained by summing the three subdivision conveyances (left, channel, and right).

Contraction and expansion losses in HEC-RAS are evaluated by using Equation (3.25):

$$h_{ce} = C\left|\frac{\alpha_2 V_2^{\,2}}{2g} - \frac{\alpha_1 V_1^{\,2}}{2g}\right|$$ ---------- **(**3. 25)

Where:

C = the contraction or expansion coefficient,

$V_1$, $V_2$ = average velocity (m/s)

HEC-RAS assumes a contraction whenever the velocity head downstream is greater than the velocity head upstream. Similarly, whenever the velocity head downstream is less than the velocity head upstream expansion loss is assumed (HEC RAS, 2016 manual).

## 3.9. Routing the Inflow Flood through the Reservoir

Dam breach analysis involves routing of the flood hydrograph, in this case the PMF, through the reservoir. Basically, there are two approaches to undertake the routing: fully dynamic routing and level pool routing. HEC-RAS offers both options.

In fully dynamic routing with HEC-RAS, the reservoir pool area is modeled as cross sections upstream of the dam and inflow is applied at the upstream end cross-section of the reservoir (see Figure 3.16.).Various literatures reported that this approach is the more accurate than that of level pool routing. But, it requires reservoir's bathymetry data (or this can be alternatively extracted from high resolution DEM) at frequent intervals for accurately representing stage-storage characteristics and, routing using this method can potentially cause instability in the HEC-RAS model (USAE HEC TD-39, 2014).

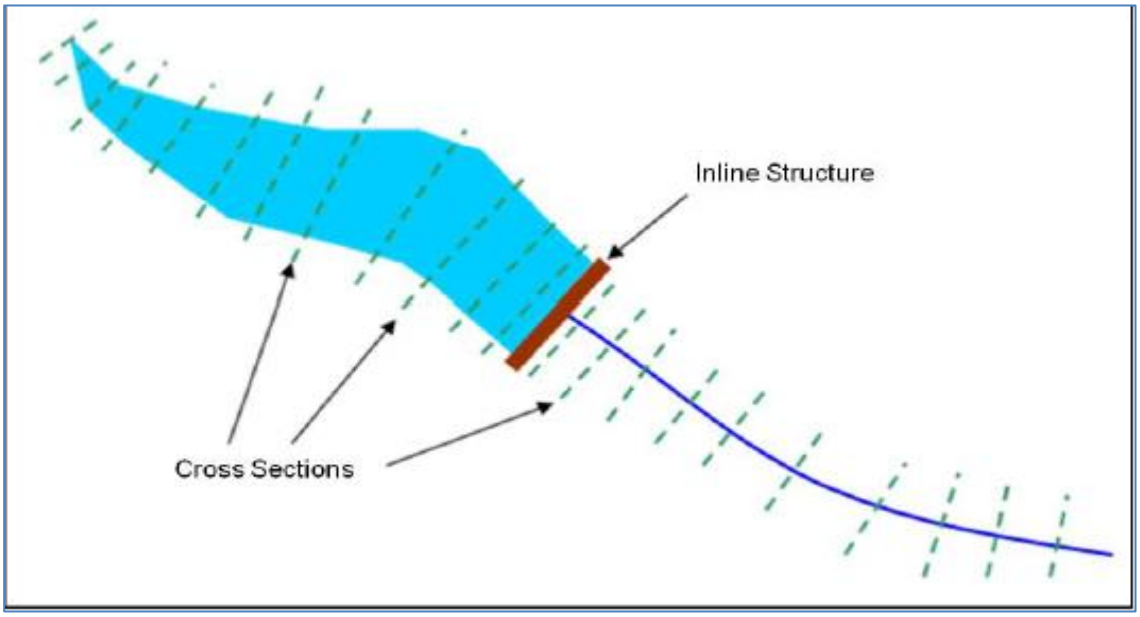



Figure 3. 15: Cross section for fully dynamic routing through a reservoir (Source: Using HEC-RAS for Dam Break Studies, TD-39, USACE HEC, 2014)

The HEC-RAS is modeling approach is by representing the reservoir pool area as a storage element. Here, the stage-discharge relationship is required, and the design inflow hydrograph (in this case the PMF) is an input to the storage element. The storage element is connected to the downstream river reach through two river cross sections located in the reservoir pool area (see Figure 3.17.). The first cross section is tied to the storage element such that the water

surface elevation in both the cross section and the reservoir (or the storage element) is the same during HEC-RAS computations. The second cross section is tied to the dam (i.e. modeled as inline structure in HEC-RAS) boundary condition and it cannot be the first cross section of the reach (USAE HEC TD-39, 2014). This approach is less data intensive and results a more stable HEC-RAS model.

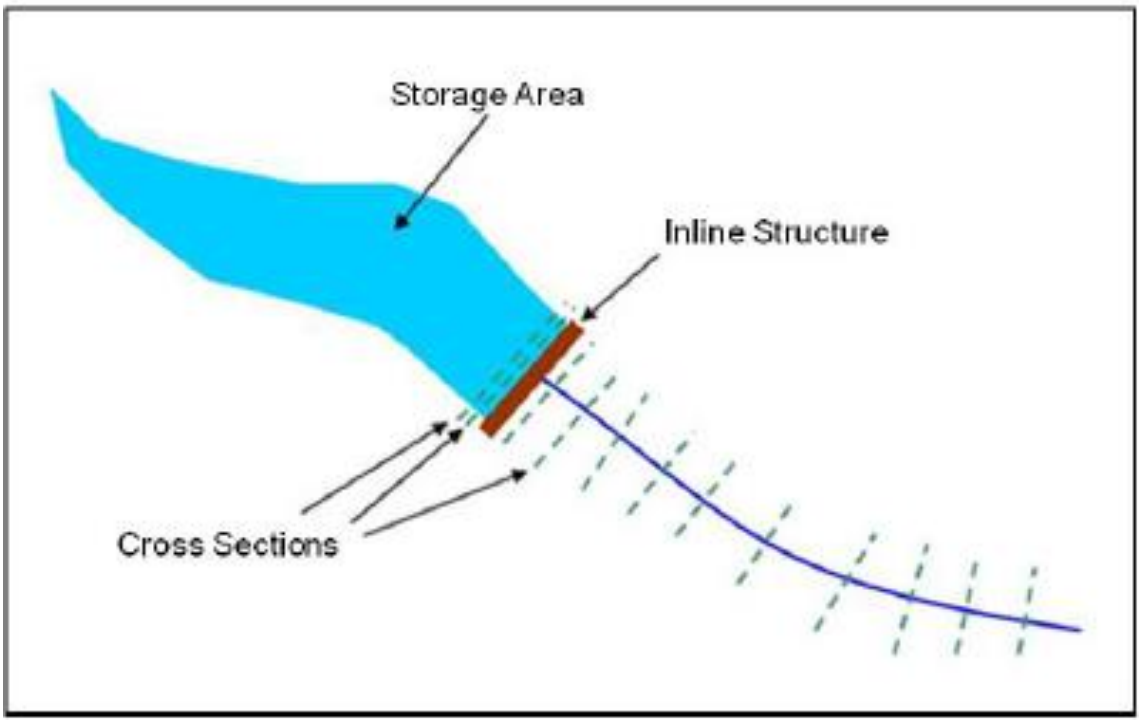



Figure 3. 16: HEC-RAS modeling approach for level pool routing (Source: Using HEC-RAS for Dam Break Studies, TD-39, USACE HEC, 2014)

The dam break analysis was undertaken following the fully dynamic reservoir routing approach as this approach, as noted from various literatures, offers more accurate results.

## 3.10. Dam Breach-Parameters and Breach Modeling

For realistic modeling of inundation map for a dam breach event, the breach shape, size, location, and timing must be estimated for the considered type of dam and its modes of failures. Koga dam is a earth/rock fill dam type with central clay-core material, and the failure modes considered for analysis are piping (i.e. under sunny day condition) and overtopping

failure(i.e. under hydrological induced condition). The breach modeling is to be conducted in both scenario that is Dam breach failure in piping and overtopping.

### 3.10.1. Breach Parameters

The breach development and breach outflow hydrograph modeling in HEC-RAS demands parameters which define breach geometry such as breach shape, average breach width ($B_{avg}$), time to full breach development ($t_f$), pool elevation at time of failure, weir and orifice coefficients, and breach side slope (see Figure 3.18). A trapezoidal breach which progresses with time sinusoidal was assumed, and the location of the breach was assumed at the centerline stations of the dam.

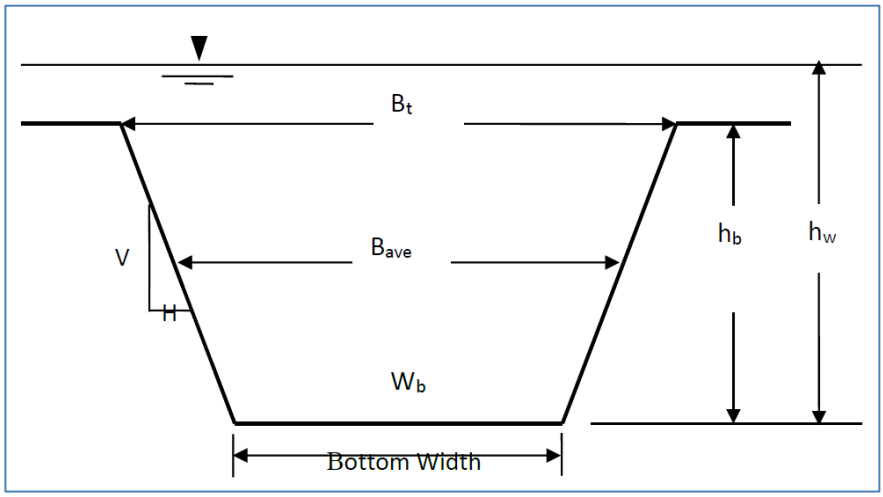



Figure 3. 17: Description of Breach parameters HEC RAS hydraulic references manual 2016.

**The important parameters for dam break analysis are:**

**Reservoir volume when breaching commences (Vw):** this is reservoir volume at the time of failure. Reservoir water surface elevation when breaching commences: this is normally taken as the top of the dam or a few meters above the MWL for overtopping failure cases.

**Breach depth ($h_b$):** this is measured from the invert level of the breach to the dam crest. The assumption here is breach is formed to the bed level of the dam or its foundation as the foundation is more resistant to erosion. Thereby $h_b$ is taken as the dam height measured from the river bed level.

**Average Breach width ($B_{avg}$):** this is the final width of the breach. The breach width has an impact on the peak discharge and downstream inundation water level.

**Breach formation time ($t_f$):** this is the time from the commencement of the breach until it attains its final form.

There are various empirical equations available for estimating breach parameters on the basis of dam and reservoir characteristics i.e. dam height, and reservoir's volume and other physical characteristics. A number of approaches and empirical equations were put to test for this analysis and the following equations were used widely for various dam breach modeling studies: Froehlich (2008), MacDonald and Langridge-Monopolis (1984), and Von Thun and Gillette (1990).

**Froehlich (2008):** Froehlich analyzed a total of 74 earthen, zoned earthen, earthen with a clay core wall, and rock fill dams' data sets and undertook regression analysis. Following these, he derived equations for the average breach width and breach formation time as presented in Equation (3.26) and (3.27):

$$\boldsymbol{B_{avg} = 0.27 K_o V_w^{0.32} h_b^{0.04}} \quad \text{---------- (3. 26)}$$

$$\boldsymbol{t_f = 63.2\sqrt{\frac{V_w}{g h_b^2}}} \text{---------- (3. 27)}$$

Where:

$B_{avg}$= average breach width (meters)
$K_o$= constant (1.3 for overtopping failures, 1.0 for piping)
$V_w$= reservoir volume at the time of failure ($m^3$)
$h_b$= height of the final breach or dam height from river bed level (i.e. which is taken as dam height) (meters)
$t_f$= breach formation time (seconds)

Froehlich states the average side slopes for overtopping failures as 1.0 H: 1Vand 0.7H: 1V for piping and seepage failure.

**MacDonald and Langridge–Monopolis (1984):** MacDonald and Langridge-Monopolis analyzed a total of 42 earthen, zoned earthen, earthen with a clay core wall, and rock fill

dams' data sets to develop "Breach Formation Factor". Breach Formation Factor is basically a product of the height of water above the dam crest and the volume of water leaving the dam. Then, they related this factor to the volume of embankment material eroded (USAE HEC TD-39, 2014).

Following are equations for volume of eroded material and breach formation time:

For earth fill dams:

$$\boldsymbol{V_{eroded} = 0.0261(V_{out} * h_w)^{0.769}} \text{ ---------- (3. 28)}$$

$$\boldsymbol{t_f = 0.0179(V_{erroded})^{0.364}} \text{ ---------- (3. 29)}$$

For earth fill with clay core or rock fill dams:

$$\mathbf{V_{eroded} = 0.00348(V_{out} * h_w)^{0.852}} \text{ ---------- (3. 30)}$$

Where:

$V_{eroded}$ = volume of eroded material from the dam embankment ($m^3$)

$V_{out}$ = volume of water leaving through the breach ($m^3$) i.e. storage volume at time of breach plus volume of inflow after breach begins, minus any spillway and gate flow after breach begins.

$h_w$ = height of water above the bottom of the breach (meters).

$t_f$ = breach formation time (hours).

$V_{out}$ is not accurately known prior to performing the breach analysis; thus, the first estimate is to set it as the volume of water in the reservoir when breach starts. With this first estimate analysis can be run and one can re-evaluate the initial estimate then make better estimates of the actual volume of water passing through the breach and redo the breach analysis. Basically, this is an iterative process where calculations continue till the estimated volume at the start of each calculation and the end of the analysis converge to some degree.

Here, breach shape is assumed trapezoidal with side slopes of 0.5H: 1V. The bottom width of the breach is then estimated with the following equation (State of Washington, 1992):

$$\boldsymbol{Wb = \frac{V_{eroded} - h_b^2(CZ_b + hbZbZ3/3)}{h_b(C + h_bZ_{3/2})}}$$ ---------- (3. 31)

**Where:**

$W_b$ = bottom width of the breach (meters)

$h_b$= height of the final breach or dam height from river bed level (i.e. which is taken as dam height) (meters)

C = crest width of the top of dam (meters)

$Z_3 = Z_1 + Z_2$

$Z_1$ = average slope ($Z_1$:1) of the upstream face of dam

$Z_2$ = average slope ($Z_2$:1) of the downstream face of dam

$Z_b$ = side slopes of the breach ($Z_b$: 1), 0.5 for the MacDonald method

**Von Thun and Gillette (1990):** Von Thun and Gillette utilized 57 dams from the Froehlich (1987) paper and the MacDonald and Langridge - Monopolis (1984) papers to derive their methodology and equations. With this, the equation for average breach width is presented as follows:

$$\boldsymbol{B_{avg} = 2.5h_w + C_b}$$ ---------- (3. 32)

Where:

$B_{avg}$= average breach width (meters)

$h_w$= height of water above the bottom of the breach (meters)

$C_b$= coefficient which is a function of reservoir size (see table 3.23 below)

Table 3. 22: Cb values

| **Reservoir size (Mm3)** | **Cb** |
|---|---|
| < 1.23 | 6.1 |
| 1.23-6.17 | 18.3 |
| 6.17-12.3 | 42.7 |
| >12.3 | 54.9 |

Here, breach shape is assumed trapezoidal with side slopes of 1H: 1V, except for dams with cohesive soils, where the method states side slops here should be between 1H: 2V to H: 3V more suitable.

As for breach formation time, Von Thun and Gillette used two sets of equations. The first set is only a function of water depth above the breach bottom, and the second set is a function of water depth above breach bottom and average width of the breach.

The first set of equations shows breach development time as a function of water depth above the breach bottom:

$\boldsymbol{t_f = 0.02h_w + 0.25}$ (Erosion resistant)---------- (3. 33)

$\boldsymbol{t_f = 0.015h_w}$ (Easily erodible)---------- (3. 34)

Where:

$t_f$= breach formation time (hours)

hw=depth of water above the bottom of the breach (m)

The second set shows $t_f$ as a function of water depth ($h_w$) above the bottom of the breach and average breach width ($B_{avg}$).

$\boldsymbol{t_f = \frac{B_{avg}}{4h_w}}$ (Erosion resistant)---------- (3. 35)

$\boldsymbol{t_f = \frac{B_{avg}}{4h_w+61}}$ (Easily erodible)---------- (3. 36)

With these, the breach parameters for Koga Dam were estimated and the parameters are presented in result part below.

### 3.10.2. Modeling the Rivers and Structures in HEC-RAS

In HEC-RAS, a dam is modeled as an inline structure. The cross sectional data corresponding to the dams extracted from DEM are imported to HEC-RAS as inline structure. Then, the dam embankment and spillway crest data were provided using inline structure weir station elevation editor, and breach parameters were estimated using the built-in parameter calculator in HEC-RAS for the selected method.

In the inline structure data window, breach parameters can be added using the breach plan data editor. Here, the trigger breach elevation was set at dam crest elevation in case of overtopping failure and at Normal Water Level for piping failure. Moreover; the breach progression with time was also defined using this same editor under breach progression menu. For the dam, sinusoidal breach progression was assumed (Figure 3.19).

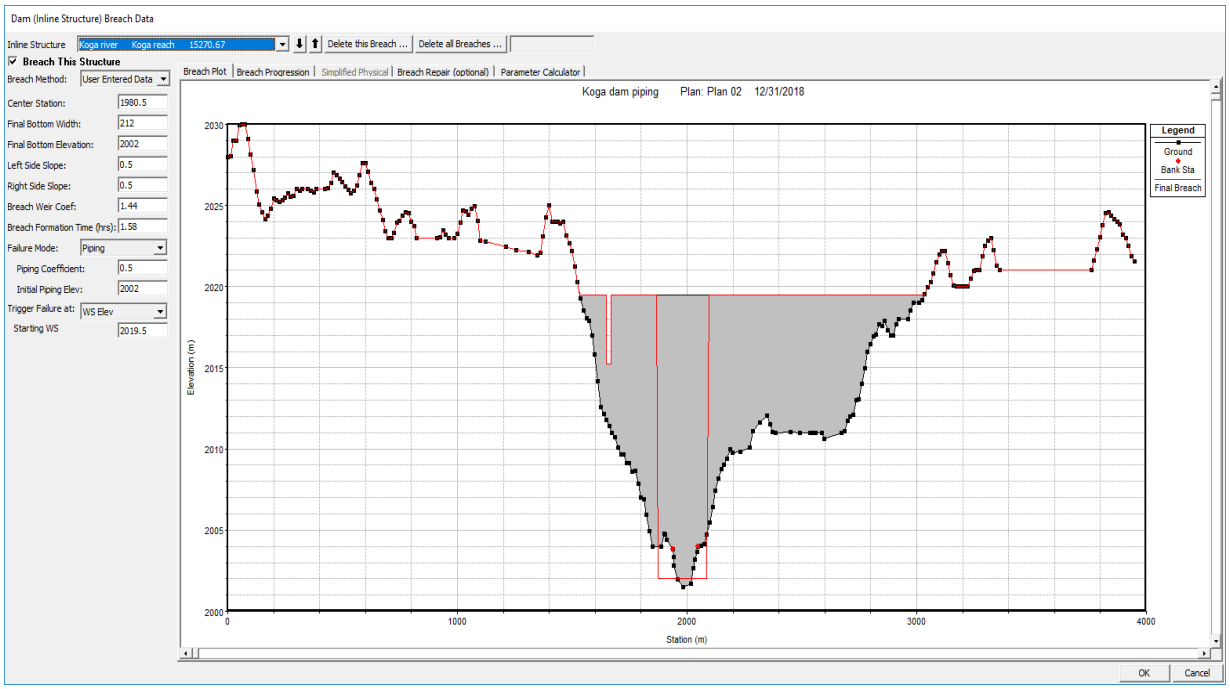



Figure 3. 18: Koga dam breach geometry according to Froehlich (2008)

## 3.11. Flood Inundation and Hazard Mapping

After the hydraulic simulations were conducted, the resulting flood hydrograph for the maximum water surface was routed through the downstream plain. The extent at which the flood area extends was mapped using a digital terrain model. The flood severity grid represents the combined effect of depth and velocity, most often communicated in categories of Low, Medium, High, Very High and Extreme Hazard. Studies have been performed in multiple countries to categorize the depth x velocity result into various flood hazard or flood severity classifications.

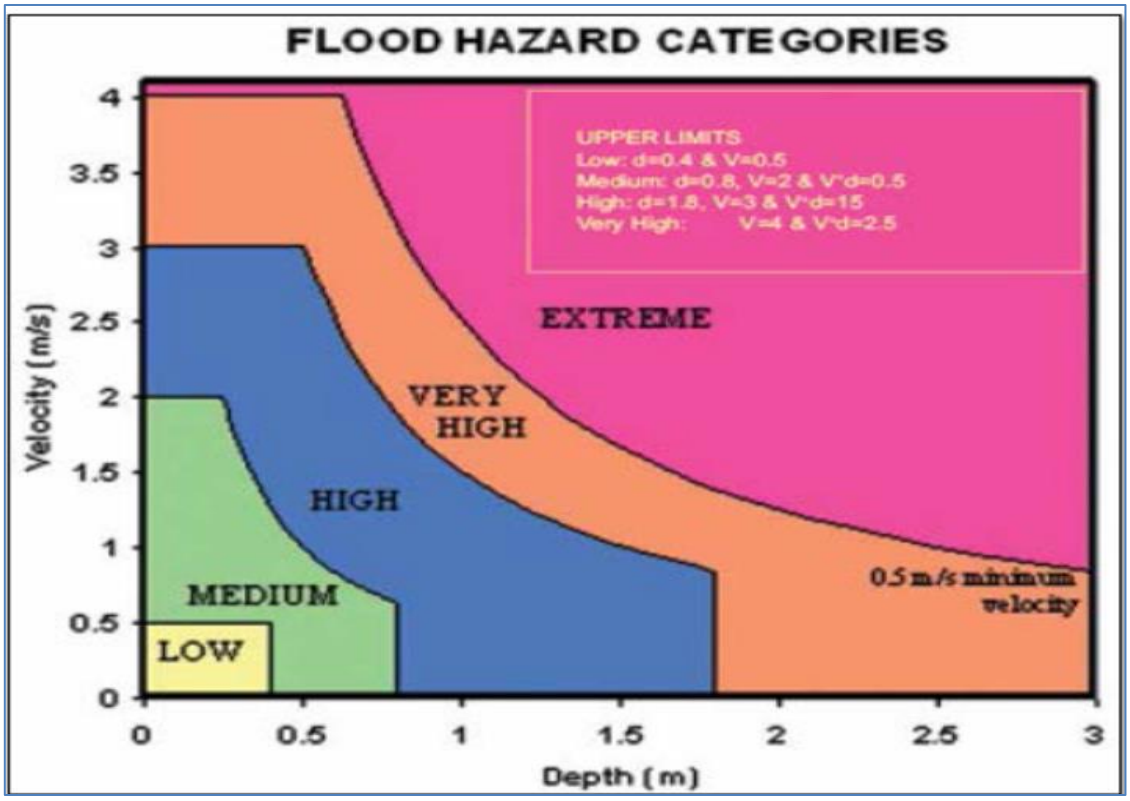



Figure 3. 19: Flood Hazard categories

To produce a flood severity grid that exactly matches the categorization shown in Figure 3.20, additional rules would need to be applied when calculating the depth * velocity product, to take into account the depth and velocity upper limits of each category. Additionally, the flood severity thresholds are different depending on whether they were would considered related to the impact on humans, vehicles, or buildings. As a simplified approach, the following depth * velocity categories can be applied when symbolizing the results of the dataset (see Table3.24). However, other categorizations of this data may be used where desired, and showed to encourage customizing the symbolization ranges shown in Table 3.24 if doing so would better communicate the hazard.

Table 3. 23: Simplified Flood Depth and Velocity Severity Grid Symbolization Categories

| Flood severity category | Depth*velocity range ($m^2$/sec) |
|---|---|
| Low | <0.2 |
| Medium | 0.2-0.5 |
| High | 0.5-1.5 |
| Very High | 1.5-2.5 |
| Extreme | >2.5 |

# 4. RESULTS AND DISCUSSIONS

## 4.1. Double Mass Curve Analysis Result for Homogeneity test

Double mass analysis is commonly used to data analysis approach for investigating the behavior of records made of hydrological or meteorological data at a number of locations. It is used to determine whether there is a need for corrections to the data to account for changes in data collection procedures or other local conditions and analysis for checking consistency of data.

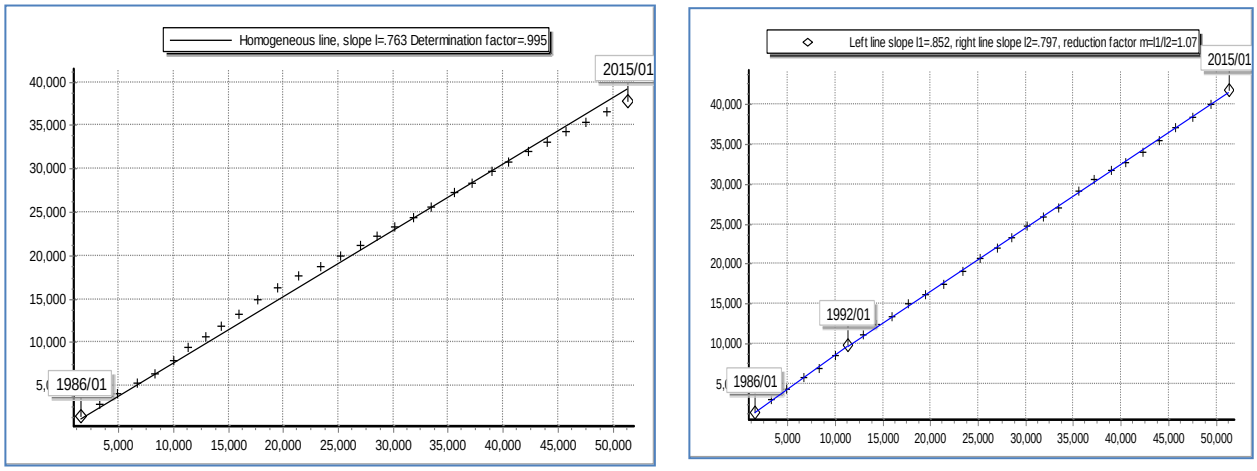



Figure 4. 1: Double mass plot of Meshenti versus other stations: DM plot of Adet versus other stations

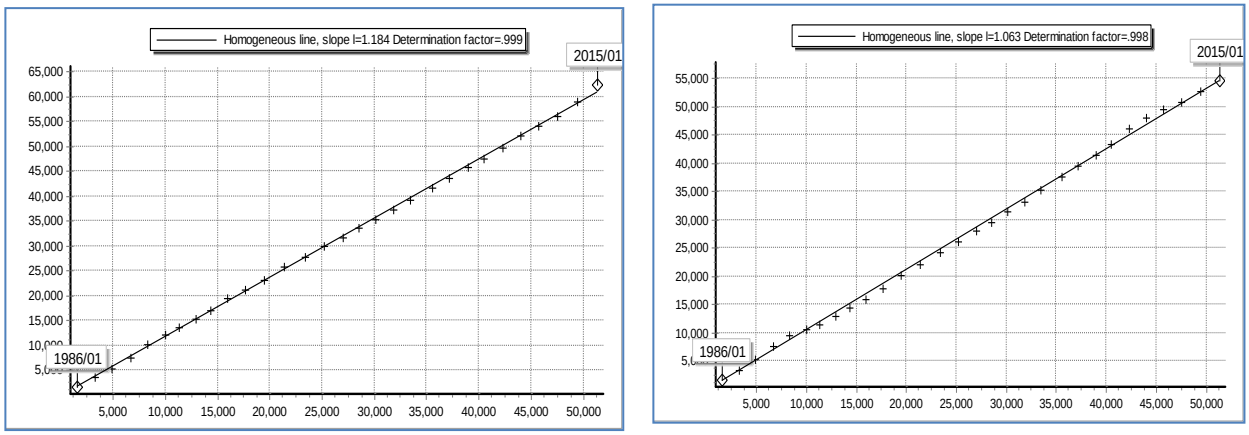



Figure 4. 2: Double mass plot of Tilli versus other stations: DM Sekela versus other stations.

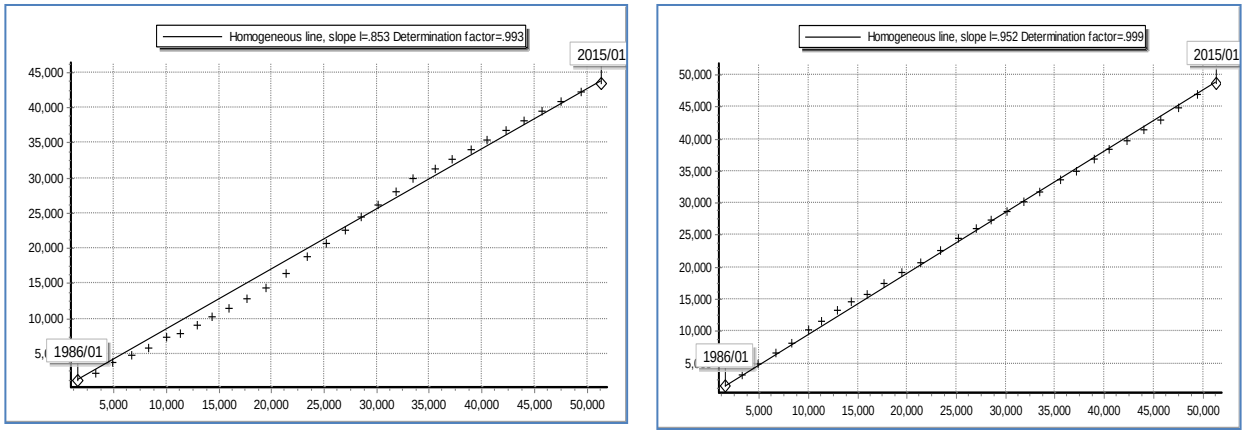



Figure 4. 3: Double mass plot of Finotselam versus other Stations. DM plot of Dangela versus other stations.

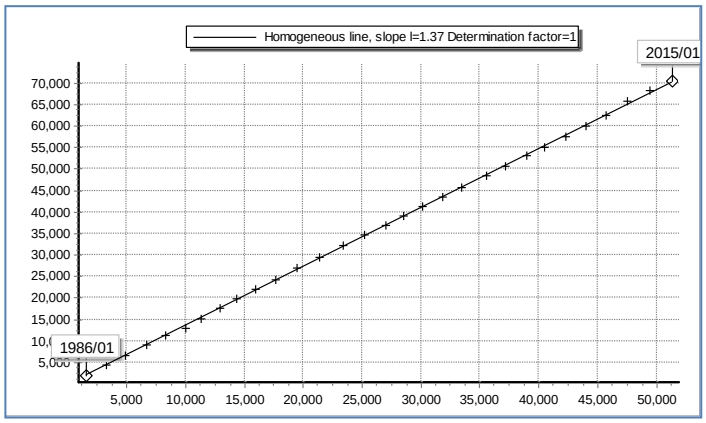



Figure 4. 4: Double mass plot of Enjebara versus other stations.

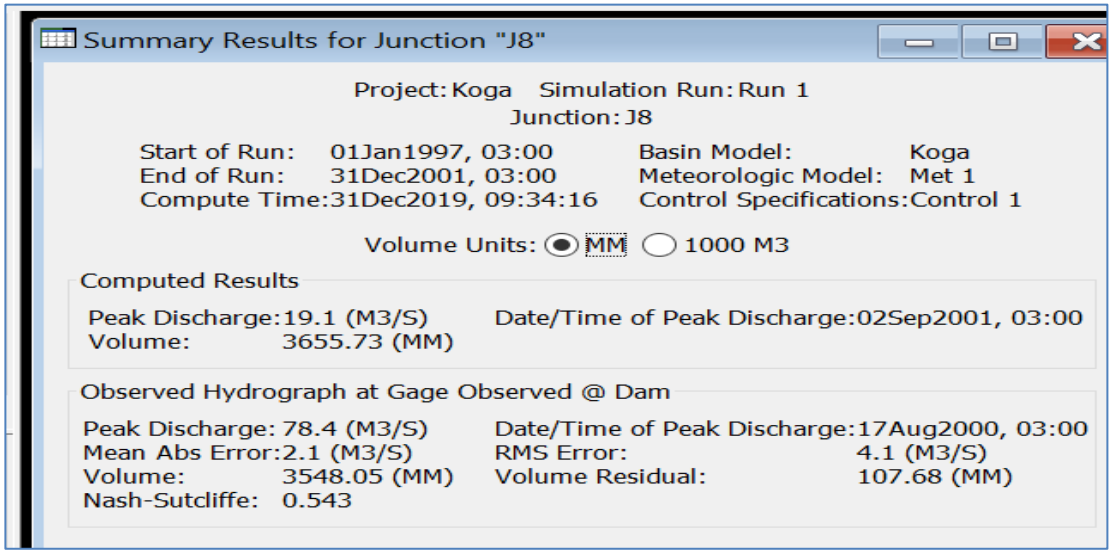
## 4.2. Calibration and Validation of HEC HMS Model

After initial model parameters were estimated, final model parameters were obtained through both manual and automatic optimization process. Some of the initial/starting physical model parameters including the catchment area, length and geometry of the reaches, the time of concentration that could be estimated from the geographic information of the basin, were derived from the 12.5m DEM of the basin using HEC GeoHMS. The model was calibrated using the observed flow records of Koga River at Koga dam upstream from 1996-2001 and validated using the 2002-2003 flow records.

For model performance evaluation, Nash Sutcliffe Efficiency (E) and coefficient of determination ($r^2$) were used. Coefficient of determination ($r^2$) measures the combined

dispersion against the single dispersion of the observed and predicted series. The value ranges between 0 and 1 which describes how much of the observed dispersion is explained by the prediction. A value of 0 suggests no correlation at all whereas a value of 1 indicates the observed dispersion is equal to the predicted dispersion. The fact that $r^2$ measures only dispersion makes it unreliable for a model which over/under estimates systematically. Such models could still show high $r^2$. Therefore, it should not be used alone. Nash Sutcliffe efficiency (E), on the other hand, measures absolute squared differences between predicted and simulated series. The value of E varies from 1 (perfect fit) to -∞. Efficiency lower than 0 means the mean of the observed series would have been a better estimate than the model.

The model performance based on these criterion was acceptable for daily simulations and very good for monthly average predictions with a Nash-Sutcliffe efficiency (E) of 0.53 (0.86 for monthly simulation) and coefficient of determination ($r^2$) of 0.7334 (0.92 for monthly simulations) during calibration and E=0.62 (0.89 for monthly simulations) and $r^2$=0.63 (0.9 for monthly simulations) during validation time. These figures are fairly acceptable and therefore the output of the model is a better choice to represent the catchment response and estimate the design variables at the required locations than the flow series available at Koga station.



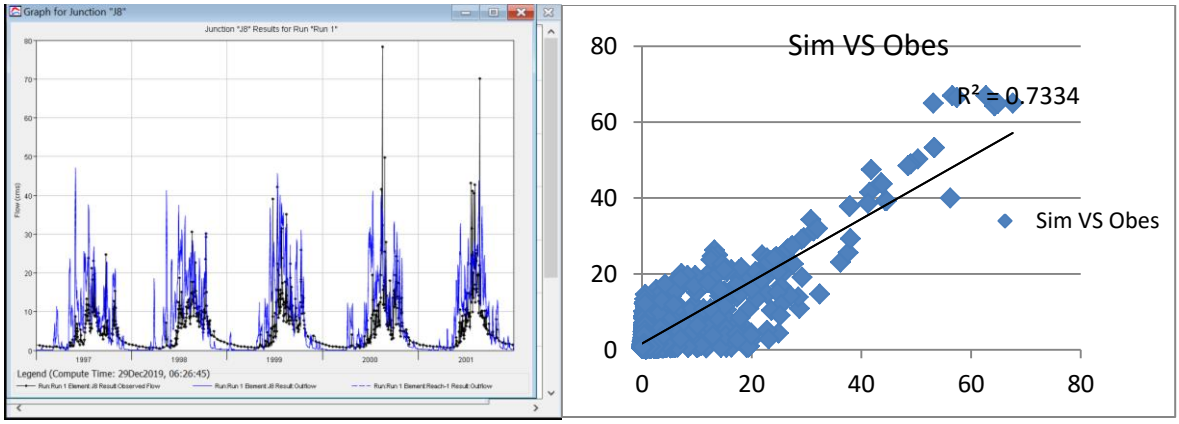



Figure 4. 5: HEC HMS Calibration observed vs simulation result

## 4.3. Probable maximum flood of Koga dam

### 4.3.1. Statically estimated using Hershfield method

Hydrology study was conducted to quantify the probable maximum flood that may enter the reservoir. A PMF of Koga Dam was with peak discharge of about 570 $m^3/s$ was computed has been obtained. This PMF can estimated by areal average rainfall was used in computing the PMP in this study while an annual maximum data from a station on the vicinity of the catchment. The approach followed here is more logical as annual maximum of daily rainfall over the catchment better represents the flood generated from all over the catchment area and flowing into the reservoir.

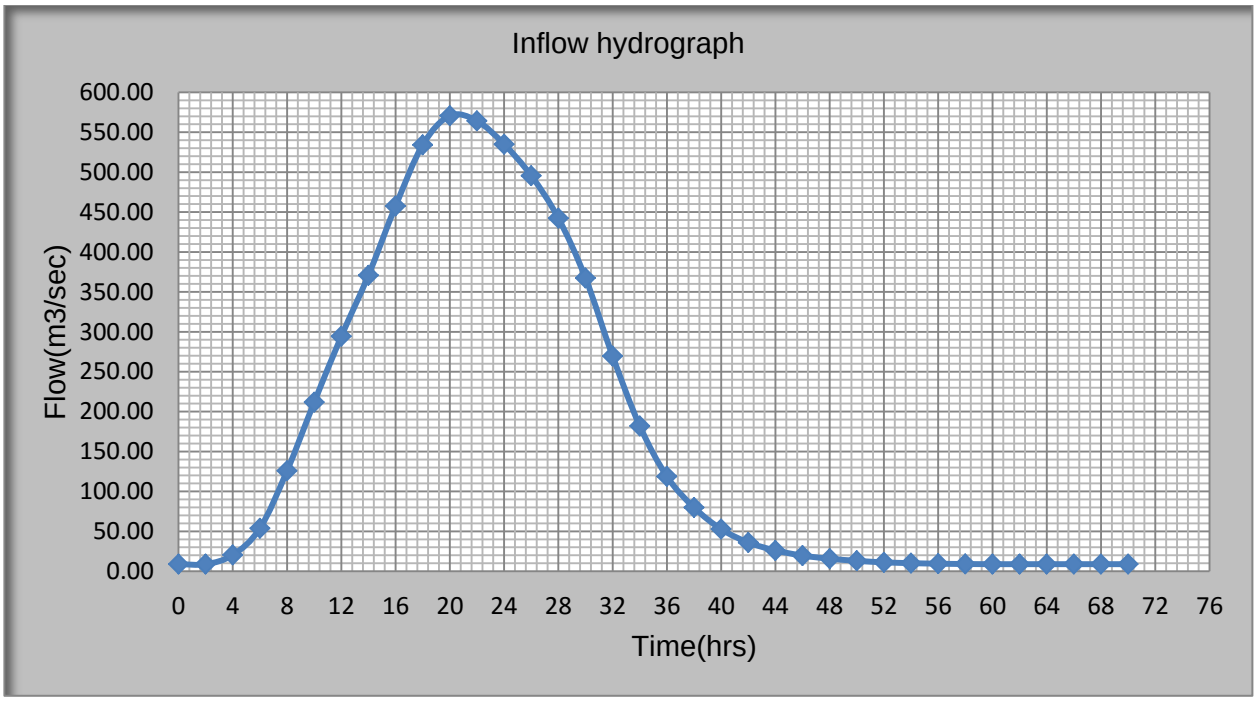



Figure 4. 6: PMF Hydrograph of Koga Dam by CSC Method

Table 4. 1: PMF of Koga Dam

| Time(hrs) | **Inflow (cms)** | Time(hrs) | **Inflow (cms)** |
|---|---|---|---|
| 0 | 8.87 | 32 | 269.51 |
| 2 | 8.87 | 34 | 181.97 |
| 4 | 20.39 | 44 | 118.76 |
| 6 | 53.77 | 46 | 79.87 |
| 8 | 125.86 | 48 | 52.80 |
| 10 | 211.71 | 50 | 36.05 |
| 12 | 294.32 | 52 | 26.07 |
| 14 | 370.83 | 54 | 19.61 |
| 16 | 457.57 | 56 | 15.72 |
| 18 | 534.19 | 58 | 13.08 |
| 20 | 570.69 | 60 | 11.17 |
| 22 | 564.15 | 62 | 10.15 |
| 24 | 534.96 | 64 | 9.47 |
| 26 | 495.53 | 66 | 9.08 |
| 28 | 442.30 | 68 | 8.87 |
| 30 | 367.34 | 70 | 8.87 |

### 4.3.2. PMF estimated by HEC HMS model

According to Hershfield method, the 24h PMP for the catchment was computed to be 306mm. This amount of precipitation was converted in to flood using the HEC-HMS rainfall-runoff model calibrated for the catchment. The corresponding PMF for the study area was found to be 537$m^3$/s at Koga dam site shown Figure below. The study was focused on extreme events due to that Herished field method was the selected for the analysis.

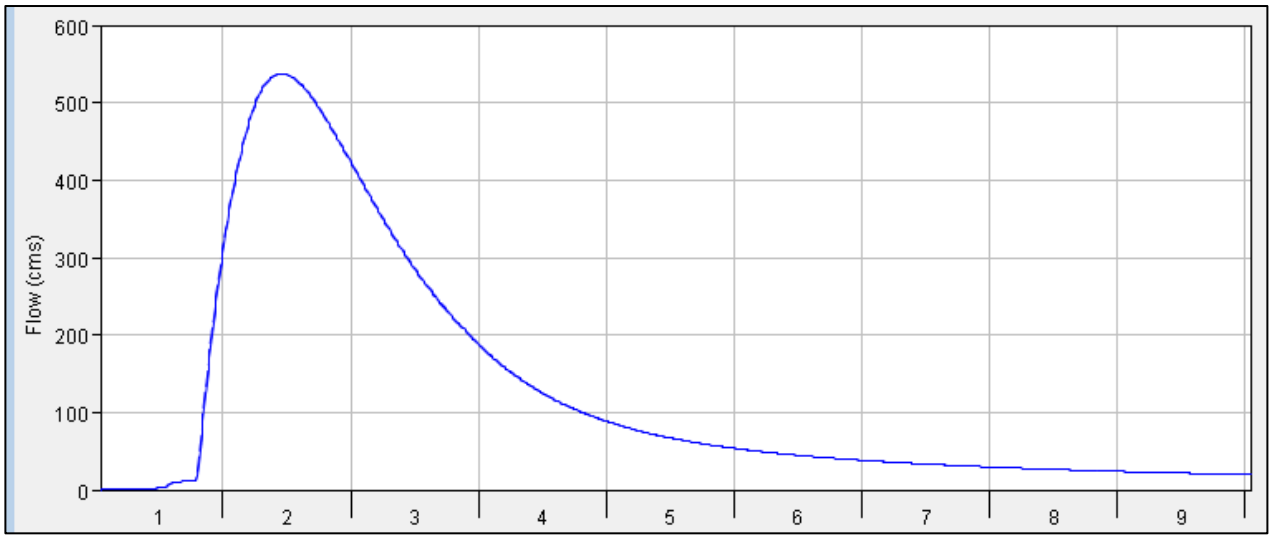



Figure 4. 7: Using HEC HMS estimated PMF

## 4.4. Dam Breach Modeling

Both overtopping and piping failure modes were checked. When overtopping failure mode is simulated, the PMF could be safely evacuated through the spillway and no breaching was observed. Hence, the dam is safe against failure induced by overtopping of flood ranging up to PMF. The dam could potentially fail due to over topping and piping flow emerged at .

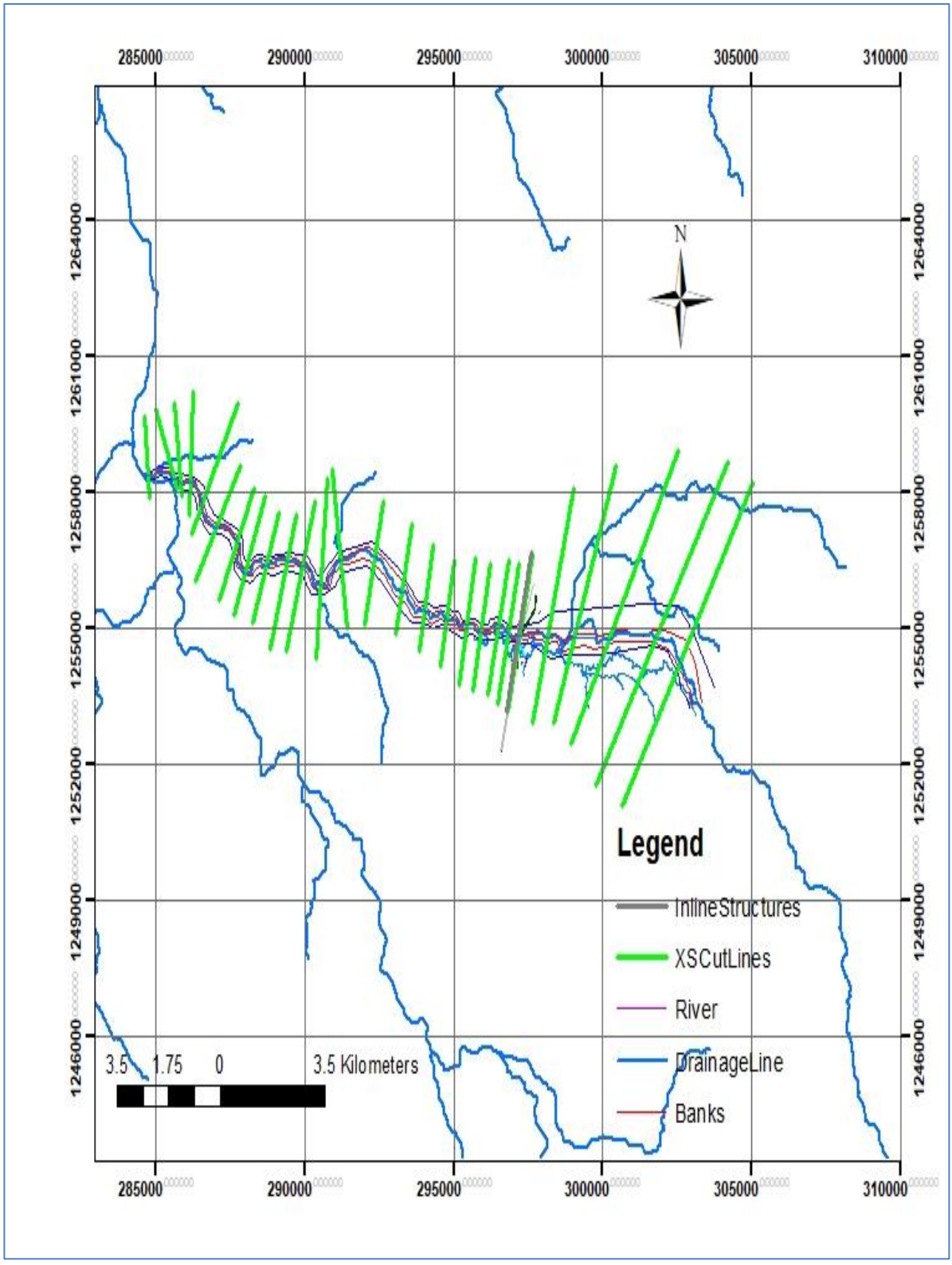



Figure 4. 8: cross sectional geometry and river

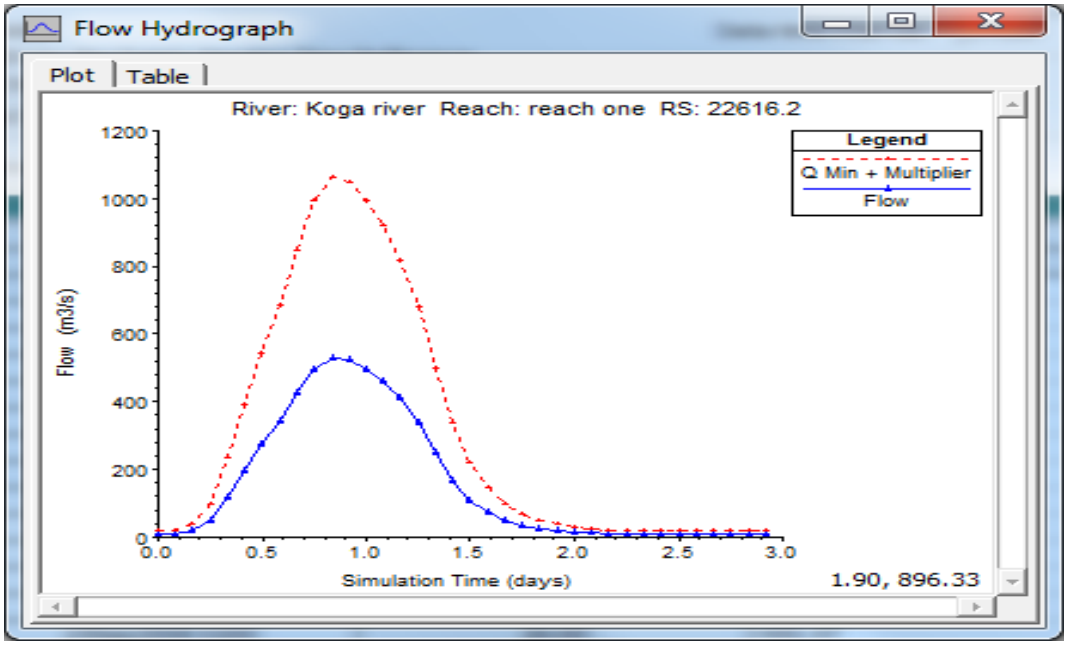



Figure 4. 9: PMF of the study area

### 4.4.1. Breach Modeling in Koga Dam by Overtopping

Koga Dam has been tested for overtopping failure applying a PMF inflow while the reservoir is at full condition i.e. when upstream water level is at spillway crest level. During simulation process the reservoir is observed to rise almost up to dam crest level and immediately after the peak flow of the PMF passes it recedes back to its initial level. From this it can be concluded that the spillway can safely evacuate the incoming PMF for which it has been designed.

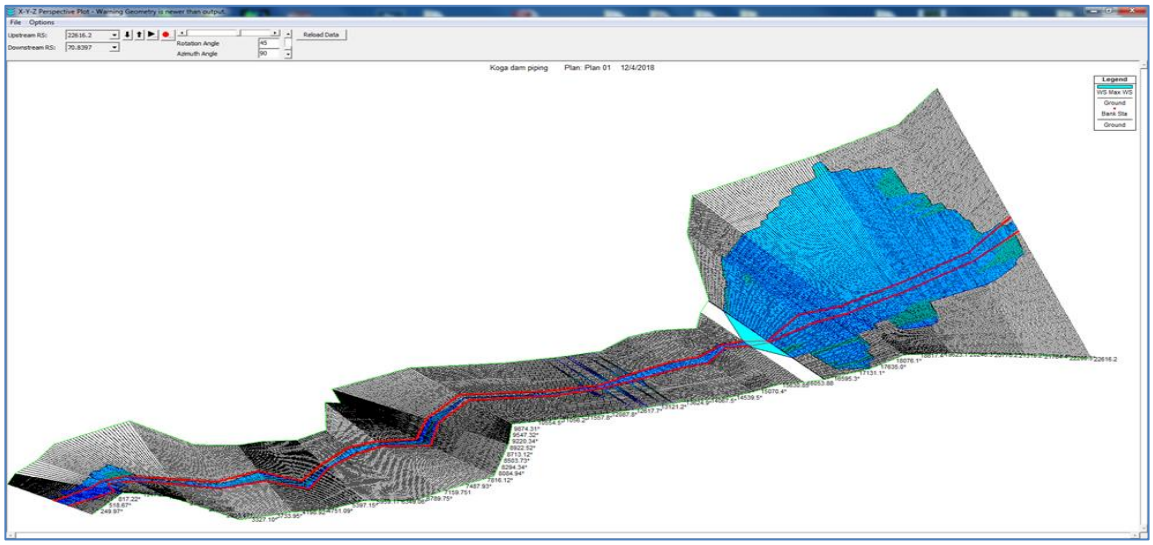


Figure 4. 10: Koga dam schematic diagram of overtopping

### 4.4.2. Breach Modeling in Koga Dam in Piping(Sunny Day Failure)

Piping through embankment body may be formed due to excessive seepage that may be triggered. When the impervious core material used is poor in quality or when the construction procedure does not follow engineering standards. The piping failure is with elevation of piping line being defined by the user. Other geometry of the dam and reservoir and engineering properties of the embankment material are as defined in the case of overtopping failure discussed earlier.

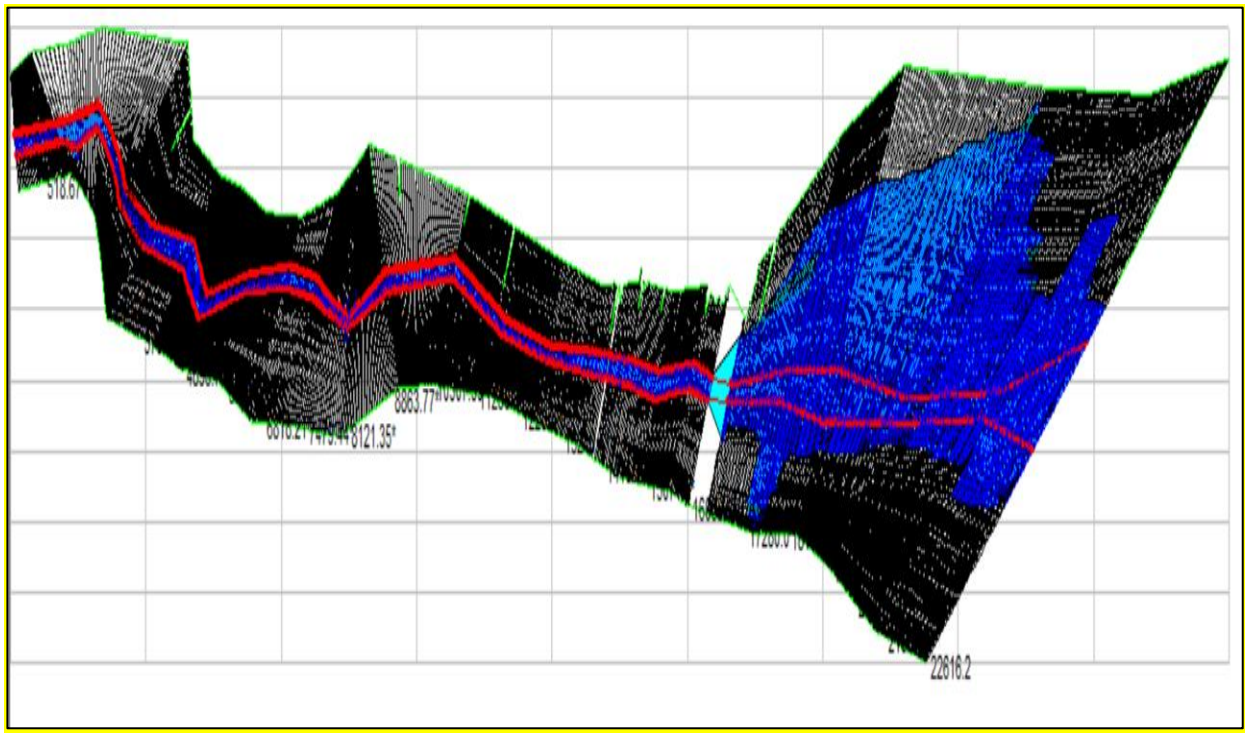
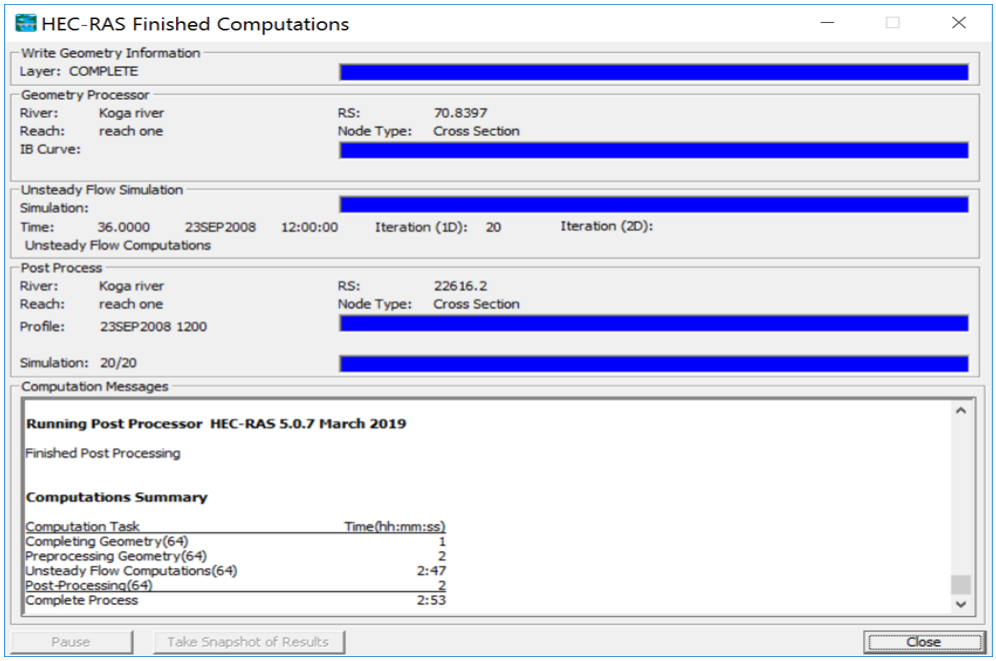


Figure 4. 11: Dam failure under piping schematic diagram

### 4.4.3. Computation Time Step

Unsteady flow analysis was run for 2 days assuming an inflow magnitude equivalent to a base flow discharge that continues after the PMF inflow ends. One of the difficulties in unsteady flow model is model instability and numerical accuracy issues. These issues can get improved by selecting a time step; too large time step normally causes numerical diffusion and model instability whereas too small time step causes lengthy computational time and model instability as well (USAE HEC CPD-68, 2010).Thus, considering this, a 10 seconds

computation interval was selected for the dam break analysis and cross sections were spaced at 20m intervals in reaches.



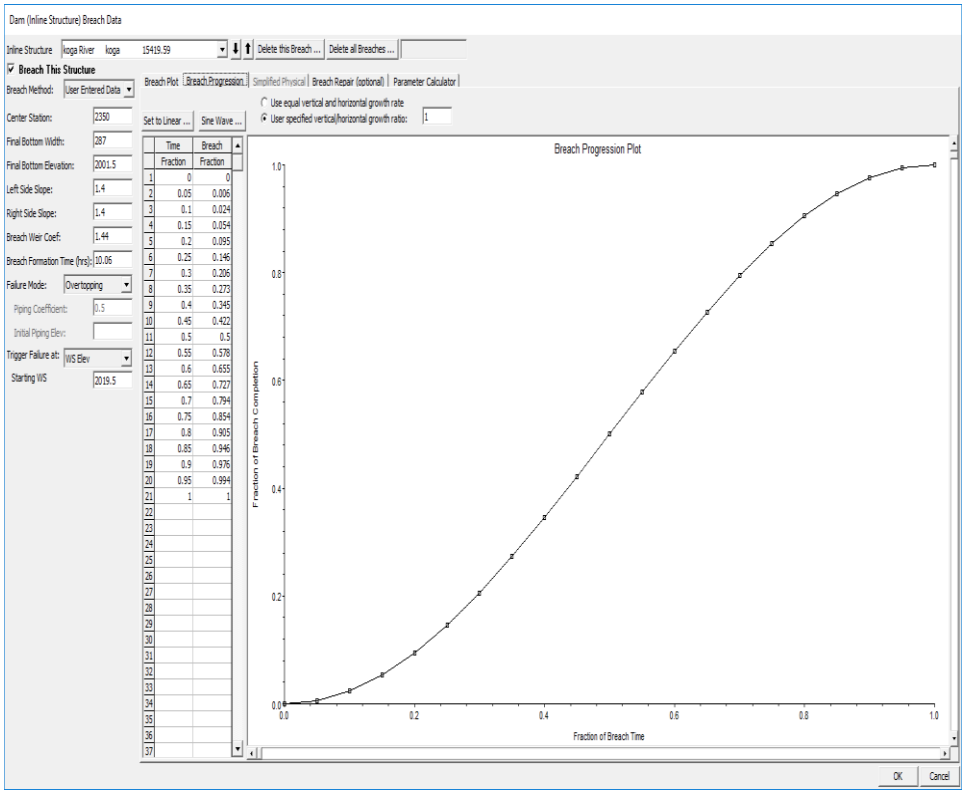




Figure 4. 12: Breach progression in time

### 4.4.4. Koga Dam breaches Parameters Result under PMF Event Overtopping Modes

The unsteady flow analyses were run for a simulation time period of about 2 days in 10 second time step. Hydrograph outputs were obtained for every 1Hour. The breach outflow hydrograph, headwater (HW) and tail water (TW) stages at Koga Dam as estimated using three methods breach dimensions are presented below table 4.1 and figure 4.13.

Table 4. 2: Koga Dam breach parameters for overtopping failure

| Method | Breach Bottom Width (m) | Side slope (H:1V) | Breach Development Time (hrs.) |
|---|---|---|---|
| MacDonald et al.(1984) | 206 | 0.5 | 1.6 |
| Froehlich (2008) | 117 | 1 | 2.84 |
| Von Thun and Gillette (1990) | 91 | 0.5 | 0.61 |

According to three methods of Koga dam breach development times and other parameter under overtopping mode show table 4.1 below. The dam breach parameters were estimated using three most currently used regression equations, i.e. Macdonald and Langridge-Monopolis (1984), Von Thun and Gillette (1990) and Froehlich (2008). For the case of overtopping failure, the bottom breach width for three methods were 206 m, 91 m, and 117m respectively. Their breach development times were 1.6 hrs, 0.61 hrs, and 2.84 hrs.

The depth of overtopping above dam crest is 0.25 m height as shown figure below 4.12.

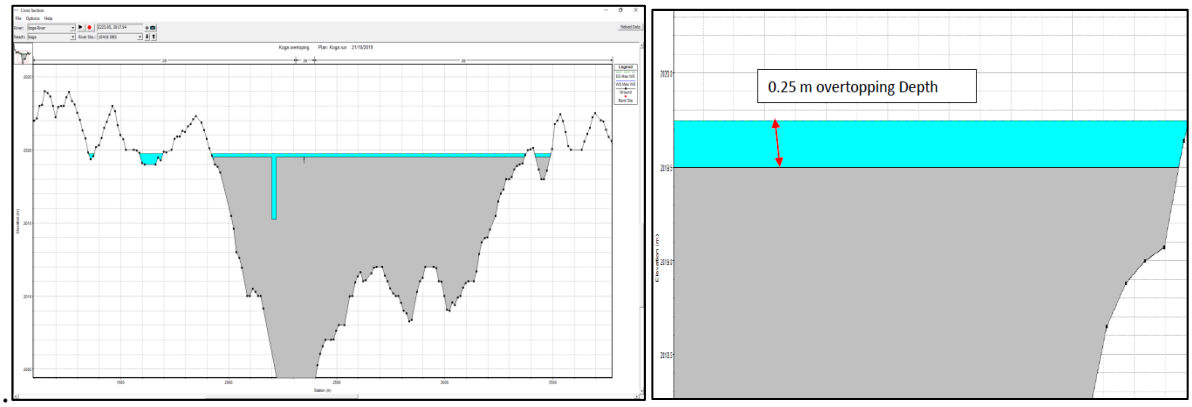
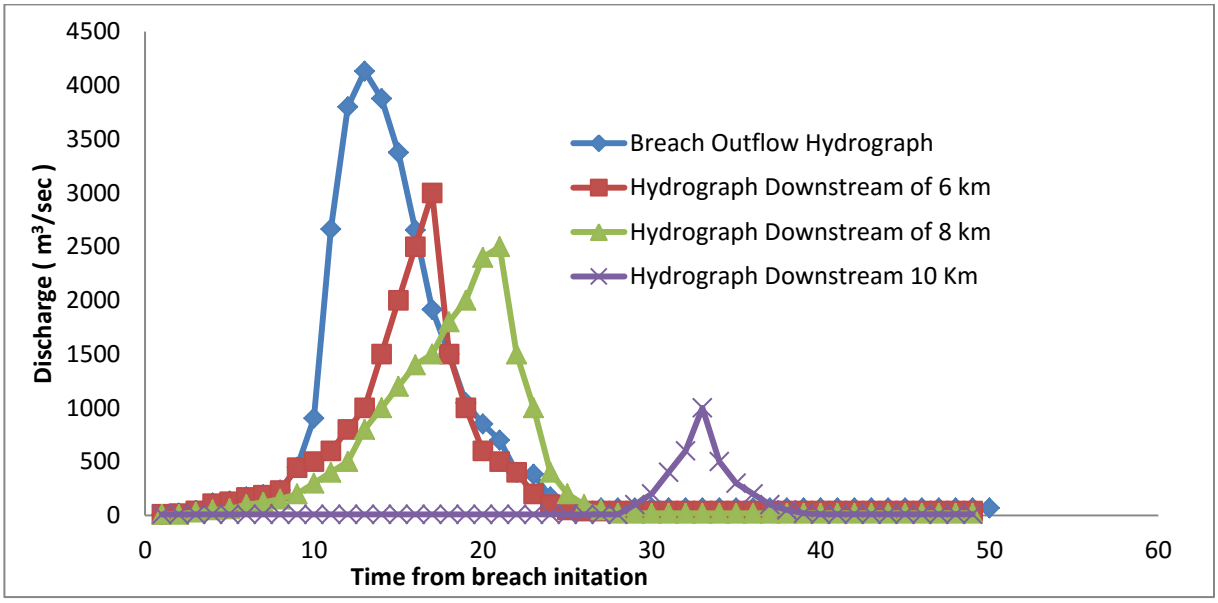



Figure 4. 13: Overtopping of dam and depth of overtopping

Under overtopping failure, the peak outflow from the dam is about 4132.51$m^3$/s (1 hour average peak) and the volume of breach outflow can reach up to 91.7M $m^3$ for a peak hour show Figure 4.14.The lag time between the peak inflow at the upstream end of the reservoir

and the time to breach the dam is about 17 hours. The head water stage and tail water stage is 2019.73m and 2007.24 m respectively as shown Figure 4. 14 below.



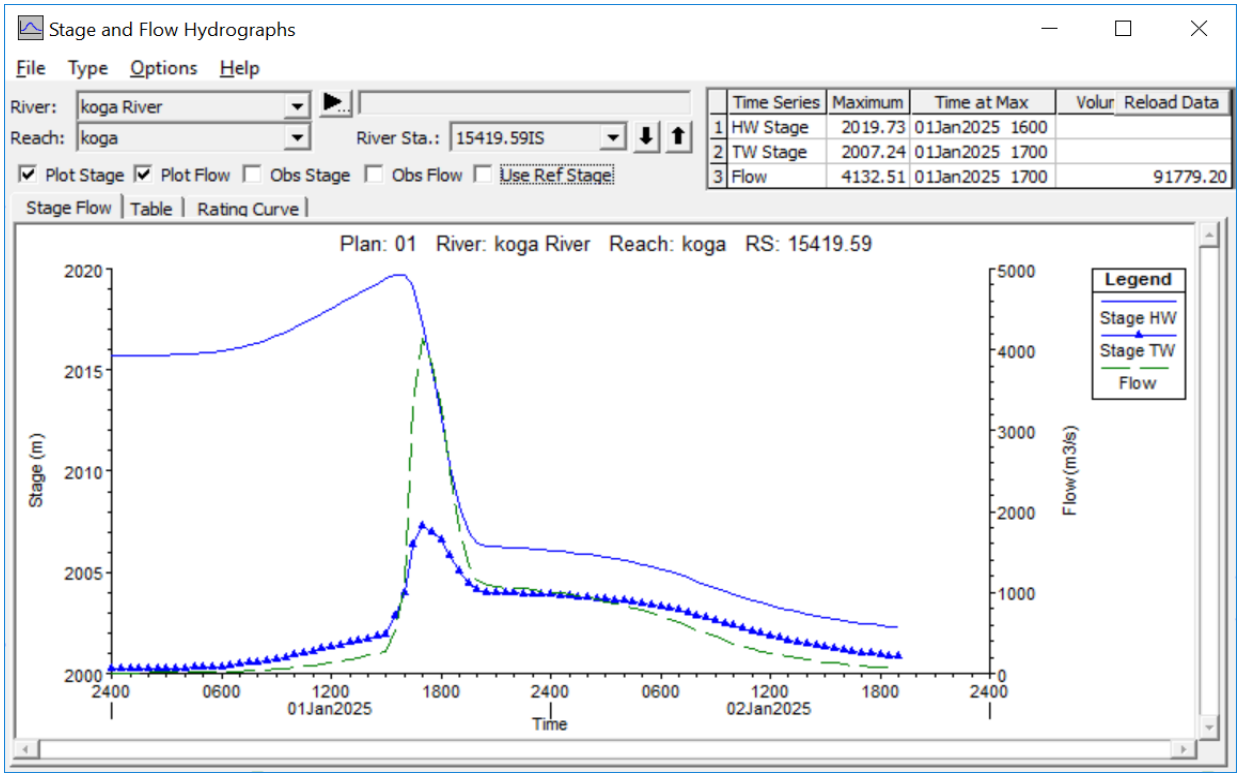




Figure 4. 14: Stage and flow hydrograph und overtopping failures.

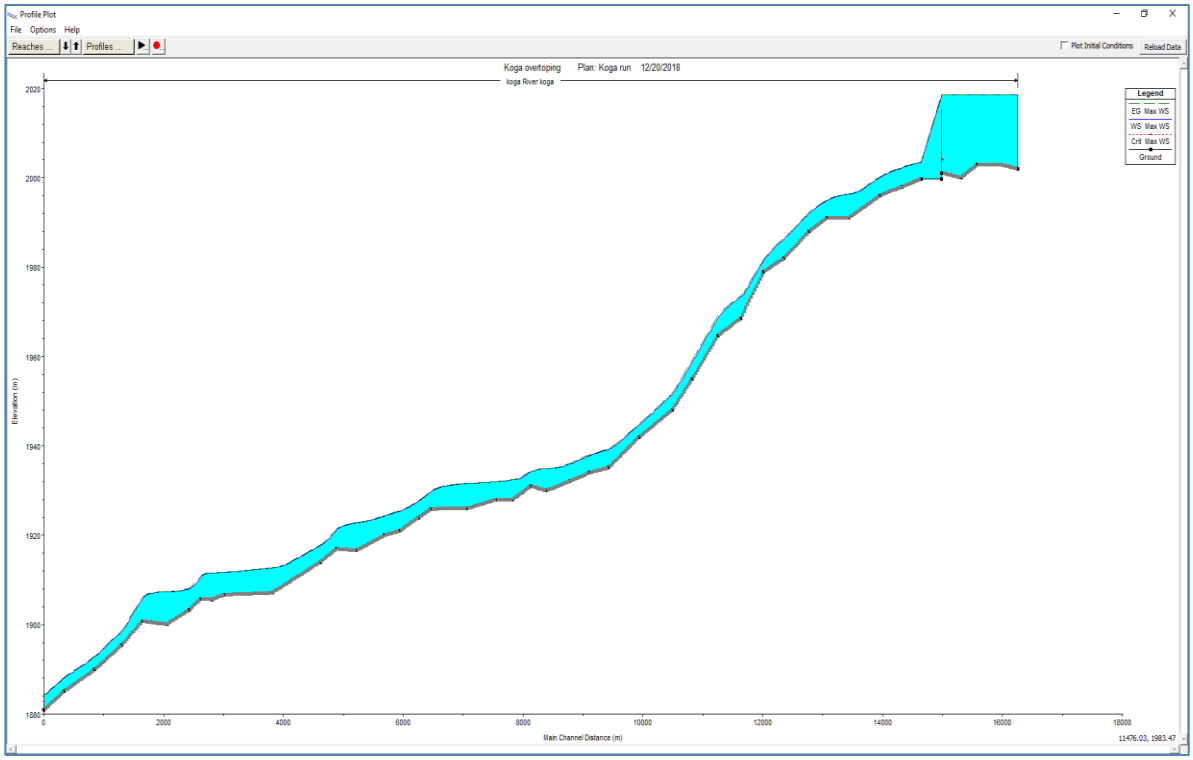



Figure 4. 15: General overtopping profile plot.

#### 4.4.4.1. Water Surface Elevation Overtopping Failures

The Water Surface Elevation (WSEL) is generally the first raster dataset that are produce as part of a Flood inundation mapping. A separate WSEL is produced for each flood event flood scenario Koga dam overtopping and piping for which modelled elevations are available. Each WSEL is provides the modelled WSEL values within the inundation extent of that particular flood event or scenario. In locations outside the corresponding mapped floodplain. The WSEL is the source from which many of the other raster datasets such as the flood depth and velocity are generated. WSEL of Koga dam dam-related WSEL could be created to reflect the flood elevations of maximum 2019.6 m from overtopping failure of the dam.

#### 4.4.4.2. Velocity Mapping of Overtopping Failures

Velocity data provides additional information about the flood hazard, and can offer a wide range of other floodplain management and risk communication benefits that may be difficult to convey with flood depths alone. The overtopping failures extents of each velocity grid are shown on Figure 4.14 produced should align with the extents of its corresponding WSEL and

depth grid. The maximum velocity in overtopping failure is 11m/sec as shown Figure below 4.16.

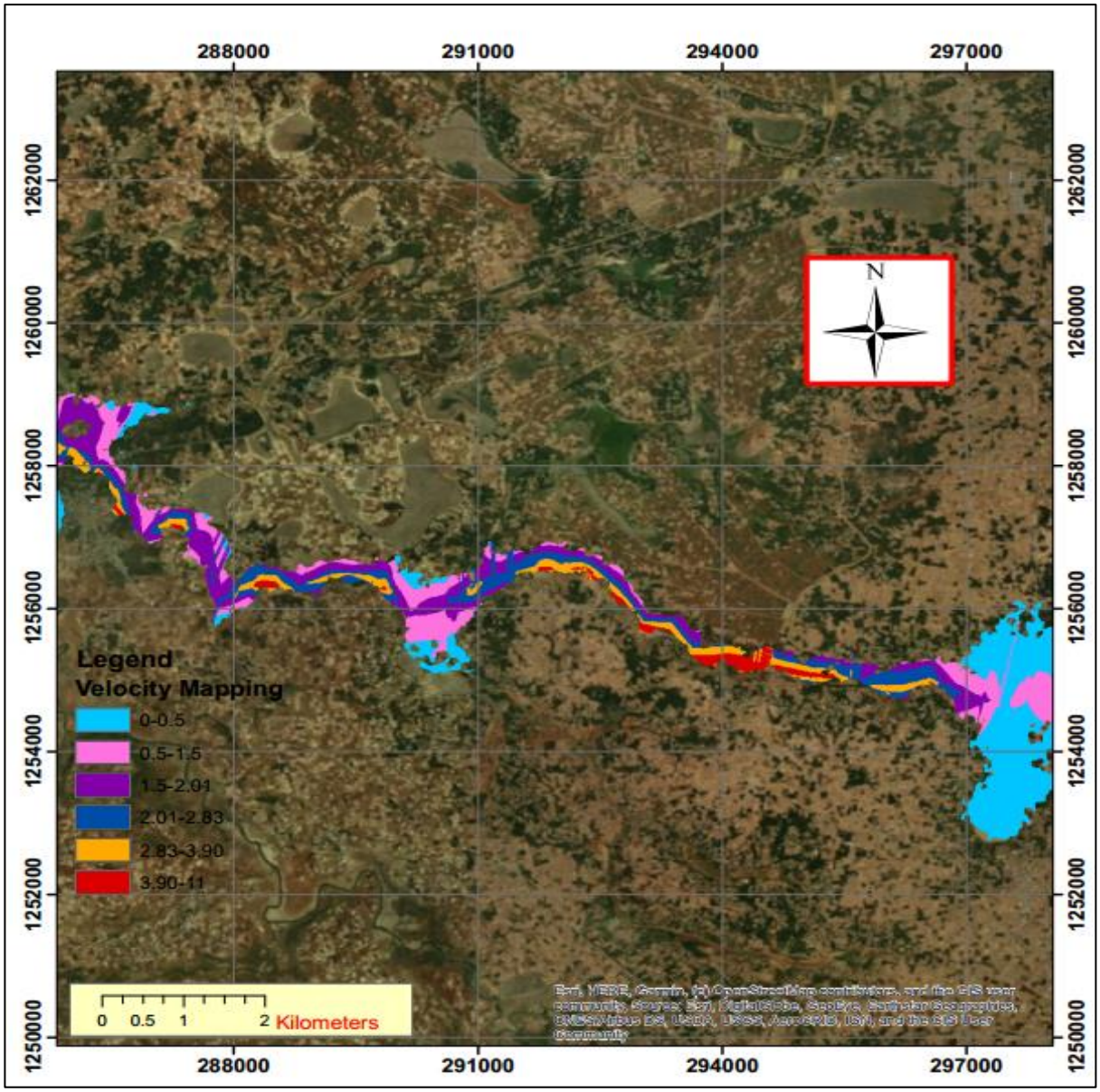



Figure 4. 16: Velocity mapping

#### 4.4.4.3. Food Depth Under Overtopping Failure

Unique combinations of flooding event, dam release type (piping, failure, or overtopping), and the hydrologic condition of the reservoir at the time of the release are used to differentiate the WSEL for dams and flood mapping area. The Koga Dam Scenario in overtopping the

Flood depth map area is provides the naming conventions that can be used for each dam WSEL, depending on the type of dam release scenario depicted.

The flood depth of the Koga dam breach in case of overtopping scenario is shown Figure below 4.17 is representing the ground elevation. The maximum of the overtopping dam breach flood depth is 15 m. The depth values for each depth cell are computed by subtracting the ground elevation value from the water surface elevation value for each flood scenario computed. The Terrain data used for the development of flood depth and should be used to generate the effective floodplain boundaries to ensure consistent and accurate results. The flood depth of Koga dam breach overtopping scenario is shown on Figure 4.17.

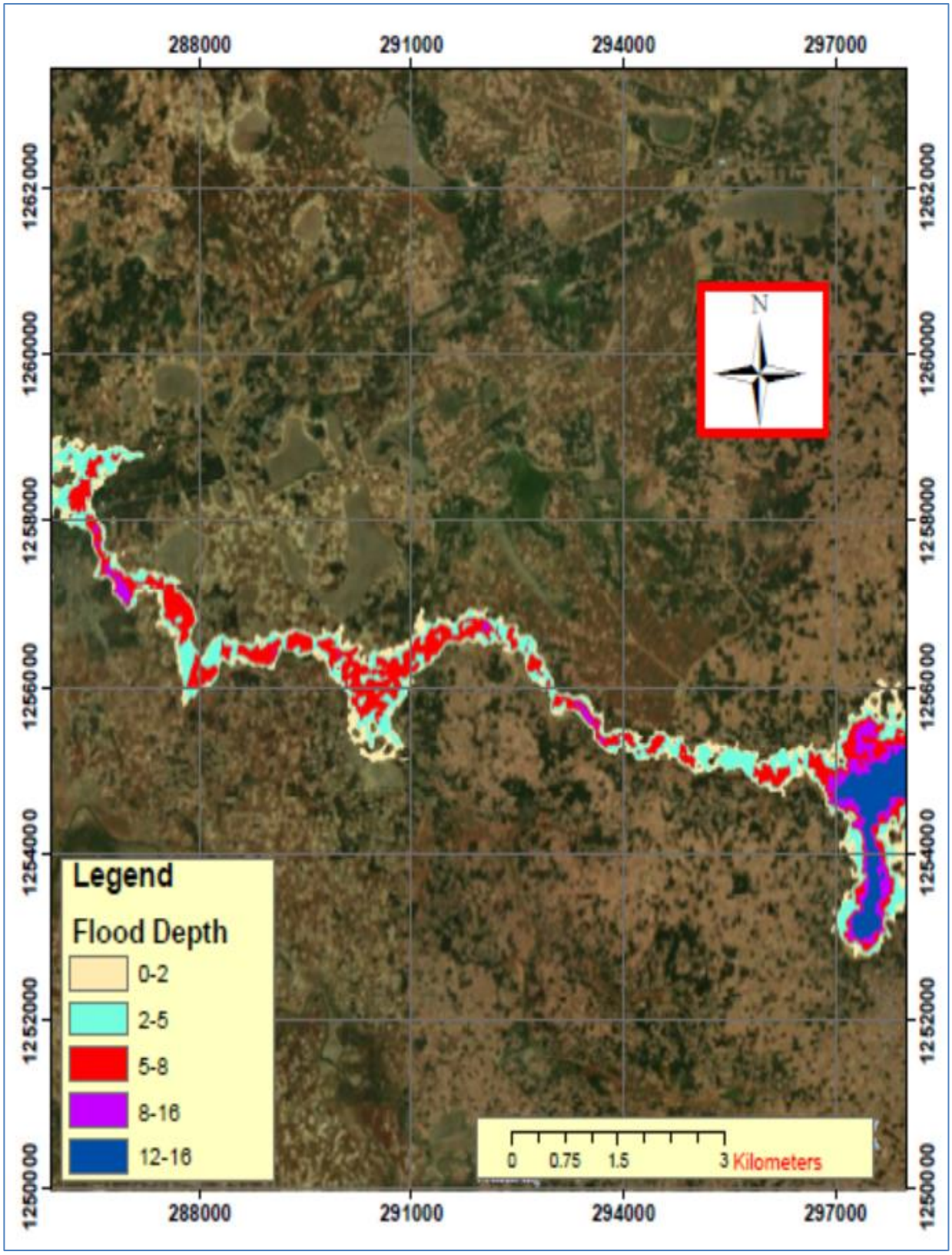



Figure 4. 17: Depth of flood mapping

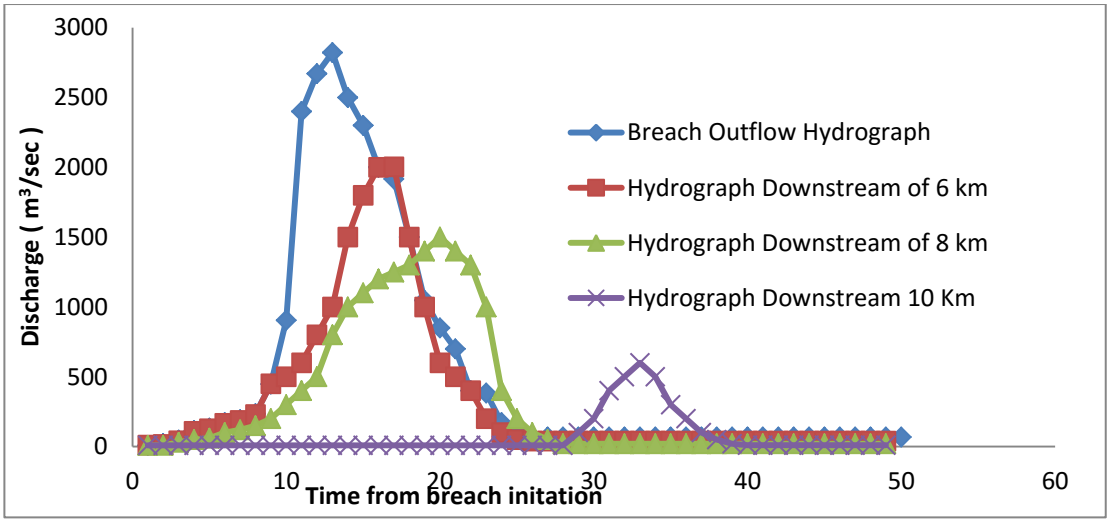
### 4.4.5. Koga Dam Breaches Parameters Result Under Piping Modes

Piping is the action of water cutting preferential channels in an embankment, following sometimes cracks and roots. The maximum breach outflow and arrival time to peak breach outflow results obtained from HEC-RAS model simulation at dam for three methods in case the of non-hydrologic (piping) breach scenario are given in tables below. The dam breach parameters were estimated using three most currently used regression equations, i.e. Macdonald and Langridge-Monopolis (1984), Von Thun and Gillette (1990) and Froehlich (2008). For the case of piping failure, the bottom breach width for three methods were 206 m, 91 m, and 117m respectively. Their breach development times were 1.6 hrs, 0.61 hrs, and 2.84 hrs respectively shown below Table 4.2.

Table 4. 3: Koga Dam breach parameters for piping failure

| Method | Breach Bottom Width (m) | Side slope (H:1V) | Breach Development Time (hrs) |
|---|---|---|---|
| MacDonald et al.(1984) | 206 | 0.5 | 1.6 |
| Froehlich (2008) | 117 | 1 | 2.84 |
| Von Thun and Gillette (1990) | 91 | 0.5 | 0.61 |

Under Piping failure, the peak outflow from the dam is about 2821.48$m^3$/s and the volume of breach outflow can reach up to 53.129M $m^3$ for a peak hour show Figure 4.18.The lag time between the peak inflow at the upstream end of the reservoir and the time to breach the dam is about 13hours. The head water stage and tail water stage is 2015.69m and 2006.09 m respectively as shown figure 4.18 below.



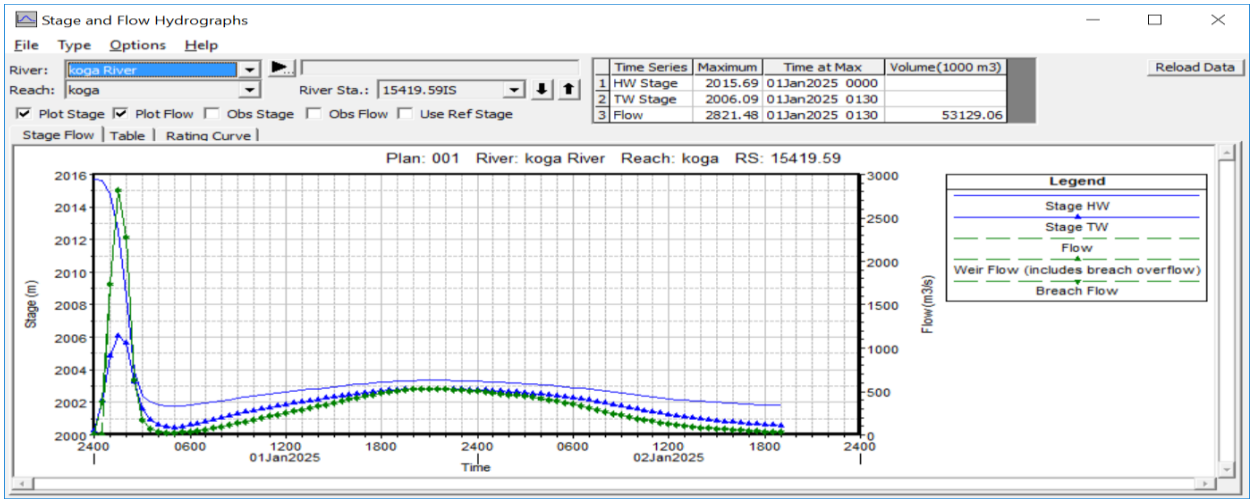



Figure 4. 18: Stage and outflow hydrograph under piping failures.

4.4.5.1. Water Surface Elevation and Cross-Sectional Depth Of Piping Failures

The Koga Dam piping failure Scenario the WSEL is the water surface profile of dam breach. WSEL of Koga dam dam-related WSEL could be created to reflect the flood elevations of maximum 2015.6 m from a sunny day piping failure of the dam where the reservoir was full to capacity. The cross-sectional depth of flooding is shown Figure below 4.19.

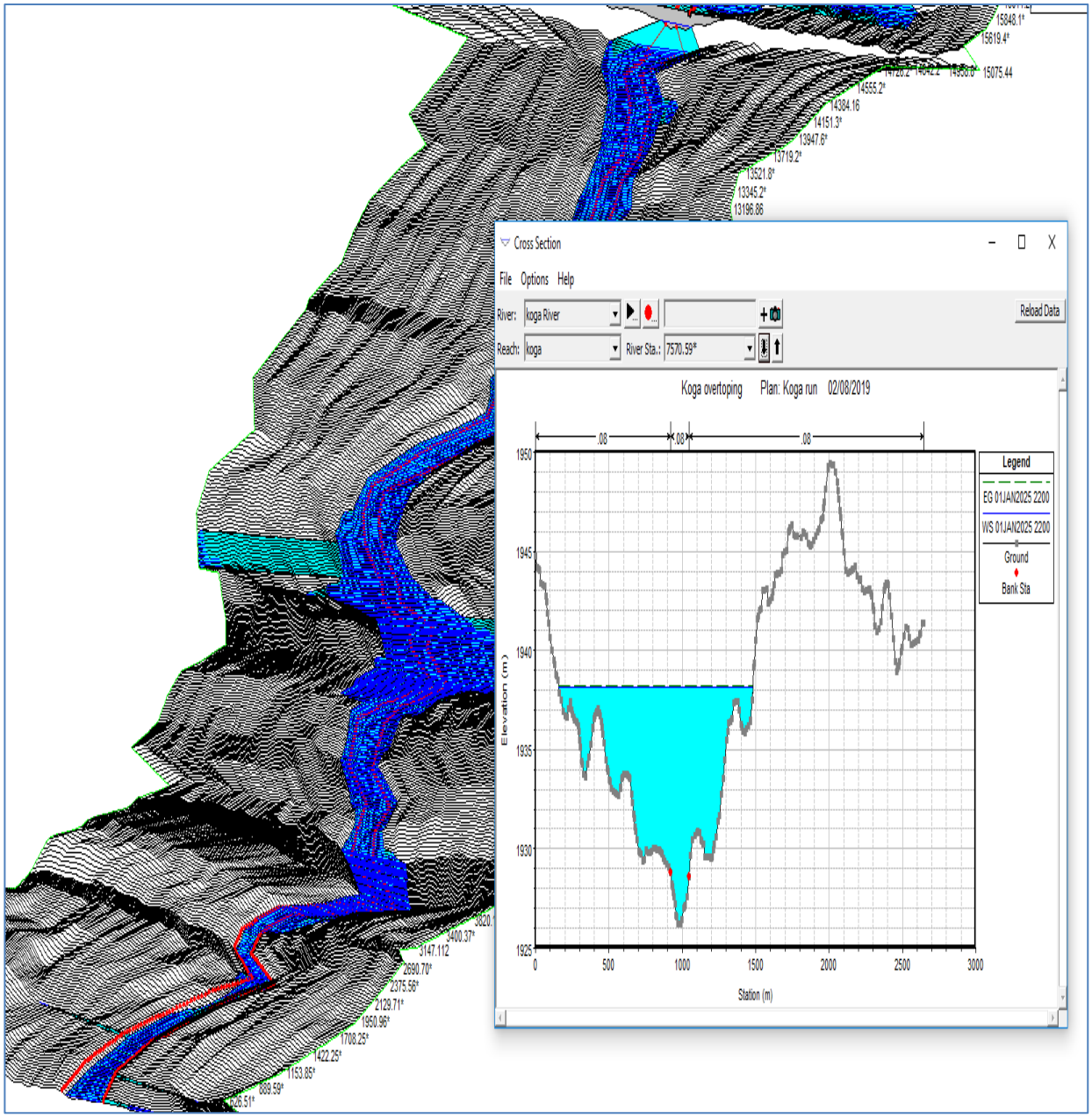



Figure 4. 19: Cross-sectional depth of flood

4.4.5.2. Velocity Mapping under Piping Failures

The Velocity mapping dataset is comprised of a digital representation of flood velocity distribution throughout the floodplain. Any point on the grid describes the average flood velocity for that floodplain location for a given scenario i.e piping of Koga dam as shown Figure below 4.20.The maximum velocity mapping of piping failure is 6.1 m/sec. The velocity ranges between 0.00 to 6.1 m/s which depends on the flood flow and water depth. The flow velocity is also influenced by the distance of certain point or location from the river.

The farther the distance from the river, the lesser the velocity due to energy losses caused by friction with the bed surface.

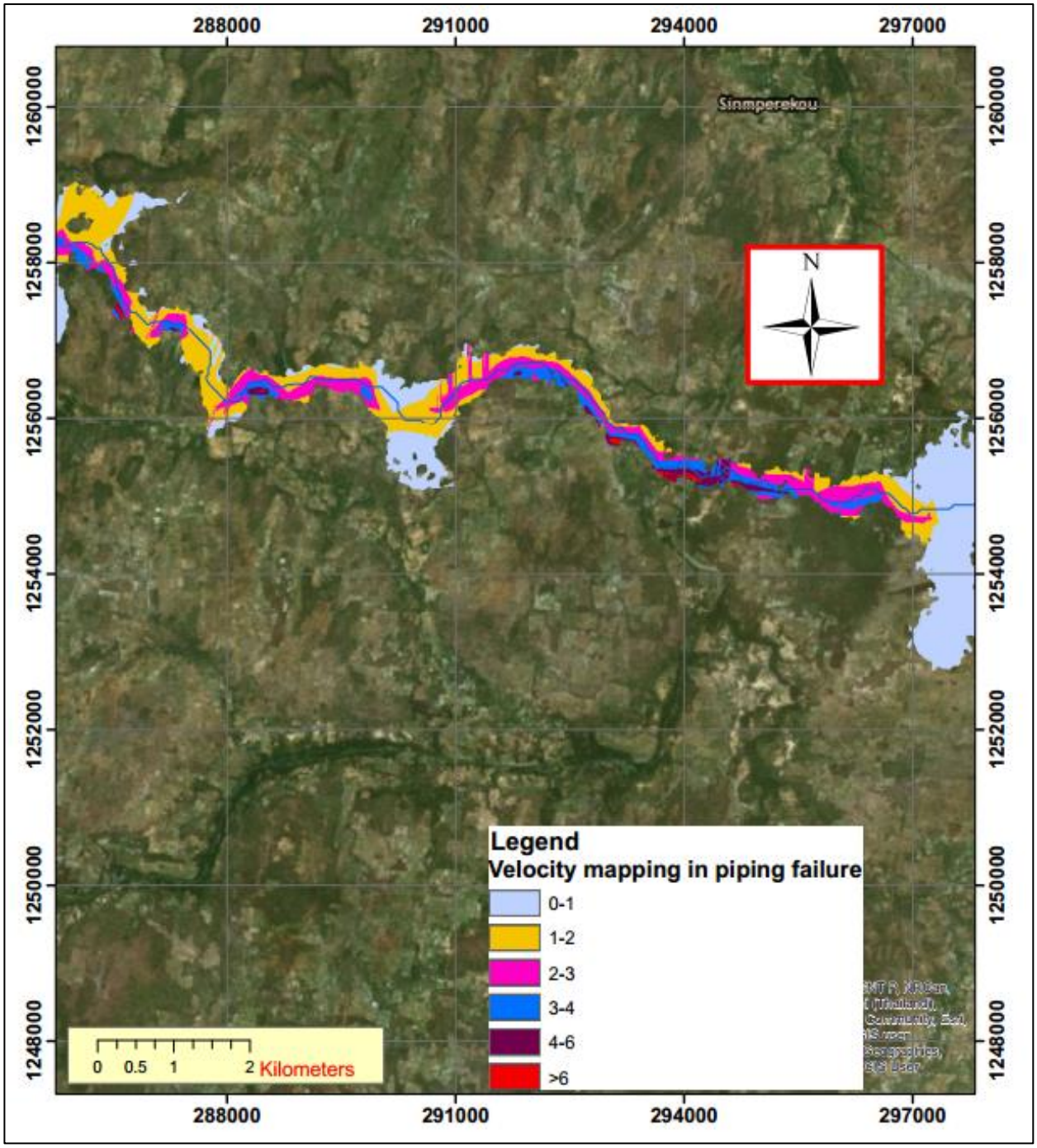



Figure 4. 20: Velocity of flood

4.4.5.3. Flood Depth of Piping Failures

The flood depth of the Koga dam breach in case of piping failures (sunny day failures) scenario is shown Figure below 4.21 is representing the ground elevation. The maximum of the piping failures of the Koga dam breach flood depth is 13 m. The depth values for each depth cell are computed by subtracting the ground elevation value from the water surface elevation value for each flood scenario computed. The Terrain data used for the development of flood depth and should be used to generate the effective floodplain boundaries to ensure consistent and accurate results. The flood depth of Koga dam breach overtopping scenario is shown on Figure 4.21.

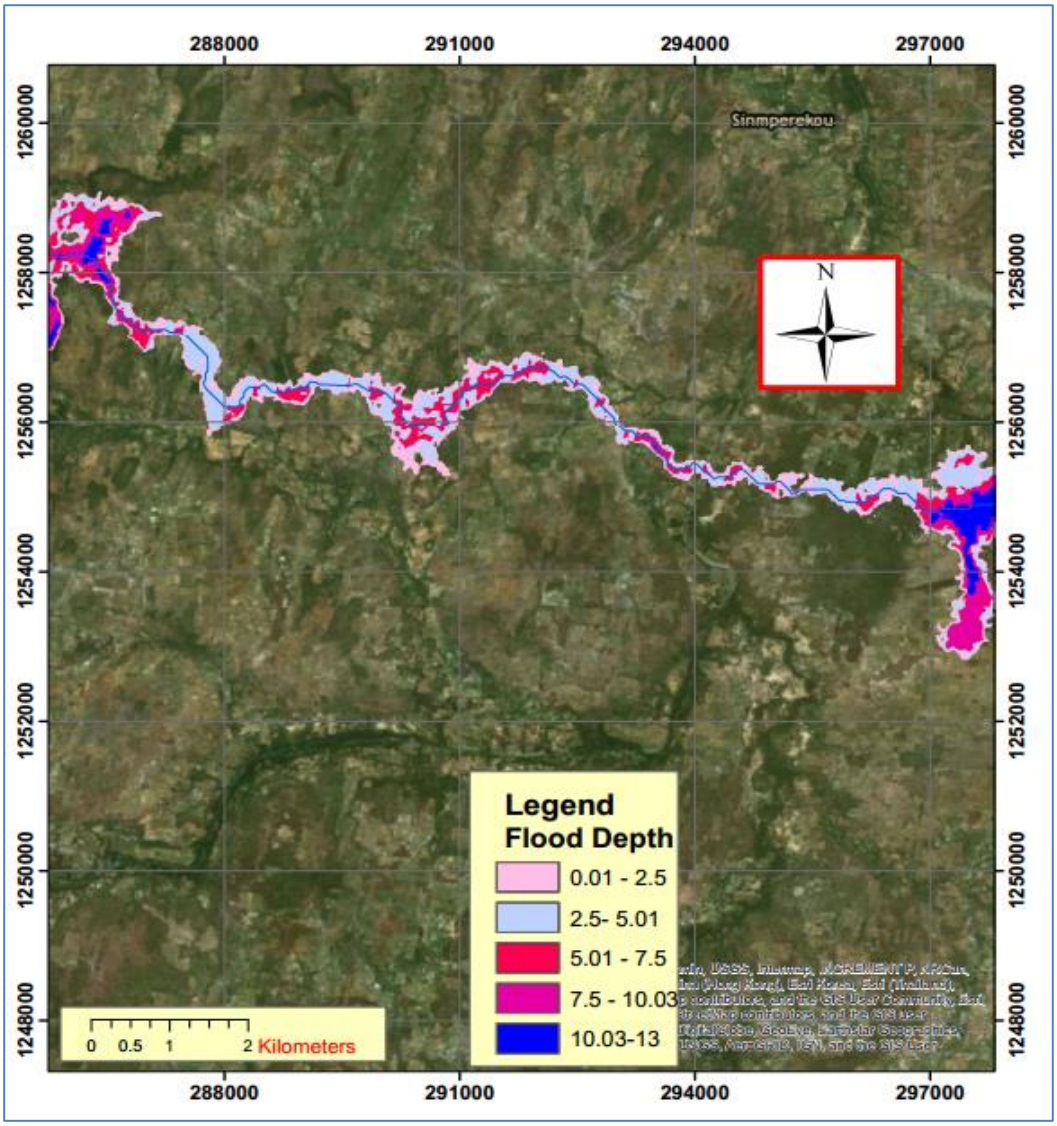



Figure 4. 21: Flood Depth of breach

## 4.5. Flood inundation

The inundation map provides a description of the areal extent of flooding which would be produced by the dam break flood. It should also identify zones of high velocity flow and depict inundation for representative cross-sections of the channel. The Koga dam overtopping and piping failure flood mapping area is as shown below. The overtopping flooding area is 10.2 $km^2$ whereas the dam failure due to ping flooding area is 9.1 $km^2$ shown Figures below 4.21 and 4.22. The flood inundation map library is a set of maps that shows where flooding may occur over a range of water levels in the community's local stream or river.




Figure 4. 22: Affected infrastructure due to flooding

The flood inundation is as shown the above Figure 4.22 *Wetit Abay* town, command area and main canal infrastructure is affected by dam failure flooding.

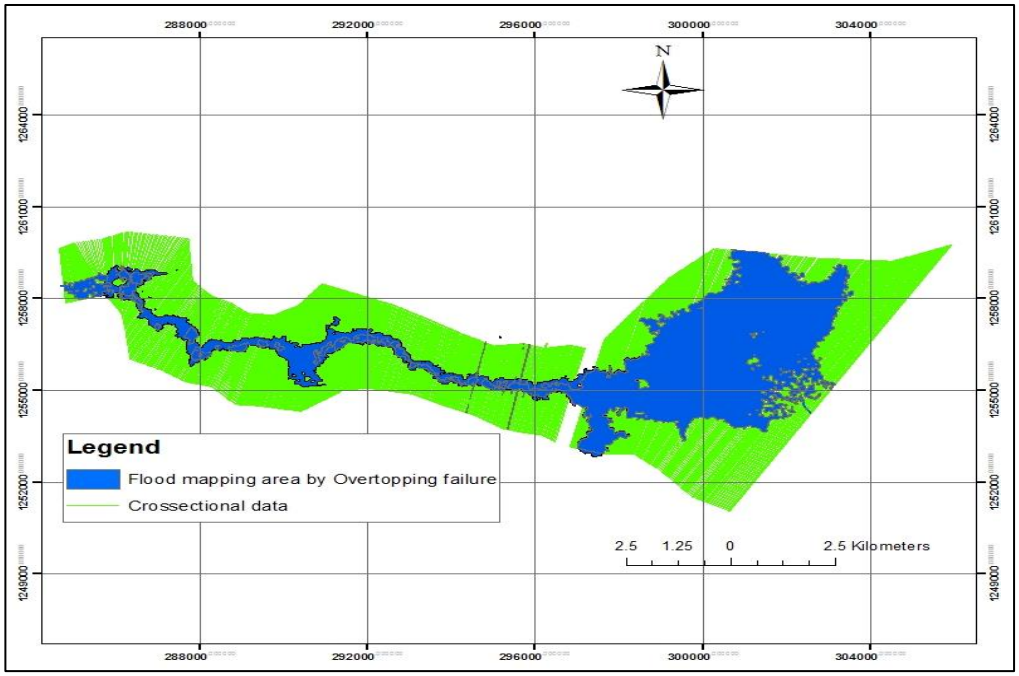



Figure 4. 23: Flooding area Dam failure due to overtopping.

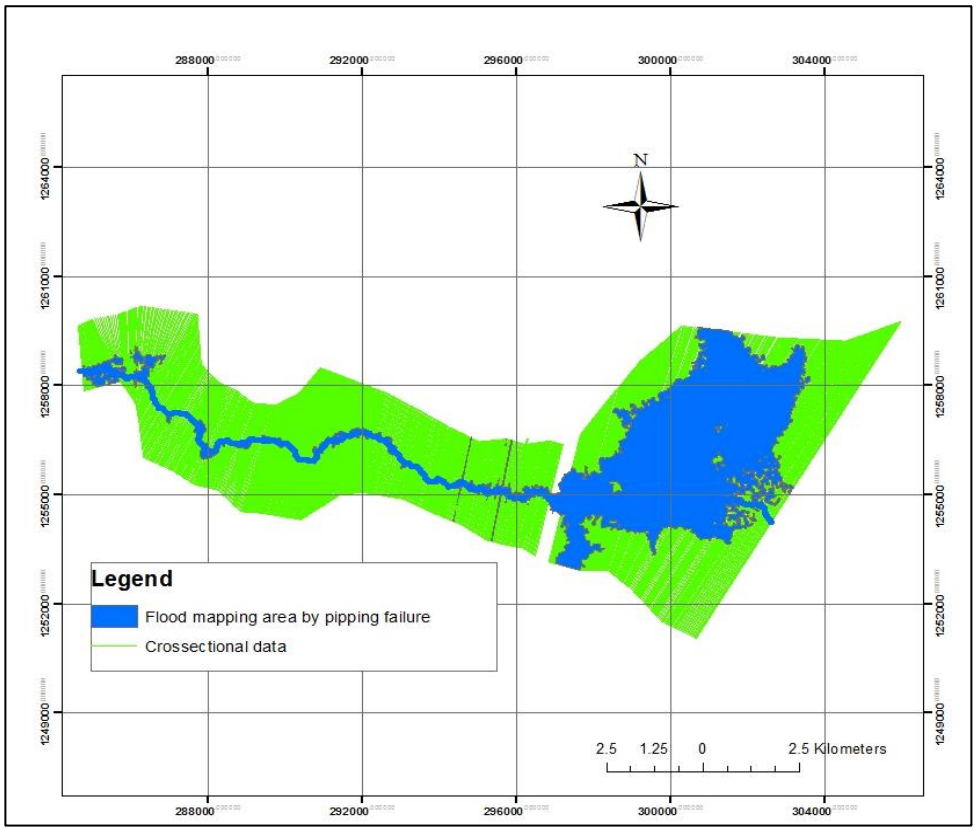



Figure 4. 24: Flood inundation boundary of Dam failure of piping

## 4.6. Flood Hazard Analysis

The classification of flood hazard which was used in this Research is derived from HEC RAS, where flood hazard rate is as function of flood depth, flow velocity. The flood hazard classification was classified into five stages i.e., low, moderate, High, Very High and extreme. The flood severity grid represents the combined effect of depth and velocity, most often communicated in categories of Low, Medium, High, Very High and Extreme Hazard.

### 4.6.1. Flood Hazard Dam Failure in Overtopping

Floods hazardous are those in rural areas, agricultural fields, forests and other land use areas. Floods hazardous in cities are densely and highly populated, they are provided with different service giving institutions, occupied with buildings, surrounded with commercial areas and industries, parts of the cities are connected with roads and railways constructed with high investments.

| **Housing** | **households (HH)** | **Space (mxm)** | **Area (m2)** | **Total(m2)** |
|---|---|---|---|---|
| Local people resettlement | 835 | 40x40 | 800 | 668000 |
| Administration | 1 | 200x200 | 40000 | 40,000 |
| Administration | 1 | 250x250 | 62500 | 62,500 |
| Farm workers | 1 | 400x400 | 160000 | 160,000 |
| Administration bldg. | 1 | 35x35 | 1225 | 1,225 |
| Work SHOP/garage | 1 | 100x100 | 10000 | 10,000 |
| Agro processing factory | 1 | 100x100 | 10,000.00 | 10,000 |
| Common services | 1 | 200*200 | 40000 | 40000 |
| At different locations as specified on the river | 1 | 300x1700 | 510,000 | 510,000 |
| Total | | | - | 9301725 |
| For road space and contingency for unseen conditions | | | - | **1,000,000** |

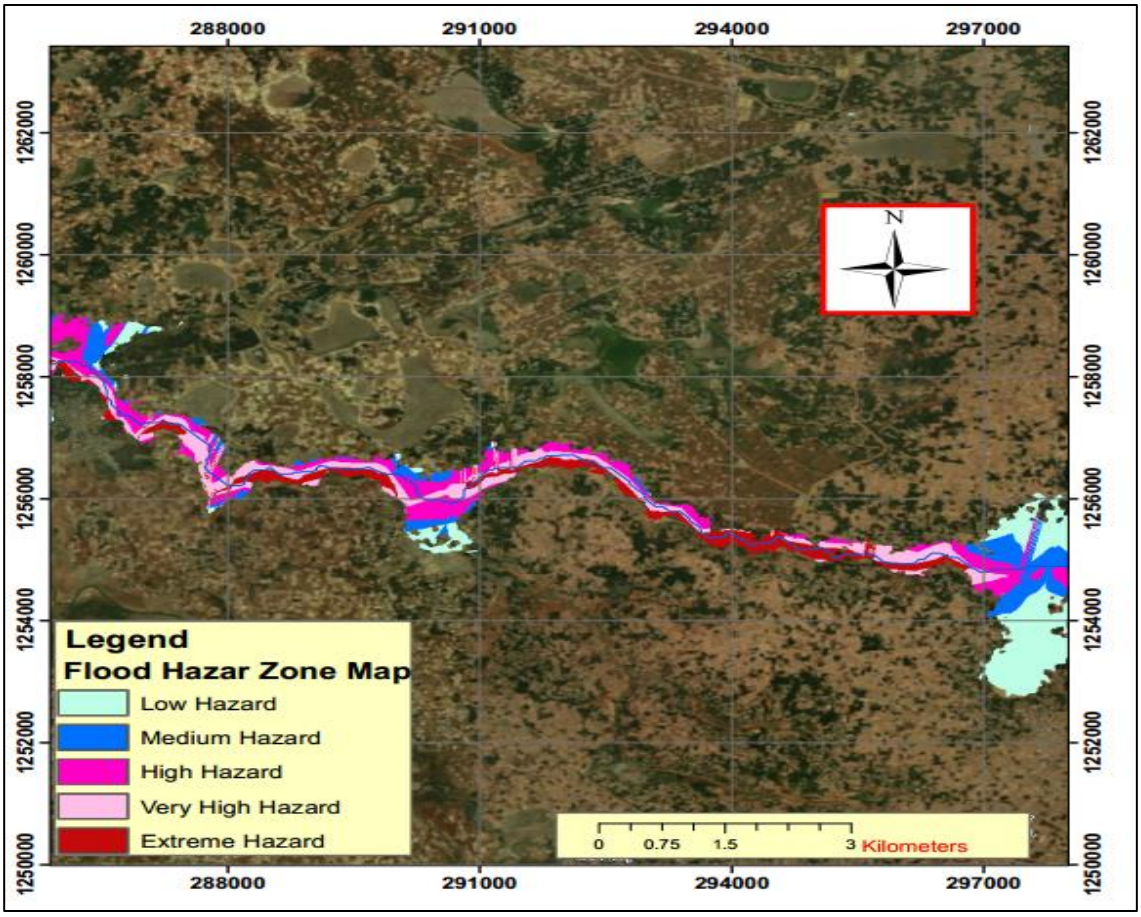



Figure 4. 25: Flood Hazard Classification in overtopping Failures.

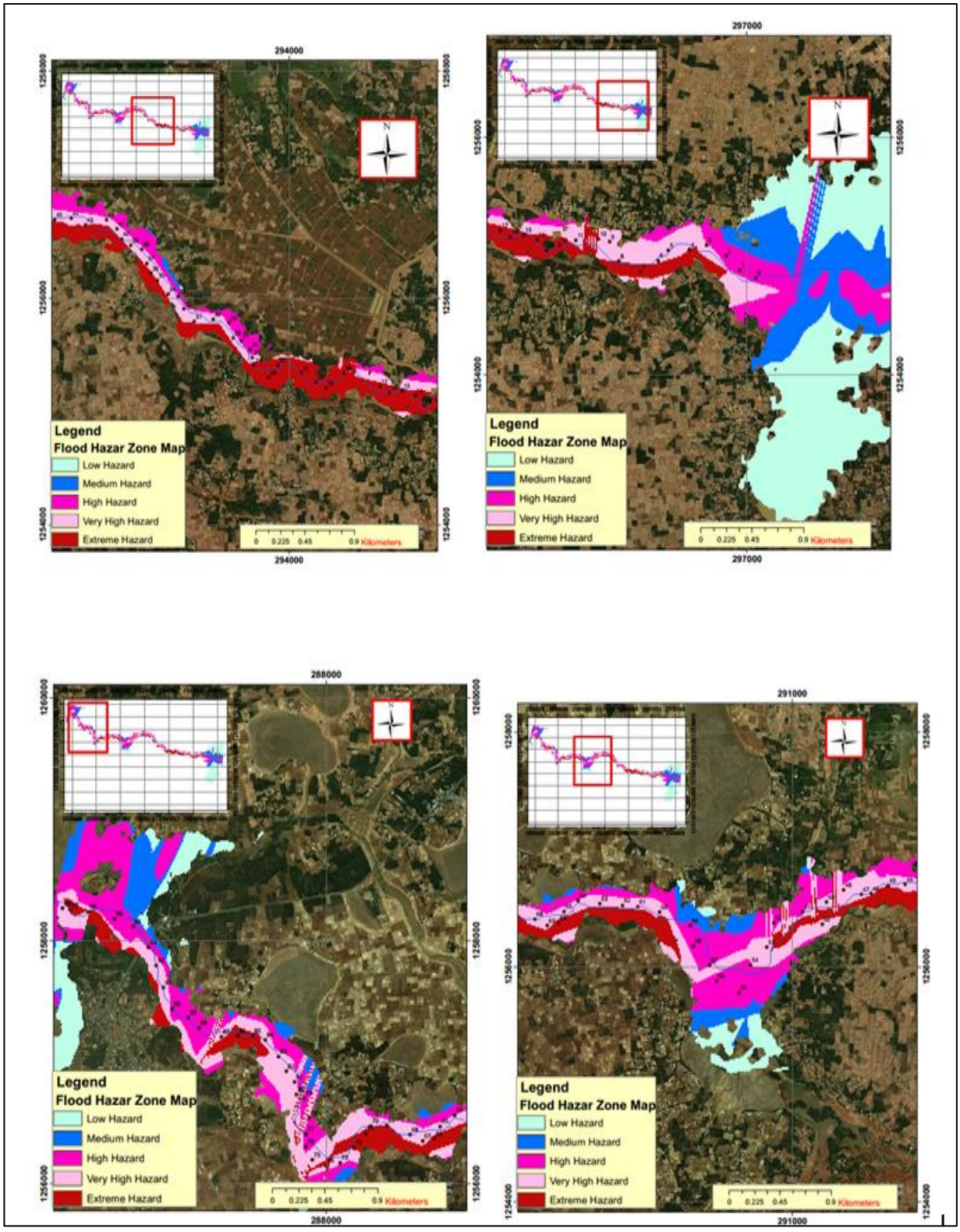



Figure 4. 26: Flood hazard at various location in piping failures

The flood hazards starting from upstream to the downstream at 98 points on the flood plains listed Table 4.3 below.

Table 4. 4: overtopping Flood hazards at various location in flood plain

| S.No | Flood Hazard | Flood Depth | Velocity | S.No | Flood Hazard | Flood Depth | Velocity |
|---|---|---|---|---|---|---|---|
| 0 | 9.01 | 14.14 | 1.23 | 50 | 25.42 | 6.74 | 2.08 |
| 1 | 9.40 | 8.97 | 1.33 | 51 | 11.91 | 7.11 | 1.90 |
| 2 | 7.68 | 6.16 | 1.27 | 52 | 8.15 | 5.06 | 1.63 |
| 3 | 15.41 | 5.37 | 1.85 | 53 | 26.45 | 6.96 | 2.14 |
| 4 | 35.59 | 3.32 | 2.70 | 54 | 10.65 | 6.76 | 1.58 |
| 5 | 23.89 | 5.10 | 2.43 | 55 | 3.77 | 6.69 | 1.06 |
| 6 | 27.53 | 7.51 | 2.60 | 56 | 6.75 | 4.52 | 1.17 |
| 7 | 98.13 | 4.50 | 3.59 | 57 | 12.05 | 6.46 | 1.39 |
| 8 | 33.89 | 5.33 | 2.41 | 58 | 7.21 | 4.21 | 1.10 |
| 9 | 19.11 | 4.96 | 1.90 | 59 | 2.42 | 6.07 | 0.75 |
| 10 | 32.39 | 4.67 | 2.14 | 60 | 30.77 | 6.13 | 2.60 |
| 11 | 30.70 | 3.76 | 2.34 | 61 | 22.73 | 4.95 | 2.17 |
| 12 | 77.91 | 2.59 | 3.53 | 62 | 22.35 | 6.29 | 2.05 |
| 13 | 120.32 | 2.54 | 4.10 | 63 | 22.84 | 5.40 | 2.05 |
| 14 | 52.01 | 3.53 | 3.23 | 64 | 13.69 | 5.34 | 1.61 |
| 15 | 45.42 | 2.24 | 3.07 | 65 | 18.59 | 6.85 | 1.78 |
| 16 | 80.81 | 6.70 | 3.74 | 66 | 80.62 | 7.69 | 2.90 |
| 17 | 49.53 | 5.43 | 3.16 | 67 | 24.53 | 7.33 | 1.97 |
| 18 | 125.96 | 7.18 | 4.61 | 68 | 26.14 | 6.83 | 2.08 |
| 19 | 119.52 | 4.72 | 4.58 | 69 | 34.46 | 4.54 | 2.78 |
| 20 | 97.13 | 3.79 | 4.37 | 70 | 34.62 | 6.18 | 2.95 |
| 21 | 99.37 | 7.05 | 4.24 | 71 | 52.46 | 5.60 | 3.52 |
| 22 | 67.63 | 6.76 | 3.37 | 72 | 57.66 | 4.81 | 3.22 |
| 23 | 143.95 | 5.03 | 4.52 | 73 | 13.47 | 6.66 | 1.83 |
| 24 | 46.26 | 7.46 | 3.29 | 74 | 18.21 | 5.09 | 2.05 |
| 25 | 22.16 | 5.72 | 2.63 | 75 | 18.70 | 5.15 | 1.82 |
| 26 | 4.14 | 9.04 | 1.95 | 76 | 10.79 | 4.83 | 1.35 |
| 27 | 10.08 | 9.00 | 2.16 | 77 | 8.44 | 4.76 | 1.27 |
| 28 | 23.74 | 12.01 | 2.71 | 78 | 4.82 | 2.70 | 1.06 |
| 29 | 9.06 | 6.45 | 2.13 | 79 | 3.77 | 6.37 | 1.01 |
| 30 | 26.70 | 7.73 | 2.71 | 80 | 32.31 | 6.15 | 1.98 |
| 31 | 35.95 | 6.20 | 3.23 | 81 | 31.28 | 5.00 | 1.93 |
| 32 | 20.51 | 4.85 | 2.13 | 82 | 27.90 | 5.76 | 1.82 |
| 33 | 15.18 | 5.38 | 1.84 | 83 | 16.27 | 5.62 | 1.50 |

| | | | | | | | |
|---|---|---|---|---|---|---|---|
| 34 | 31.26 | 4.78 | 2.79 | 84 | 22.30 | 5.23 | 1.93 |
| 35 | 34.98 | 4.47 | 3.01 | 85 | 46.73 | 6.81 | 3.24 |
| 36 | 38.45 | 6.25 | 3.15 | 86 | 75.43 | 4.71 | 3.38 |
| 37 | 33.22 | 5.49 | 2.87 | 87 | 30.09 | 5.94 | 2.14 |
| 38 | 19.77 | 4.43 | 2.28 | 88 | 7.03 | 7.59 | 1.12 |
| 39 | 32.73 | 2.23 | 2.79 | 89 | 8.02 | 8.17 | 1.36 |
| 40 | 35.90 | 6.28 | 2.88 | 90 | 9.37 | 9.15 | 2.20 |
| 41 | 26.12 | 5.58 | 2.44 | 91 | 21.94 | 6.66 | 2.71 |
| 42 | 22.54 | 4.73 | 2.27 | 92 | 21.96 | 6.77 | 2.21 |
| 43 | 34.25 | 4.76 | 2.79 | 93 | 11.97 | 7.61 | 1.77 |
| 44 | 26.31 | 8.02 | 2.48 | 94 | 4.18 | 5.13 | 1.22 |
| 45 | 36.35 | 6.95 | 2.96 | 95 | 8.40 | 6.03 | 2.04 |
| 46 | 32.39 | 6.21 | 2.66 | 96 | 32.47 | 3.18 | 2.72 |
| 47 | 28.44 | 5.80 | 2.47 | 97 | 35.97 | 4.16 | 3.11 |
| 48 | 16.24 | 5.22 | 1.97 | 98 | 23.74 | 3.29 | 2.62 |
| 49 | 16.59 | 6.85 | 1.79 | | | | |

### 4.6.2. Flood Hazard Dam Failure in Piping

The flood hazard classification had five stage i.e Low, Medium, High, very high and extreme high classification based on depth and velocity range as shown figure below. The hazard classification is lesser severity in piping failures where as in overtopping failure increase severity.

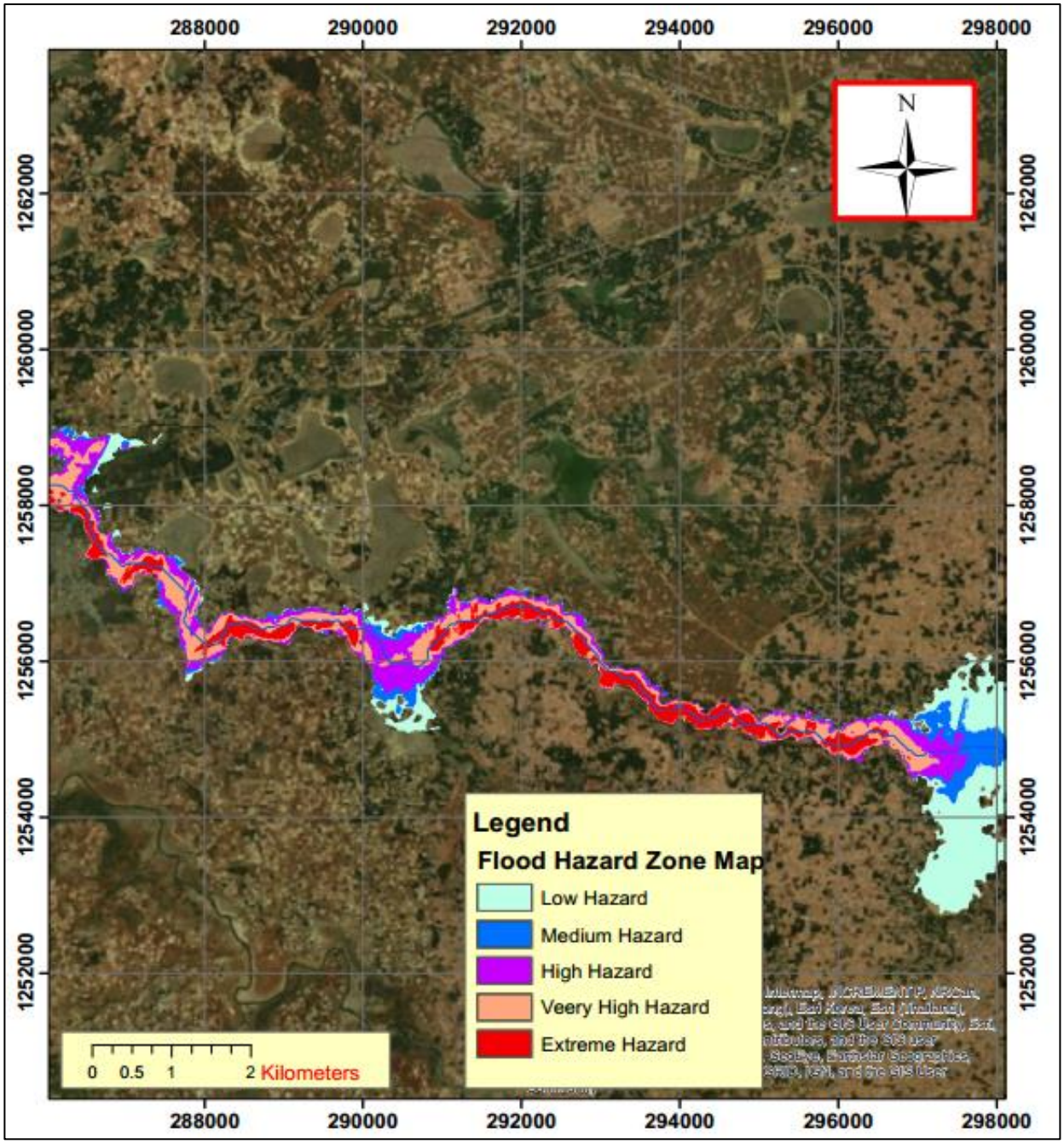



Figure 4. 27: Flood Hazard Classification in Piping Failures.

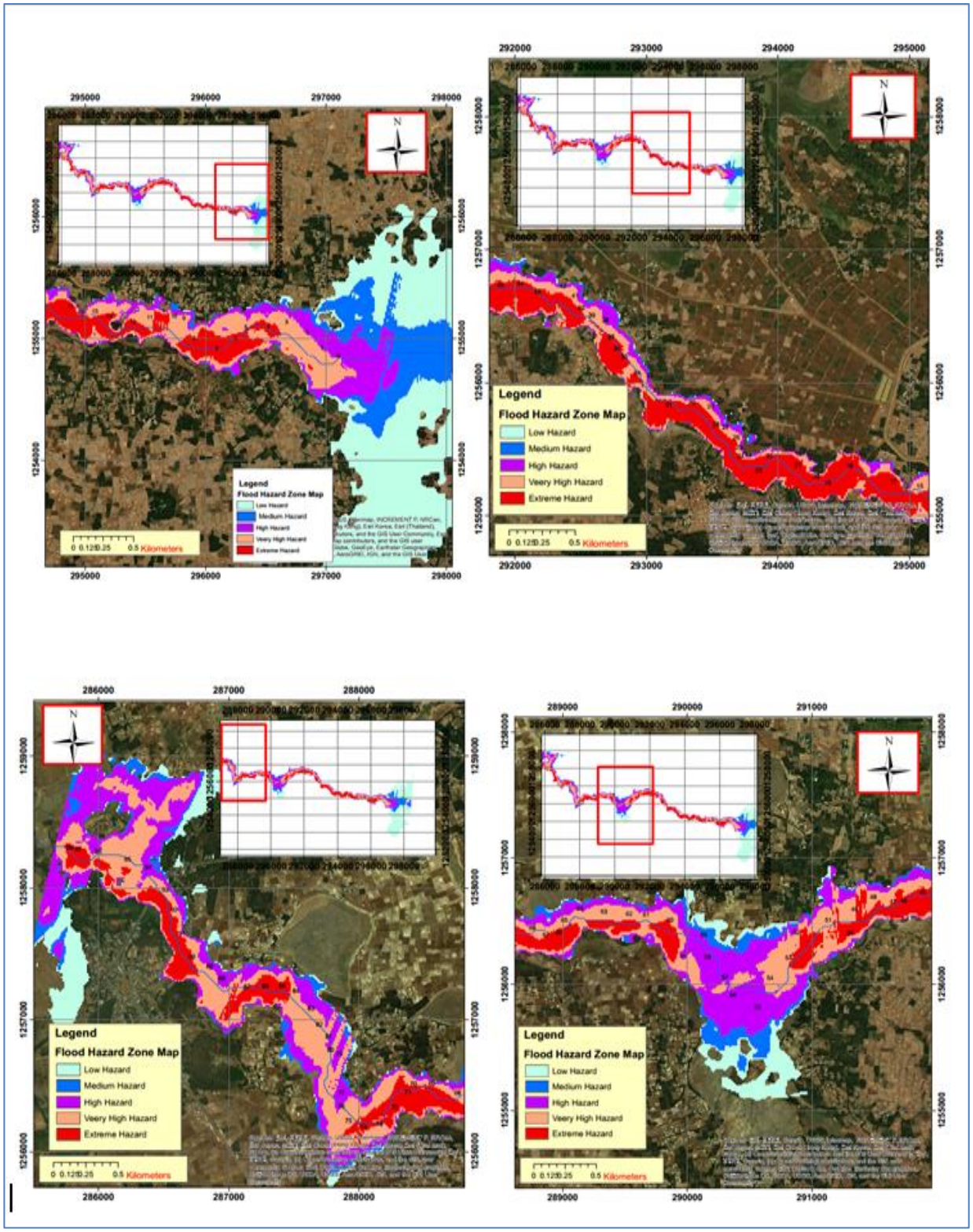



Figure 4. 28: Flood Hazard piping Failure at various locations.

Table 4. 5: piping Flood hazards at various location

| S.No | Flood Hazard | Flood Depth | Velocity | S.No | Flood Hazard | Flood Depth | Velocity |
|---|---|---|---|---|---|---|---|
| 0 | 14.744 | 10.935 | 1.620 | 50 | 38.430 | 5.852 | 2.355 |
| 1 | 16.099 | 6.991 | 1.589 | 51 | 30.049 | 6.205 | 2.047 |
| 2 | 14.983 | 5.045 | 1.457 | 52 | 12.683 | 3.847 | 1.671 |
| 3 | 26.034 | 4.255 | 2.033 | 53 | 32.056 | 5.739 | 2.245 |
| 4 | 38.699 | 2.302 | 3.048 | 54 | 14.379 | 5.512 | 1.552 |
| 5 | 44.144 | 4.108 | 2.730 | 55 | 6.915 | 5.442 | 1.087 |
| 6 | 69.920 | 6.479 | 2.890 | 56 | 5.169 | 3.271 | 1.202 |
| 7 | 70.540 | 3.328 | 3.600 | 57 | 11.624 | 5.210 | 1.456 |
| 8 | 46.524 | 4.007 | 2.710 | 58 | 5.721 | 2.987 | 1.118 |
| 9 | 26.295 | 3.640 | 2.100 | 59 | 3.606 | 4.845 | 0.749 |
| 10 | 38.720 | 3.378 | 2.619 | 60 | 49.028 | 4.784 | 2.712 |
| 11 | 32.655 | 2.549 | 2.649 | 61 | 28.949 | 3.376 | 2.274 |
| 12 | 49.271 | 1.460 | 3.810 | 62 | 33.299 | 4.668 | 2.185 |
| 13 | 68.778 | 1.462 | 4.548 | 63 | 30.118 | 3.787 | 2.222 |
| 14 | 54.710 | 2.471 | 3.559 | 64 | 18.350 | 3.741 | 1.741 |
| 15 | 34.840 | 1.121 | 3.384 | 65 | 28.405 | 5.268 | 1.938 |
| 16 | 120.104 | 5.539 | 3.998 | 66 | 64.071 | 6.125 | 2.759 |
| 17 | 78.660 | 4.263 | 3.548 | 67 | 42.740 | 5.777 | 2.303 |
| 18 | 231.166 | 6.180 | 5.404 | 68 | 38.687 | 5.354 | 2.267 |
| 19 | 131.869 | 3.682 | 4.912 | 69 | 49.715 | 3.332 | 3.117 |
| 20 | 102.488 | 2.667 | 4.727 | 70 | 72.481 | 5.146 | 3.291 |
| 21 | 168.624 | 5.738 | 4.607 | 71 | 91.746 | 4.595 | 3.877 |
| 22 | 107.776 | 5.448 | 3.768 | 72 | 57.028 | 3.785 | 3.269 |
| 23 | 120.576 | 3.773 | 4.549 | 73 | 29.112 | 5.603 | 2.003 |
| 24 | 116.064 | 6.357 | 3.771 | 74 | 46.378 | 3.785 | 2.821 |
| 25 | 60.840 | 4.637 | 3.083 | 75 | 21.516 | 3.533 | 1.899 |
| 26 | 54.472 | 7.966 | 2.369 | 76 | 12.167 | 3.186 | 1.466 |
| 27 | 68.810 | 7.964 | 2.673 | 77 | 10.543 | 3.112 | 1.374 |
| 28 | 131.946 | 11.010 | 3.232 | 78 | 4.678 | 1.053 | 1.151 |
| 29 | 48.546 | 5.468 | 2.624 | 79 | 9.016 | 4.723 | 1.119 |
| 30 | 83.454 | 6.759 | 3.166 | 80 | 32.300 | 4.512 | 2.151 |
| 31 | 93.539 | 5.112 | 3.713 | 81 | 23.252 | 3.376 | 1.996 |
| 32 | 34.770 | 3.819 | 2.534 | 82 | 25.014 | 4.159 | 1.948 |
| 33 | 28.806 | 4.447 | 2.205 | 83 | 17.851 | 4.047 | 1.663 |
| 34 | 53.369 | 3.887 | 3.170 | 84 | 27.266 | 3.703 | 2.125 |
| 35 | 56.149 | 3.580 | 3.355 | 85 | 100.103 | 5.296 | 3.626 |
| 36 | 80.918 | 5.320 | 3.454 | 86 | 87.368 | 3.117 | 3.988 |
| 37 | 59.697 | 4.516 | 3.145 | 87 | 39.464 | 4.416 | 2.430 |
| 38 | 31.598 | 3.407 | 2.517 | 88 | 14.172 | 6.115 | 1.307 |

| | | | | | | | |
|---|---|---|---|---|---|---|---|
| 39 | 26.223 | 1.140 | 3.064 | 89 | 22.696 | 6.780 | 1.604 |
| 40 | 68.663 | 5.157 | 3.169 | 90 | 77.422 | 7.993 | 2.824 |
| 41 | 45.136 | 4.459 | 2.716 | 91 | 77.372 | 5.567 | 3.282 |
| 42 | 35.633 | 3.644 | 2.616 | 92 | 49.024 | 7.370 | 2.590 |
| 43 | 53.743 | 3.732 | 3.208 | 93 | 40.563 | 10.219 | 2.237 |
| 44 | 62.617 | 7.021 | 2.723 | 94 | 10.977 | 8.997 | 1.417 |
| 45 | 75.473 | 5.992 | 3.210 | 95 | 35.197 | 10.157 | 2.351 |
| 46 | 53.996 | 5.227 | 2.869 | 96 | 28.965 | 7.370 | 2.877 |
| 47 | 43.640 | 4.817 | 2.671 | 97 | 53.621 | 6.380 | 3.468 |
| 48 | 24.954 | 4.270 | 2.134 | 98 | 26.744 | 6.187 | 2.715 |
| 49 | 27.527 | 5.949 | 1.975 | | | | |

# 5. CONCULSION AND RECOMMENDATION

## 5.1. Conclusion

According to this study conclusion the Urgent Phase works have reduced the risk of irrigation canal being flooded by the Koga River. Considerable further inputs are required to maintain the present level of flood protection, increase the level of protection to that required by a canal and also to secure the protection by the construction of further lengths of river bank protection works. The dam breach parameters were estimated using three most currently used regression equations, i.e. Macdonald and Langridge-Monopolis (1984), Von Thun and Gillette (1990) and Froehlich (2008).Flood management planning and implementation should consider information regarding consequential damages if a dam fails. This should involve accurate estimation of the severity and extent of dam break flood prior to the construction of a dam. Therefore, damages that could occur in human and animal life, the surrounding settlements, agricultural areas, and industries can be minimized and even controlled. .

A Flood Map informs for the community about the local flood risk. It helps set minimum floodplain standards so that the community builds safely and resiliently. It determines the cost of flood insurance, which helps property owners to financially protect themselves against flooding.

The dam breach modeling and flood maps results in this study can adequately inform the user the extents of hydrological and seismic induced dam break and the subsequent flood. In almost all scenarios considered in this study, the flood inundation extent is not significantly different except the depth of flood.

The following conclusions can be drawn from the overall study.

- The dam site PMF was 570$m^3$/s obtained using Hershifield's technique whereas using HEC HMS model the Dam site PMF was 537 $m^3$/s.
- The dam is safe from breaching out due to overtopping failure mode, since the PMF does not overtop the dam due to that scaled the PMF two times.

- The depth of the flood depth in overtopping ranges from 0 to 16 m on the flood plains.
- The velocity mapping in piping and overtopping failures ranges from 0 to 6 m/s and 0 to 11 m/sec respectively.
- The breach outflow inundates area of overtopping and piping is 10.2 and 9.2 $km^2$ downstream of the dam respectively.
- The right side irrigation farm at downstream are the main canal structure is inundated whereas the left and right side farms and settlement are partly flooded.
- Resettlement villages around the flooding area.
- The town is drowned while some of part of the town is submerged at the downstream.
- Flood depth grids can help identify potentially compromised evacuation or emergency routes in the event of a flood.
- Flood hazards Analyzing and precisely determining the magnitude and extent of flood on a specific area helps as a good quality input data for preparing the flood extent maps
- The flood maps in turn are used to delineate the areas at risk and help to revise the settlement and infrastructure planning in the area.
- Flood depth can help identify potentially compromised evacuation or emergency routes in the event of a flood.
- WSEL can help inform mitigation efforts and the elevation of individual structures. Some infrastructure, require that certain flood protection measures.
- Velocity mapping can help identify areas of swift-moving water where scour or erosion may be an issue.

## 5.2. Recommendation

Floodplain managers and emergency management personnel may then utilize the resulting contingencies to protect against the loss of life and property damage. After analyzing the results obtained in this research, the following recommendations are Suggested Finally, in order to improve the results obtained in this analysis, it is recommended to

- Use fine resolution DEM or Survey Data
- Further study the economic and life damage consequences in detail
- The mitigating potential of some structural measures could be further analyzed and planned to minimize the damage (for example, If Koga dam breaches, the Debre markos –Bahir Dar road could be protected by a dike of less than 1km) and Koga irrigation project
- Effective dam monitoring system should be in place in the future
- This result should be supplemented with effective real time/ near real time flood forecasting and earthquake warning so that comprehensive warning system would be developed and early warning system would be effective.
- Resettlement action plan or structural mitigation is which one best for further analysis study.
- Re-channelizing streams and river training works are essential in making natural drains more stable
- Flood protection structures such as dykes can be proposed based on the result of the research
- Settlements that are in highly hazardous areas will be sorted out for resettlement action plan
- The structural flood control measurement to be recommended is to construct flood dike and flood gate. The non-structural measurement one is to improve watershed management and socialization of flood awareness.

# 6. REFERENCES


Ackerman, C. T.2011 HEC-Geo RAS GIS tools for support of HEC-RAS using ArcGIS© user's manual version 4.3. 93: Davis, Calif. US Army Corps of Engineers, Hydrologic Engineering Center, CPD-83.

Adams, T., Chen, S., Davis, R., Schade, T., & Lee, D. 2010 The Ohio river community HEC-RAS model. In World Environmental and Water Resources Congress 2010: Challenges of Change (pp. 1512-1523).

Ahmad Asnaashari, D. M. (2014). DAM BREACH INUNDATION ANALYSIS USING HEC-RAS AND GIS. CDA 2014 Annual Conference. Banff, Alberta: CANADIAN DAM ASSOCIATION.

Basheer, T. A., Wayayok, A., Yusuf, B., & KAMAL, M. R. 2017 Dam Breach parameters and their influence on flood hydrographs for Mosul Dam. Journal of Engineering Science and Technology, 12(11), 2896-2908.

Brunner, G. W. (not dated). Hydraulic Model Development for Dam Break Studies. Davis: U.S Army Corps of Engineers Hydrologic Engineering Center.

Cameron T. Ackerman, P.E. and Gary W. Brunner, P.E. Hydraulic Engineer and Senior Technical Hydraulic Engineer, Hydrologic Engineering Center, Davis, CA 95616 Dam Failure Analysis Using HEC-RAS and HEC-Geo RAS

Canale, L., & Wüthrich, D. 2014. Dam Break Analysis for Serra degli Ulivi Dam (No. CONF).

Chow V.T. 1951. A general formula for hydrologic frequency analysis. Transactions American Geophysical Union32: 231–237.

Chow, V. T., Open Channel Hydraulics, Caldwell, New Jersey, USA: The Blackburn Press, 1959.

Colorado Dam Safety Office/CDSO (Feb. 10, 2010), "Guidelines for Dam Breach Analysis", Office of the State Engineer, Dam Safety Branch, Colorado; website: http://water.state.co.us

Cunderlik, J. M., & Simonovic, S. P. (2007, August). Hydrologic models for inverse climate change impact modeling. In *Proceedings of the 18th Canadian Hydrotechnical Conference, Challenges for Water Resources Engineering in a Changing World Winnipeg*.

Dam, K. G., & Abidin, N. B. Z. 2015. Dam Break Flood Inundation Modelling.

ERA, 2013 Drainage Design Manual, Ethiopian Roads Authority, 2013

FEMA, 2014. Guidance for Flood Risk Analysis and Mapping: Flood Depth and Analysis Grids

Froehlich, D. C. 2008, Embankment Dam Breach Parameters and Their Uncertainties, Journal of Hydraulic Engineering, Vol. 134, No. 12,.

Gee, D. Michael, Senior Hydraulic Engineer, Corps of Engineers Hydrologic Engineering Center, 2010. USE OF BREACH PROCESS MODELS TO ESTIMATE HEC-RAS DAM BREACH PARAMETERS 609 2nd St., Davis, CA 95616; email: michael.gee@usace.army.mil

Hershfield DM. 1961. Estimating the probable maximum precipitation. Proceedings American Society of Civil Engineers, Journal Hydraulics Division87(HY5): 99–106

Hershfield DM. 1965. Method for estimating probable maximum precipitation. Journal American Water works Association 57: 965–972.

Hydrologic Engineering Center, 2014 Using HEC-RAS for Dam Break Studies, TD-39, U.S. Army Corps of Engineers, Davis, CA, Aug.

Hydrologic Engineering Center, HEC-Geo RAS, GIS Tools for Support of HEC-RAS using GIS, User's Manual, 2012,CPD-83, Version 10, U.S. Army Corps of Engineers, Davis, CA, may..

Hydrologic Engineering Center, HEC-RAS, River Analysis System Hydraulic Reference Manual, CPD-69, Version 4.1, U.S. 2016, Army Corps of Engineers, Davis, CA, Jan..

Hydrologic Engineering Center, HEC-RAS, River Analysis System User's Manual, CPD-68, Version 4.1, 2010 U.S. Army Corps of Engineers, Davis, CA, Jan..

Koga Dam and Irrigation Project - Interim Report. Mott MacDonald in association with MCE and WWDSE, May 2004.

MacDonald, Thomas C.and Jennifer Langridge-Monopolis, 1984, "Breaching Characteristics of Dam Failures," Journal of Hydraulic Engineering, Vol. 110, No. 5, p. 567-586.

D. Michael Gee1 Senior Hydraulic Engineer, Corps of Engineers Hydrologic Engineering Center, 609 2nd St., Davis, CA 95616; email:michael.gee@usace.army.mil. Comparison of Dam Breach Parameter Estimators

Mott MacDonald in association with MCE and WWDSE, 10 November 2004 ,KOGA IRRIGATION AND WATERSHED MANAGEMENT PROJECT Koga Irrigation and Drainage System. Hydrology Factual Report.

Mott MacDonald in association with MCE and WWDSE 10 April 2006 Koga Dam and Irrigation Project Design Report.Part 1: Koga Dam

Mrunal M. Joshi and Dr. S. S. Shahapure 2017 Study of Two Dimensional Dam Break Analysis Using HECRAS for Vir Dam, Civil Engineering Department, Rajarshi Shahu College of Engineering, Tathawade, Pune , India

Purvang. H. Pandya Thakor Dixitsinh Jitaji 2013 A Brief Review of Method Available for Dam Break Analysis.indian journal of research

Singh, V. a. (1998). Retrieved June 27, 2014, from /American Society of Civil Engineers: http://dx.doi.org/10.1061/(ASCE)0733-9429(1988)114:1(21)

Sun, Zhandong, Qun Huang, Christian Opp, Thomas Hennig, and Ulf Marold. "Impacts and implications of major changes caused by the Three Gorges Dam in the middle reaches of the Yangtze River, China." *Water resources management* 26, no. 12 (2012): 3367-3378.

Tony L. Wahl, Hydraulic Engineer (June 27 - July 1, 2010), "Dam Breach Modeling an Overview of Analysis Methods", Bureau of Reclamation 2nd Joint Federal Interagency Conference, Las Vegas, Denver, CO, twahl@usbr.gov

USACE (2016). HEC-RAS hydraulic reference manual. Version 5.0.1, U.S. Army Corps of Engineers, Hydrologic Engineering Center.

USACE (2014). Using HEC-RAS for dam break studies. Report No. TD-39. U.S. Army Corps of Engineers, Hydrologic Engineering Center. Retrieved March 20, 2017, from http://www.hec.usace.army.mil/publications

USBR, 1987 Design of Small Dams, Third Edition. United State Department of the Interior, Bureau of Reclamation, Denver, Colorado, 1987.

USGS 2005a. U.S. Geological Survey, 199904, Major Dams of the United States: U.S. Geological Survey, Reston, VA. (http://nationalatlas.gov/atlasftp.html)

Von Thun, J.L.; and Gillette, D.R 1990 Guidance on breach parameters. Unpublished internal document, U.S. Bureau of Reclamation, Denver, Colorado

Wahl, T.L. 1998 Prediction of embankment dam breach parameters – a literature review and needs assessment. Dam Safety Report DSO-98-004, U.S. Bureau of Reclamation. Retrieved March 20, 2017, from https://www. usbr.gov

Wayne J. Graham, P.E, 1999. A Procedure for Estimating Loss of Life Caused by Dam Failure DSO-99-06. Sedimentation & River Hydraulics September. U.S. Department of Interior Bureau of Reclamation Dam Safety Office Denver, Colorado

World Meteorological Organization (WMO), 1986. Manual for Estimation of Probable Maximum Precipitation. Operational Hydrology Report no. 1, WMO No. 332.

Wurbs, R.A. 1987 Dam-breach flood wave models. Journal of Hydraulic Engineering, 113(1), 29-46.

Xiong, Y. 2011. A dam break analysis using HEC-RAS. Journal of Water Resource and Protection, 3(6), 370-379.

Xu, Y. and Zhang, L.M., (2009), "Breaching Parameters for Earth and Rockfill Dams," Journal of Geotechnical and Geoenvironmental Engineering, ASCE, pp. 1957-1970, December 2009.

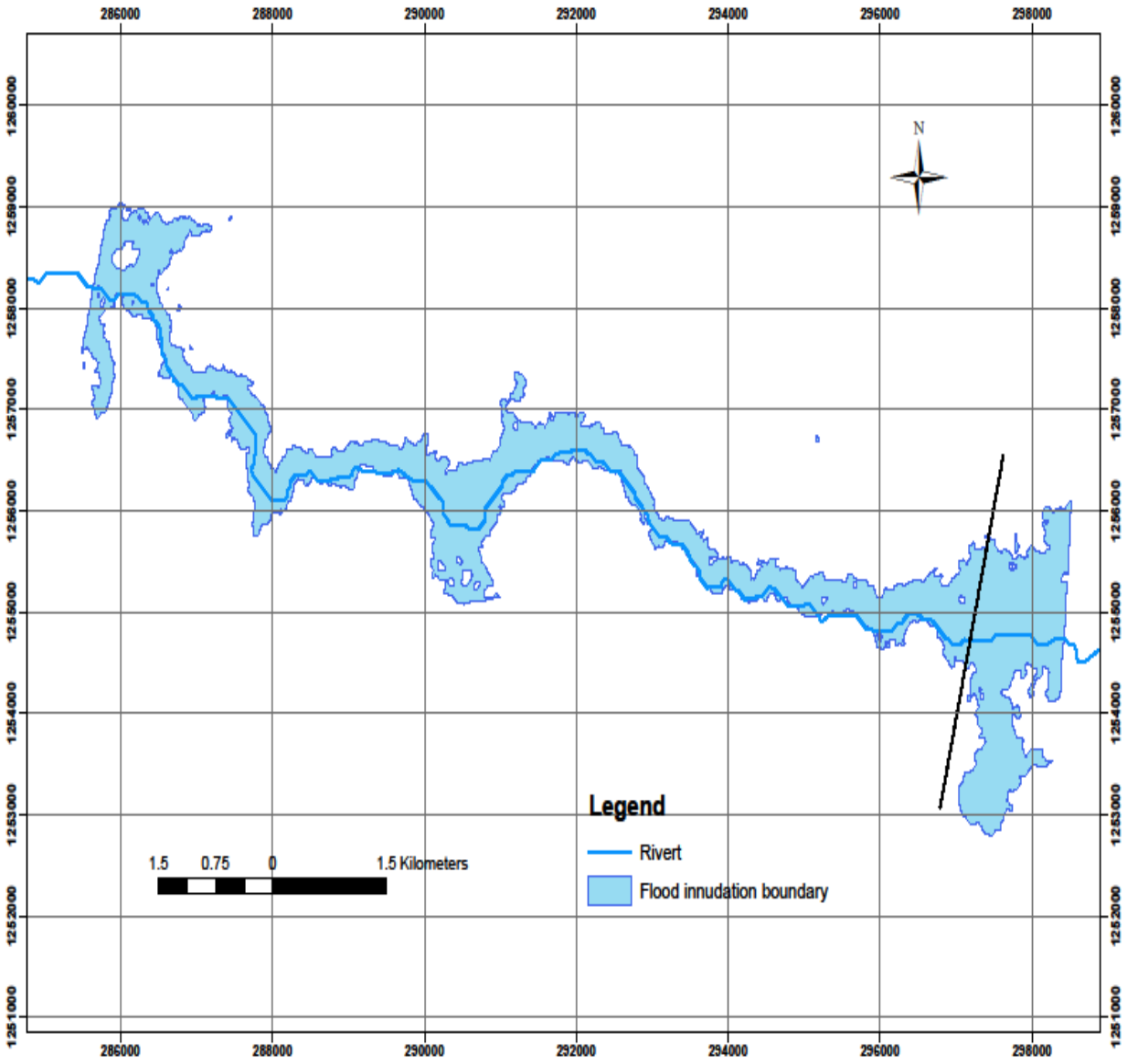
Yared Michael, 2015 MSc thesis Arba Minch University Dam Breach Modeling and Flood Inundation Mapping: a case study on Kesem Dam

Zagonjolli, M. 2007 Dam break Modeling, Risk Assessment and Uncertainty Analysis for Flood Mitigation. ISBN 9 780415 455947 (Taylor & Francis Group). London, UK: Taylor & Francis.

# 7. ANNEX

**Annex Table 7. 1: station annual maximum precipitation**

| | meshenti | dangla | adet | enjibara | tilili | fnotslam | sekela | |
|---|---|---|---|---|---|---|---|---|
| | yr mx(mm) | yr mx(mm) | yr mx(mm) | yr mx(mm) | yr mx(mm) | yr mx(mm) | yr mx(mm) | Average |
| 1986 | 1399.7 | 1585.2 | 1563.8 | 1952.4 | 1683.3 | 1239.7 | 1590.5 | 1573.5 |
| 1987 | 1614.4 | 1581.9 | 1292.5 | 2380.5 | 1937.8 | 1106.6 | 1719.9 | 1661.9 |
| 1988 | 1248.6 | 1786.1 | 1298.4 | 2297.6 | 1823.2 | 1416.7 | 1971.2 | 1691.7 |
| 1989 | 1401.9 | 1646.2 | 1232.3 | 2556.3 | 2159.2 | 1062.8 | 2274.5 | 1761.9 |
| 1990 | 1165.8 | 1559.5 | 939.8 | 1990.3 | 2496.8 | 1037.7 | 2010.7 | 1600.1 |
| 1991 | 1638.2 | 2001.6 | 1646.4 | 1879.0 | 2086.8 | 1560.8 | 995.2 | 1686.9 |
| 1992 | 1258.5 | 1422.2 | 1434.9 | 2186.2 | 1509.8 | 397.0 | 930.2 | 1305.5 |
| 1993 | 1304.9 | 1715.6 | 1193.7 | 2506.4 | 1725.8 | 1355.3 | 1490.5 | 1613.2 |
| 1994 | 1290.7 | 1317.9 | 1271.9 | 2231.6 | 1517.2 | 1192.1 | 1328.2 | 1450.0 |
| 1995 | 1059.3 | 1184.6 | 1347.6 | 1953.6 | 2511.2 | 1208.1 | 1646.4 | 1558.7 |
| 1996 | 1540.3 | 1654.7 | 1675.1 | 2386.9 | 1764.3 | 1253.3 | 1899.7 | 1739.2 |
| 1997 | 1228.6 | 1667.2 | 1381.2 | 2816.5 | 1964.9 | 1608.4 | 2233.0 | 1842.8 |
| 1998 | 1368.1 | 1577.4 | 1347.6 | 2301.2 | 2556.6 | 2050.6 | 1857.1 | 1865.5 |
| 1999 | 1576.3 | 1959.4 | 1156.6 | 2709.6 | 2076.3 | 2300.6 | 2267.2 | 2006.6 |
| 2000 | 1544.0 | 1895.7 | 1115.1 | 2570.9 | 2075.3 | 1912.9 | 1935.4 | 1864.2 |
| 2001 | 1404.7 | 1411.1 | 1358.8 | 2285.0 | 1882.4 | 1899.8 | 1958.3 | 1742.9 |
| 2002 | 1190.6 | 1349.8 | 955.7 | 2157.0 | 1900.4 | 1847.4 | 1481.6 | 1554.7 |
| 2003 | 1461.0 | 1369.4 | 1118.2 | 2106.4 | 1743.0 | 1780.8 | 1801.8 | 1625.8 |
| 2004 | 1186.9 | 1627.9 | 1132.3 | 2201.7 | 1889.5 | 1792.2 | 1832.2 | 1666.1 |
| 2005 | 1181.5 | 1405.4 | 1130.7 | 2194.8 | 1954.5 | 1952.2 | 1943.8 | 1680.4 |
| 2006 | 2043.1 | 1869.0 | 1620.2 | 2759.2 | 2303.0 | 1347.7 | 2349.8 | 2041.7 |
| 2007 | 1451.2 | 1478.7 | 1151.1 | 2157.7 | 1967.7 | 1282.5 | 1932.4 | 1631.6 |
| 2008 | 1243.2 | 1858.1 | 1399.3 | 2483.8 | 2213.6 | 1393.2 | 2072.1 | 1809.0 |
| 2009 | 929.8 | 1454.6 | 1031.5 | 2136.2 | 1690.1 | 1370.4 | 1894.1 | 1501.0 |
| 2010 | 1295.2 | 1404.1 | 1174.5 | 2358.5 | 2216.3 | 1342.4 | 2775.4 | 1795.2 |
| 2011 | 1478.0 | 1599.2 | 1140.3 | 2349.1 | 2442.0 | 1449.8 | 1854.4 | 1759.0 |
| 2012 | 1561.1 | 1640.4 | 1135.5 | 2484.6 | 1943.4 | 1366.5 | 1451.6 | 1654.7 |
| 2013 | 1402.5 | 1945.4 | 1175.5 | 3335.7 | 1978.5 | 1323.5 | 1354.8 | 1788.0 |
| 2014 | 1522.5 | 2008.2 | 1246.7 | 2635.6 | 2895.0 | 1332.3 | 1927.0 | 1938.2 |
| 2015 | 1849.8 | 1716.3 | 1139.5 | 2136.4 | 3455.2 | 1305.7 | 1887.3 | 1927.2 |

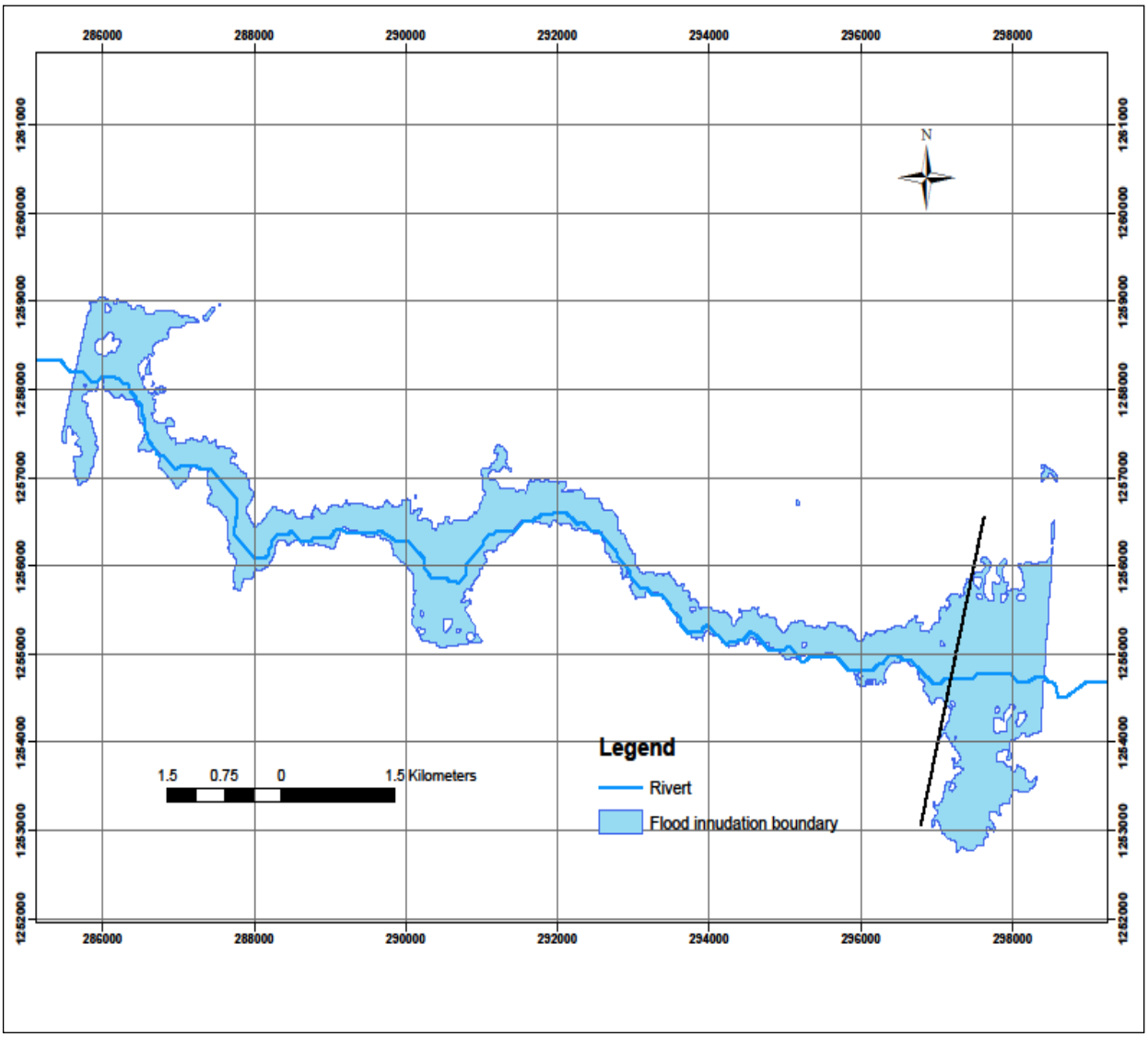



**Annex Figure 7. 1: Flood mapping area by overtopping.**





**Annex Figure 7. 2: Intake Tower and Spillway of the Koga Dam**




**Annex Figure 7. 3: Flood mapping area by overtopping.**



**Annex Figure 7. 4: Koga Dam crest**

**Annex Table 7. 2: Probability Fitting a Distribution Kolmogorov _Simonov test**

| Kolmogorov-Smirnov test for: All data | a=1% | a=5% | a=10% | Attained a | DMax |
|---|---|---|---|---|---|
| Normal | ACCEPT | ACCEPT | ACCEPT | 65.49% | 0.12663 |
| Normal (L-Moments) | ACCEPT | ACCEPT | ACCEPT | 69.38% | 0.1224 |
| LogNormal | ACCEPT | ACCEPT | ACCEPT | 88.86% | 0.09875 |
| Galton | ACCEPT | ACCEPT | ACCEPT | 73.68% | 0.11768 |
| Exponential | ACCEPT | ACCEPT | ACCEPT | 36.81% | 0.16033 |
| Exponential (L-Moments) | ACCEPT | ACCEPT | ACCEPT | 48.82% | 0.14516 |
| Gamma | ACCEPT | ACCEPT | ACCEPT | 83.03% | 0.10671 |
| Pearson III | ACCEPT | ACCEPT | ACCEPT | 73.81% | 0.11753 |
| Log Pearson III | ACCEPT | ACCEPT | ACCEPT | 90.01% | 0.09696 |
| EV1-Max (Gumbel) | ACCEPT | ACCEPT | ACCEPT | 98.98% | 0.07627 |
| EV2-Max | ACCEPT | ACCEPT | ACCEPT | 37.28% | 0.15969 |
| EV1-Min (Gumbel) | ACCEPT | ACCEPT | ACCEPT | 20.42% | 0.18767 |
| EV3-Min (Weibull) | ACCEPT | ACCEPT | ACCEPT | 44.42% | 0.15046 |
| GEV-Max | ACCEPT | ACCEPT | ACCEPT | 79.45% | 0.11108 |
| GEV-Min | ACCEPT | ACCEPT | ACCEPT | 78.24% | 0.1125 |
| Pareto | ACCEPT | ACCEPT | ACCEPT | 65.63% | 0.12648 |
| GEV-Max (L-Moments) | ACCEPT | ACCEPT | ACCEPT | 87.40% | 0.10088 |
| GEV-Min (L-Moments) | ACCEPT | ACCEPT | ACCEPT | 88.47% | 0.09933 |
| EV1-Max (Gumbel, L-Moments) | ACCEPT | ACCEPT | ACCEPT | 74.78% | 0.11645 |
| EV2-Max (L-Momments) | ACCEPT | ACCEPT | ACCEPT | 48.12% | 0.14599 |
| EV1-Min (Gumbel, L-Moments) | ACCEPT | ACCEPT | ACCEPT | 24.70% | 0.17931 |
| EV3-Min (Weibull, L-Moments) | ACCEPT | ACCEPT | ACCEPT | 49.64% | 0.14421 |
| Pareto (L-Moments) | ACCEPT | ACCEPT | ACCEPT | 98.98% | 0.07334 |
| GEV-Max (kappa specified) | ACCEPT | ACCEPT | ACCEPT | 32.71% | 0.1662 |
| GEV-Min (kappa specified) | ACCEPT | ACCEPT | ACCEPT | 43.81% | 0.15121 |
| GEV-Max (kappa specified, L-Moments) | ACCEPT | ACCEPT | ACCEPT | 47.43% | 0.14681 |
| GEV-Min (kappa specified, L-Moments) | ACCEPT | ACCEPT | ACCEPT | 47.40% | 0.14685 |

**Annex Table 7. 3: Probability Fitting a Distribution test by X-square test**

| X-Square test for All data | a=1% | a=5% | a=10% | Attained a | Pearson Param. |
|---|---|---|---|---|---|
| Normal | ACCEPT | ACCEPT | ACCEPT | 11.46% | 4.33333 |
| Normal (L-Moments) | ACCEPT | ACCEPT | ACCEPT | 11.46% | 4.33333 |
| LogNormal | ACCEPT | ACCEPT | REJECT | 8.21% | 5 |
| Galton | ACCEPT | REJECT | REJECT | 2.53% | 5 |
| Exponential | ACCEPT | ACCEPT | ACCEPT | 26.36% | 2.66667 |

| | | | | | |
|---|---|---|---|---|---|
| Exponential (L-Moments) | ACCEPT | ACCEPT | ACCEPT | 36.79% | 2 |
| Gamma | ACCEPT | ACCEPT | REJECT | 8.21% | 5 |
| Pearson III | | | | | |
| Log Pearson III | ACCEPT | REJECT | REJECT | 2.53% | 5 |
| EV1-Max (Gumbel) | ACCEPT | ACCEPT | ACCEPT | 6.66% | 2.33333 |
| EV2-Max | ACCEPT | ACCEPT | REJECT | 9.70% | 4.66667 |
| EV1-Min (Gumbel) | ACCEPT | ACCEPT | REJECT | 6.95% | 5.33333 |
| EV3-Min (Weibull) | ACCEPT | ACCEPT | ACCEPT | 11.46% | 4.33333 |
| GEV-Max | ACCEPT | REJECT | REJECT | 3.74% | 4.33333 |
| GEV-Min | ACCEPT | REJECT | REJECT | 3.74% | 4.33333 |
| Pareto | ACCEPT | ACCEPT | ACCEPT | 11.46% | 4.33333 |
| GEV-Max (L-Moments) | ACCEPT | REJECT | REJECT | 3.74% | 4.33333 |
| GEV-Min (L-Moments) | ACCEPT | REJECT | REJECT | 3.74% | 4.33333 |
| EV1-Max (Gumbel, L-Moments) | ACCEPT | ACCEPT | ACCEPT | 22.31% | 3 |
| EV2-Max (L-Momments) | ACCEPT | ACCEPT | ACCEPT | 36.79% | 2 |
| EV1-Min (Gumbel, L-Moments) | ACCEPT | ACCEPT | REJECT | 9.70% | 4.66667 |
| EV3-Min (Weibull, L-Moments) | ACCEPT | ACCEPT | ACCEPT | 11.46% | 4.33333 |
| Pareto (L-Moments) | ACCEPT | ACCEPT | ACCEPT | 12.66% | 2.33333 |
| GEV-Max (kappa specified) | ACCEPT | ACCEPT | REJECT | 9.70% | 4.66667 |
| GEV-Min (kappa specified) | ACCEPT | ACCEPT | ACCEPT | 11.46% | 4.33333 |
| GEV-Max (kappa specified, L-Moments) | ACCEPT | ACCEPT | ACCEPT | 36.79% | 2 |
| GEV-Min (kappa specified, L-Moments) | ACCEPT | ACCEPT | ACCEPT | 11.46% | 4.33333 |

**Annex Table 7. 4: Dimensional unit hydrograph**

| | | | | |
|---|---|---|---|---|
| **SCS Dimensionless UH** | | | | Interpolation |

| **Method** | | | | | |
|---|---|---|---|---|---|
| | | Koga Dam | | To 2hrs time step | |
| ti/tp | q/qp | t=tp*t/tp | q=qp*q/qp | t | q |
| 0 | 0 | 0 | 0.00 | 0 | 0.00 |
| 0.1 | 0.03 | 1 | 1.39 | 2 | 8.82 |
| 0.2 | 0.1 | 1 | 4.64 | 4 | 21.81 |
| 0.3 | 0.19 | 2 | 8.82 | 6 | 45.94 |
| 0.4 | 0.31 | 3 | 14.39 | 8 | 45.94 |
| 0.5 | 0.47 | 4 | 21.81 | 10 | 36.20 |
| 0.6 | 0.66 | 4 | 30.63 | 12 | 21.35 |
| 0.7 | 0.82 | 5 | 38.05 | 14 | 15.31 |
| 0.8 | 0.93 | 6 | 43.16 | 16 | 9.61 |
| 0.9 | 0.99 | 6 | 45.94 | 18 | 5.52 |
| 1 | 1 | 7 | 46.40 | 20 | 3.57 |
| 1.1 | 0.99 | 8 | 45.94 | 22 | 2.06 |
| 1.2 | 0.93 | 9 | 43.16 | 24 | 1.35 |
| 1.3 | 0.86 | 9 | 39.91 | 26 | 1.16 |
| 1.4 | 0.78 | 10 | 36.20 | 28 | 0.57 |
| 1.5 | 0.68 | 11 | 31.56 | 30 | 0.43 |
| 1.6 | 0.56 | 11 | 25.99 | 32 | 0.23 |
| 1.7 | 0.46 | 12 | 21.35 | 34 | 0.17 |
| 1.8 | 0.39 | 13 | 18.10 | 36 | 0.00 |
| 1.9 | 0.33 | 14 | 15.31 | 38 | 0.00 |
| 2 | 0.28 | 14 | 12.99 | 40 | 0.00 |
| 2.2 | 0.207 | 16 | 9.61 | 42 | 0.00 |
| 2.4 | 0.147 | 17 | 6.82 | 44 | 0.00 |
| 2.6 | 0.107 | 19 | 4.97 | 46 | 0.00 |
| 2.8 | 0.077 | 20 | 3.57 | 48 | 0.00 |
| 3 | 0.055 | 21 | 2.55 | 50 | 0.00 |
| 3.2 | 0.04 | 23 | 1.86 | 52 | 0.00 |
| 3.4 | 0.029 | 24 | 1.35 | 54 | 0.00 |
| 3.6 | 0.025 | 26 | 1.16 | 56 | |
| 3.8 | 0.015 | 27 | 0.70 | 58 | |
| 4 | 0.011 | 29 | 0.51 | 60 | |
| 4.5 | 0.005 | 32 | 0.23 | 62 | |
| 5 | 0 | 36 | 0.00 | 64 | |

**Annex Table 7. 5: percent of accumulated rainfall and duration**

| % of rainfall and duration | | % of rainfall and duration | |
|---|---|---|---|
| Duration (%) | Accumulated RF (%) | Duration (%) | Accumulated RF (%) |
| 0.0 | 0.00 | 52.1 | 43.18 |
| 2.1 | 1.91 | 54.2 | 45.80 |
| 4.2 | 2.67 | 56.3 | 47.71 |
| 6.3 | 4.27 | 58.3 | 49.62 |
| 8.3 | 5.73 | 60.4 | 51.53 |
| 10.4 | 7.18 | 62.5 | 53.44 |
| 12.5 | 8.63 | 64.6 | 55.34 |
| 14.6 | 10.08 | 66.7 | 57.25 |
| 16.7 | 11.53 | 68.8 | 59.16 |
| 18.8 | 12.98 | 70.8 | 61.07 |
| 20.8 | 15.27 | 72.9 | 63.74 |
| 22.9 | 17.00 | 75.0 | 66.41 |
| 25.0 | 18.87 | 77.1 | 69.08 |
| 27.1 | 20.74 | 79.2 | 71.76 |
| 29.2 | 22.61 | 81.3 | 74.43 |
| 31.3 | 24.48 | 83.3 | 77.10 |

| | | | |
|---|---|---|---|
| 33.3 | 26.35 | 85.4 | 79.77 |
| 35.4 | 28.22 | 87.5 | 82.44 |
| 37.5 | 30.09 | 89.6 | 85.11 |
| 39.6 | 31.96 | 91.7 | 87.79 |
| 41.7 | 33.83 | 93.8 | 90.46 |
| 43.8 | 35.70 | 95.8 | 93.13 |
| 45.8 | 37.57 | 97.9 | 95.80 |
| 47.9 | 39.44 | 100.0 | 100.00 |
| 50.0 | 41.31 | | |

**Annex Table 7. 6**: Unit Hydrograph for Koga dam site catchment based on CSC Method

| Time(hrs) | Discharge (cms) | RF0 | RF2 | RF4 | RF6 | RF8 | RF10 | RF12 | RF14 | RF16 | RF18 | RF20 | RF22 | RF24 | Commuluted DRH | Baseflow (cms) | Flood Hydrograph ordinates (cms) |
|---|---|---|---|---|---|---|---|---|---|---|---|---|---|---|---|---|---|
| | | 0.00 | 1.31 | 1.86 | 1.86 | 1.91 | 2.91 | 3.41 | 2.91 | 2.41 | 2.13 | 1.86 | 1.81 | 1.28 | | | |
| 0 | 0.000 | 0.00 | | | | | | | | | | | | | 0.00 | 8.87 | 8.87 |
| 2 | 8.817 | 0.00 | 0.00 | | | | | | | | | | | | 0.00 | 8.87 | 8.87 |
| 4 | 21.810 | 0.00 | 11.52 | 0.00 | | | | | | | | | | | 11.52 | 8.87 | 20.39 |
| 6 | 45.940 | 0.00 | 28.51 | 16.39 | 0.00 | | | | | | | | | | 44.90 | 8.87 | 53.77 |
| 8 | 45.940 | 0.00 | 60.05 | 40.55 | 16.39 | 0.00 | | | | | | | | | 116.99 | 8.87 | 125.86 |
| 10 | 36.196 | 0.00 | 60.05 | 85.41 | 40.55 | 16.83 | 0.00 | | | | | | | | 202.84 | 8.87 | 211.71 |
| 12 | 21.346 | 0.00 | 47.31 | 85.41 | 85.41 | 41.64 | 25.68 | 0.00 | | | | | | | 285.45 | 8.87 | 294.32 |
| 14 | 15.313 | 0.00 | 27.90 | 67.29 | 85.41 | 87.71 | 63.53 | 30.11 | 0.00 | | | | | | 361.96 | 8.87 | 370.83 |
| 16 | 9.606 | 0.00 | 20.02 | 39.68 | 67.29 | 87.71 | 133.83 | 74.48 | 25.68 | 0.00 | | | | | 448.70 | 8.87 | 457.57 |
| 18 | 5.520 | 0.00 | 12.56 | 28.47 | 39.68 | 69.11 | 133.83 | 156.88 | 63.53 | 21.26 | 0.00 | | | | 525.32 | 8.87 | 534.19 |
| 20 | 3.573 | 0.00 | 7.21 | 17.86 | 28.47 | 40.76 | 105.44 | 156.88 | 133.83 | 52.59 | 18.79 | 0.00 | | | 561.82 | 8.87 | **570.69** |
| 22 | 2.064 | 0.00 | 4.67 | 10.26 | 17.86 | 29.24 | 62.18 | 123.60 | 133.83 | 110.77 | 46.48 | 16.39 | 0.00 | | 555.28 | 8.87 | 564.15 |

| | | | | | | | | | | | | | | | | | |
|---|---|---|---|---|---|---|---|---|---|---|---|---|---|---|---|---|---|
| 24 | 1.346 | 0.00 | 2.70 | 6.64 | 10.26 | 18.34 | 44.61 | 72.89 | 105.44 | 110.77 | 97.90 | 40.55 | 15.99 | 0.00 | 526.09 | 8.87 | 534.96 |
| 26 | 1.160 | 0.00 | 1.76 | 3.84 | 6.64 | 10.54 | 27.98 | 52.29 | 62.18 | 87.27 | 97.90 | 85.41 | 39.54 | 11.30 | 486.66 | 8.87 | 495.53 |
| 28 | 0.566 | 0.00 | 1.52 | 2.50 | 3.84 | 6.82 | 16.08 | 32.80 | 44.61 | 51.47 | 77.13 | 85.41 | 83.30 | 27.96 | 433.43 | 8.87 | 442.30 |
| 30 | 0.432 | 0.00 | 0.74 | 2.16 | 2.50 | 3.94 | 10.41 | 18.85 | 27.98 | 36.92 | 45.49 | 67.29 | 83.30 | 58.89 | 358.47 | 8.87 | 367.34 |
| 32 | 0.232 | 0.00 | 0.57 | 1.05 | 2.16 | 2.57 | 6.01 | 12.20 | 16.08 | 23.16 | 32.63 | 39.68 | 65.63 | 58.89 | 260.64 | 8.87 | 269.51 |
| 34 | 0.167 | 0.00 | 0.30 | 0.80 | 1.05 | 2.22 | 3.92 | 7.05 | 10.41 | 13.31 | 20.47 | 28.47 | 38.70 | 46.40 | 173.10 | 8.87 | 181.97 |
| 36 | 0.000 | 0.00 | 0.22 | 0.43 | 0.80 | 1.08 | 3.38 | 4.60 | 6.01 | 8.62 | 11.76 | 17.86 | 27.77 | 27.37 | 109.89 | 8.87 | 118.76 |
| 38 | 0.000 | 0.00 | 0.00 | 0.31 | 0.43 | 0.83 | 1.65 | 3.96 | 3.92 | 4.98 | 7.61 | 10.26 | 17.42 | 19.63 | 71.00 | 8.87 | 79.87 |
| 40 | 0.000 | 0.00 | 0.00 | 0.00 | 0.31 | 0.44 | 1.26 | 1.93 | 3.38 | 3.24 | 4.40 | 6.64 | 10.01 | 12.31 | 43.93 | 8.87 | 52.80 |
| 42 | 0.000 | 0.00 | 0.00 | 0.00 | 0.00 | 0.32 | 0.68 | 1.48 | 1.65 | 2.80 | 2.87 | 3.84 | 6.48 | 7.08 | 27.18 | 8.87 | 36.05 |
| 44 | 0.000 | 0.00 | 0.00 | 0.00 | 0.00 | 0.00 | 0.49 | 0.79 | 1.26 | 1.36 | 2.47 | 2.50 | 3.74 | 4.58 | 17.20 | 8.87 | 26.07 |
| 46 | 0.000 | 0.00 | 0.00 | 0.00 | 0.00 | 0.00 | 0.00 | 0.57 | 0.68 | 1.04 | 1.21 | 2.16 | 2.44 | 2.65 | 10.74 | 8.87 | 19.61 |
| 48 | 0.000 | 0.00 | 0.00 | 0.00 | 0.00 | 0.00 | 0.00 | 0.00 | 0.49 | 0.56 | 0.92 | 1.05 | 2.10 | 1.73 | 6.85 | 8.87 | 15.72 |
| 50 | 0.000 | 0.00 | 0.00 | 0.00 | 0.00 | 0.00 | 0.00 | 0.00 | 0.00 | 0.40 | 0.49 | 0.80 | 1.03 | 1.49 | 4.21 | 8.87 | 13.08 |
| 52 | 0.000 | 0.00 | 0.00 | 0.00 | 0.00 | 0.00 | 0.00 | 0.00 | 0.00 | 0.00 | 0.36 | 0.43 | 0.78 | 0.73 | 2.30 | 8.87 | 11.17 |
| 54 | 0.000 | 0.00 | 0.00 | 0.00 | 0.00 | 0.00 | 0.00 | 0.00 | 0.00 | 0.00 | 0.00 | 0.31 | 0.42 | 0.55 | 1.29 | 8.87 | 10.15 |
| 56 | 0.000 | 0.00 | 0.00 | 0.00 | 0.00 | 0.00 | 0.00 | 0.00 | 0.00 | 0.00 | 0.00 | 0.00 | 0.30 | 0.30 | 0.60 | 8.87 | 9.47 |
| 58 | 0.000 | 0.00 | 0.00 | 0.00 | 0.00 | 0.00 | 0.00 | 0.00 | 0.00 | 0.00 | 0.00 | 0.00 | 0.00 | 0.21 | 0.21 | 8.87 | 9.08 |
| 60 | 0.000 | 0.00 | 0.00 | 0.00 | 0.00 | 0.00 | 0.00 | 0.00 | 0.00 | 0.00 | 0.00 | 0.00 | 0.00 | 0.00 | 0.00 | 8.87 | 8.87 |
| 62 | 0.000 | 0.00 | 0.00 | 0.00 | 0.00 | 0.00 | 0.00 | 0.00 | 0.00 | 0.00 | 0.00 | 0.00 | 0.00 | 0.00 | 0.00 | 8.87 | 8.87 |
| 64 | 0.000 | 0.00 | 0.00 | 0.00 | 0.00 | 0.00 | 0.00 | 0.00 | 0.00 | 0.00 | 0.00 | 0.00 | 0.00 | 0.00 | 0.00 | 8.87 | 8.87 |
| 66 | 0.000 | 0.00 | 0.00 | 0.00 | 0.00 | 0.00 | 0.00 | 0.00 | 0.00 | 0.00 | 0.00 | 0.00 | 0.00 | 0.00 | 0.00 | 8.87 | 8.87 |
| 68 | 0.000 | 0.00 | 0.00 | 0.00 | 0.00 | 0.00 | 0.00 | 0.00 | 0.00 | 0.00 | 0.00 | 0.00 | 0.00 | 0.00 | 0.00 | 8.87 | 8.87 |
| 70 | 0.000 | 0.00 | 0.00 | 0.00 | 0.00 | 0.00 | 0.00 | 0.00 | 0.00 | 0.00 | 0.00 | 0.00 | 0.00 | 0.00 | 0.00 | 8.87 | 8.87 |

**Annex Table 7. 7: Weighted maximum precipitation**

| Year | ADET | BAHIR | DANGLA | MESHETI | SEKELA | Max precipitation |
|---|---|---|---|---|---|---|
| **1986** | 37.2 | 58.3 | 37.2 | 33.6 | 31.8 | 34.3 |
| **1987** | 42.6 | 47.4 | 48.0 | 36.3 | 31.6 | 37.5 |
| **1988** | 76.1 | 57.1 | 46.0 | 49.8 | 56.3 | 54.7 |
| **1989** | 79.5 | 61.1 | 78.5 | 83.2 | 60.4 | 82.5 |
| **1990** | 37.8 | 114.1 | 76.4 | 63.4 | 40.0 | 58.6 |
| **1991** | 53.9 | 90.5 | 39.6 | 60.3 | 29.0 | 59.1 |
| **1992** | 64.7 | 53.8 | 40.0 | 73.5 | 26.8 | 71.8 |
| **1993** | 41.5 | 71.3 | 43.2 | 59.9 | 54.9 | 56.4 |
| **1994** | 43.6 | 39.0 | 58.8 | 50.1 | 27.0 | 48.9 |
| **1995** | 64.5 | 58.6 | 38.2 | 51.3 | 44.1 | 53.8 |
| **1996** | 56.3 | 51.1 | 47.2 | 60.1 | 40.0 | 59.4 |
| **1997** | 56.6 | 69.2 | 48.5 | 74.0 | 60.0 | 70.7 |
| **1998** | 81.9 | 51.5 | 46.7 | 57.9 | 49.0 | 62.4 |
| **1999** | 40.3 | 64.6 | 68.0 | 79.0 | 84.4 | 71.7 |
| **2000** | 35.8 | 105.3 | 67.0 | 49.4 | 66.9 | 46.8 |
| **2001** | 46.7 | 124.7 | 42.5 | 44.8 | 50.0 | 45.2 |
| **2002** | 46.0 | 89.5 | 39.5 | 47.6 | 48.3 | 47.3 |
| **2003** | 43.6 | 39.0 | 45.0 | 62.9 | 48.1 | 59.3 |
| **2004** | 35.6 | 77.5 | 59.0 | 56.7 | 74.3 | 52.7 |

| | | | | | | |
|---|---|---|---|---|---|---|
| **2005** | 53.8 | 87.1 | 59.8 | 65.4 | 103.5 | 63.2 |
| **2006** | 70.2 | 85.7 | 61.0 | 61.9 | 60.0 | 63.5 |

| Meshenti | Jan | Feb | Mar | Apr | May | Jun | Jul | Aug | Sep | Oct | Nov | Dec | Sum | Mean | Stdev | Var coef |
|---|---|---|---|---|---|---|---|---|---|---|---|---|---|---|---|---|

| | | | | | | |
|---|---|---|---|---|---|---|
| **2007** | 34.2 | 74.1 | 37.0 | 57.9 | 37.3 | 53.5 |
| **2008** | 65.9 | 68.3 | 58.5 | 41.2 | 55.2 | 45.8 |
| **2009** | 38.0 | 64.5 | 57.7 | 41.2 | 55.7 | 40.6 |
| **2010** | 35.4 | 58.1 | 53.8 | 82.3 | 72.3 | 73.5 |
| **2011** | 69.5 | 72.8 | 53.5 | 84.2 | 67.7 | 81.4 |
| **2012** | 45.5 | 96.7 | 53.0 | 91.3 | 29.2 | 82.7 |
| **2013** | 38.8 | 86.4 | 44.3 | 102.9 | 39.1 | 90.9 |
| **2014** | 49.5 | 48.2 | 57.5 | 57.8 | 34.1 | 56.2 |
| **2015** | 38.5 | 66.7 | 47.0 | 84.4 | 45.3 | 75.8 |

Annex Table 7. 8: Monthly rainfall of different station

| | | | | | | | | | | | | | | | | |
|---|---|---|---|---|---|---|---|---|---|---|---|---|---|---|---|---|
| **1986** | 0 | 0.3 | 5.1 | 16.5 | 9.4 | 225.4 | 400 | 271.1 | 171 | 116 | 0 | 0 | 1214 | 101.19 | 136.27 | 1.35 |
| **1987** | 0 | 0.9 | 0 | 8.3 | 235.3 | 215.1 | 219 | 297.5 | 158 | 57.9 | 0 | 0.1 | 1192 | 99.31 | 115.98 | 1.17 |
| **1988** | 3.9 | 24.1 | 0 | 16.4 | 55.9 | 188 | 444 | 304 | 124 | 120 | 21.6 | 8.8 | 1311 | 109.26 | 140.19 | 1.28 |
| **1989** | 0 | 0 | 7.9 | 9.8 | 123 | 222.6 | 387 | 508.7 | 253 | 86.5 | 1.4 | 3.3 | 1603 | 133.55 | 173.32 | 1.3 |
| **1990** | 4.9 | 6 | 1 | 29 | 6.7 | 97.8 | 575 | 452.4 | 206 | 39.3 | 0 | 0 | 1418 | 118.18 | 195.95 | 1.66 |
| **1991** | 0 | 0.93 | 7.85 | 19.5 | 74.76 | 277 | 584 | 330.8 | 298 | 106 | 0.9 | 1.8 | 1702 | 141.81 | 188.78 | 1.33 |
| **1992** | 0 | 0 | 4.3 | 63.7 | 49.9 | 122.6 | 291 | 438.3 | 160 | 203 | 65.3 | 0 | 1399 | 116.55 | 137.06 | 1.18 |
| **1993** | 5.5 | 0 | 15.2 | 24.3 | 117.3 | 222.7 | 479 | 362.4 | 235 | 104 | 18.9 | 0 | 1584 | 132.02 | 160.13 | 1.21 |
| **1994** | 0 | 0.8 | 0 | 21.9 | 103.3 | 190.5 | 322 | 272.8 | 136 | 19.2 | 3.7 | 5.6 | 1077 | 89.71 | 116.07 | 1.29 |
| **1995** | 0 | 4.1 | 8.4 | 19.2 | 76.5 | 277 | 402 | 269.9 | 95.8 | 28.9 | 0 | 4.7 | 1186 | 98.87 | 138.22 | 1.4 |
| **1996** | 0 | 0.7 | 29.5 | 47.5 | 100.9 | 284.7 | 302 | 365.2 | 175 | 47.6 | 26.7 | 0 | 1380 | 115 | 132.78 | 1.15 |
| **1997** | 0 | 0 | 19.4 | 29.13 | 238.11 | 144.5 | 236 | 200.1 | 174 | 150 | 17.2 | 10.1 | 1218 | 101.46 | 97.15 | 0.96 |
| **1998** | 0 | 0 | 18.8 | 0.8 | 122.73 | 196.5 | 423 | 357.6 | 202 | 115 | 1.1 | 0 | 1438 | 119.83 | 148.57 | 1.24 |
| **1999** | 9 | 0 | 0 | 12.9 | 48.1 | 129 | 415 | 463.8 | 196 | 197 | 3 | 0 | 1474 | 122.87 | 165.93 | 1.35 |
| **2000** | 0 | 0 | 0.3 | 90.3 | 61.2 | 160.4 | 315 | 510 | 239 | 160 | 27.8 | 0 | 1564 | 130.32 | 158.54 | 1.22 |
| **2001** | 0 | 0 | 1 | 22.7 | 55.5 | 249.2 | 398 | 555.3 | 132 | 102 | 2.6 | 16.9 | 1535 | 127.92 | 181.96 | 1.42 |
| **2002** | 0 | 4.1 | 5.3 | 15.9 | 2 | 452.7 | 451 | 423.6 | 135 | 18.3 | 0 | 1 | 1509 | 125.73 | 194.62 | 1.55 |
| **2003** | 0 | 0.4 | 0.9 | 0 | 82.55 | 193.6 | 410 | 372.3 | 184 | 88.7 | 10.4 | 2.46 | 196.9 | 32.82 | 78.77 | 2.4 |
| **2004** | 0 | 0.2 | 10.72 | 23.48 | 82.55 | 193.6 | 410 | 420.3 | 171 | 74.7 | 7.2 | 0 | 673.6 | 134.72 | 173.86 | 1.29 |
| **2005** | 0.7 | 0 | 85.6 | 9.9 | 80.6 | 194 | 528 | 250.6 | 282 | 49.6 | 7.4 | 0 | 1488 | 124.03 | 162.57 | 1.31 |
| **2006** | 3.1 | 0.2 | 0.1 | 6.7 | 151.2 | 226.4 | 571 | 356.3 | 214 | 121 | 0.3 | 4.9 | 1656 | 137.97 | 180.7 | 1.31 |
| **2007** | 0 | 0 | 1.1 | 29.2 | 14.9 | 286.3 | 317 | 326 | 229 | 45.4 | 11.4 | 0 | 1260 | 105 | 138.82 | 1.32 |
| **2008** | 1.8 | 0 | 0 | 107 | 86.5 | 174.4 | 483 | 369.1 | 117 | 69.4 | 20.2 | 0 | 1429 | 119.04 | 156.06 | 1.31 |
| **2009** | 0 | 0 | 10.9 | 0.5 | 82.55 | 87 | 358 | 343.7 | 104 | 56.8 | 3 | 0 | 963.5 | 87.59 | 135.43 | 1.55 |
| **2010** | 13 | 0 | 0 | 42 | 64.1 | 137.7 | 410 | 434.2 | 179 | 45.1 | 1.5 | 0 | 916.9 | 83.35 | 130.84 | 1.57 |
| **2011** | 0 | | 22.7 | 12.9 | 104 | 169 | 405 | 344 | 115 | 29.5 | 26.1 | 0 | 1228 | 111.66 | 141.53 | 1.27 |
| **2012** | 0 | 0 | 0 | 0 | 25.4 | 122 | 501 | 472.1 | 251 | 7.6 | 2 | 11.2 | 1392 | 115.99 | 188.46 | 1.62 |
| **2013** | 0 | 0 | 1.4 | 1.4 | 82.55 | 172.9 | 590 | 343.2 | 139 | 166 | 16.6 | 0 | 1431 | 130.05 | 188.99 | 1.45 |
| **2014** | 0 | 2.2 | 63.7 | 23.48 | 23.48 | 193.2 | 366 | 486.1 | 241 | 117 | 0 | 0.4 | 1469 | 146.92 | 172.29 | 1.17 |
| **2015** | 0 | 0.8 | 0.4 | 0 | 137 | 98.9 | 296 | 268.5 | 201 | 117 | 16.2 | | 1135 | 103.2 | 111.91 | 1.08 |
| **Mean** | 1.5 | 1.63 | 10.72 | 23.48 | 82.55 | 196.9 | 410 | 372.3 | 184 | 88.7 | 10.4 | 2.46 | 1301 | | | |
| **Standard deviation** | 3.2 | 4.65 | 19.63 | 26.22 | 62.43 | 74.85 | 105 | 89.63 | 54.5 | 53.8 | 14.2 | 4.36 | | | | |
| **Variance coefficient** | 2.2 | 2.86 | 1.83 | 1.12 | 0.76 | 0.38 | 0.26 | 0.24 | 0.3 | 0.61 | 1.36 | 1.78 | | | | |
| **Maximum value** | 13 | 24.1 | 85.6 | 107 | 238.11 | 452.7 | 590 | 555.3 | 298 | 203 | 65.3 | 16.9 | | | | |
| **Minimum** | 0 | 0 | 0 | 0 | 2 | 87 | 219 | 200.1 | 95.8 | 7.6 | 0 | 0 | | | | |

| Sekela | Jan | Feb | Mar | Apr | May | Jun | Jul | Aug | Sep | Oct | Nov | Dec | Sum |
|---|---|---|---|---|---|---|---|---|---|---|---|---|---|
| **1986** | 0 | 0.3 | 5.1 | 16.5 | 9.4 | 225.4 | 400 | 271.1 | 171 | 116 | 0 | 0 | 1214 |
| **1987** | 0 | 0.9 | 0 | 8.3 | 235.3 | 215.1 | 219 | 297.5 | 158 | 57.9 | 0 | 0.1 | 1192 |
| **1988** | 3.9 | 24.1 | 0 | 16.4 | 55.9 | 188 | 444 | 304 | 124 | 120 | 21.6 | 8.8 | 1311 |
| **1989** | 0 | 0 | 7.9 | 9.8 | 123 | 222.6 | 387 | 508.7 | 253 | 86.5 | 1.4 | 3.3 | 1603 |
| **1990** | 4.9 | 6 | 1 | 29 | 6.7 | 97.8 | 575 | 452.4 | 206 | 39.3 | 0 | 0 | 1418 |

| | | | | | | | | | | | | | |
|---|---|---|---|---|---|---|---|---|---|---|---|---|---|
| **1991** | 0 | 0.93 | 7.85 | 19.5 | 74.76 | 277 | 584 | 330.8 | 298 | 106 | 0.9 | 1.8 | 1702 |
| **1992** | 0 | 0 | 4.3 | 63.7 | 49.9 | 122.6 | 291 | 438.3 | 160 | 203 | 65.3 | 0 | 1399 |
| **1993** | 5.5 | 0 | 15.2 | 24.3 | 117.3 | 222.7 | 479 | 362.4 | 235 | 104 | 18.9 | 0 | 1584 |
| **1994** | 0 | 0.8 | 0 | 21.9 | 103.3 | 190.5 | 322 | 272.8 | 136 | 19.2 | 3.7 | 5.6 | 1077 |
| **1995** | 0 | 4.1 | 8.4 | 19.2 | 76.5 | 277 | 402 | 269.9 | 95.8 | 28.9 | 0 | 4.7 | 1186 |
| **1996** | 0 | 0.7 | 29.5 | 47.5 | 100.9 | 284.7 | 302 | 365.2 | 175 | 47.6 | 26.7 | 0 | 1380 |
| **1997** | 0 | 0 | 19.4 | 29.13 | 238.11 | 144.5 | 236 | 200.1 | 174 | 150 | 17.2 | 10.1 | 1218 |
| **1998** | 0 | 0 | 18.8 | 0.8 | 122.73 | 196.5 | 423 | 357.6 | 202 | 115 | 1.1 | 0 | 1438 |
| **1999** | 9 | 0 | 0 | 12.9 | 48.1 | 129 | 415 | 463.8 | 196 | 197 | 3 | 0 | 1474 |
| **2000** | 0 | 0 | 0.3 | 90.3 | 61.2 | 160.4 | 315 | 510 | 239 | 160 | 27.8 | 0 | 1564 |
| **2001** | 0 | 0 | 1 | 22.7 | 55.5 | 249.2 | 398 | 555.3 | 132 | 102 | 2.6 | 16.9 | 1535 |
| **2002** | 0 | 4.1 | 5.3 | 15.9 | 2 | 452.7 | 451 | 423.6 | 135 | 18.3 | 0 | 1 | 1509 |
| **2003** | 0 | 0.4 | 0.9 | 0 | 2 | 193.6 | 410 | 372.3 | 184 | 88.7 | 10.4 | 2.46 | 196.9 |
| **2004** | 1.5 | 1.63 | 10.72 | 23.48 | 82.55 | 196.9 | 410 | 420.3 | 171 | 74.7 | 7.2 | 0 | 673.6 |
| **2005** | 0.7 | 0 | 85.6 | 9.9 | 80.6 | 194 | 528 | 250.6 | 282 | 49.6 | 7.4 | 0 | 1488 |
| **2006** | 3.1 | 0.2 | 0.1 | 6.7 | 151.2 | 226.4 | 571 | 356.3 | 214 | 121 | 0.3 | 4.9 | 1656 |
| **2007** | 0 | 0 | 1.1 | 29.2 | 14.9 | 286.3 | 317 | 326 | 229 | 45.4 | 11.4 | 0 | 1260 |
| **2008** | 1.8 | 0 | 0 | 107 | 86.5 | 174.4 | 483 | 369.1 | 117 | 69.4 | 20.2 | 0 | 1429 |
| **2009** | 0 | 0 | 10.9 | 0.5 | | 87 | 358 | 343.7 | 104 | 56.8 | 3 | 0 | 963.5 |
| **2010** | 13 | 0 | 0 | 42 | 64.1 | 137.7 | | 434.2 | 179 | 45.1 | 1.5 | 0 | 916.9 |
| **2011** | 0 | | 22.7 | 12.9 | 104 | 169 | 405 | 344 | 115 | 29.5 | 26.1 | 0 | 1228 |
| **2012** | 0 | 0 | 0 | 0 | 25.4 | 122 | 501 | 472.1 | 251 | 7.6 | 2 | 11.2 | 1392 |
| **2013** | 0 | 0 | 1.4 | 1.4 | | 172.9 | 590 | 343.2 | 139 | 166 | 16.6 | 0 | 1431 |
| **2014** | 0 | 2.2 | 63.7 | | | 193.2 | 366 | 486.1 | 241 | 117 | 0 | 0.4 | 1469 |
| **2015** | 0 | 0.8 | 0.4 | 0 | 137 | 98.9 | 296 | 268.5 | 201 | 117 | 16.2 | | 1135 |
| **Mean** | 1.5 | 1.63 | 10.72 | 23.48 | 82.55 | 196.9 | 410 | 372.3 | 184 | 88.7 | 10.4 | 2.46 | 1301 |
| **Standard deviation** | 3.2 | 4.65 | 19.63 | 26.22 | 62.43 | 74.85 | 105 | 89.63 | 54.5 | 53.8 | 14.2 | 4.36 | |
| **Variance coefficient** | 2.2 | 2.86 | 1.83 | 1.12 | 0.76 | 0.38 | 0.26 | 0.24 | 0.3 | 0.61 | 1.36 | 1.78 | |
| **Maximum value** | 13 | 24.1 | 85.6 | 107 | 238.11 | 452.7 | 590 | 555.3 | 298 | 203 | 65.3 | 16.9 | |
| **Minimum value** | 0 | 0 | 0 | 0 | 2 | 87 | 219 | 200.1 | 95.8 | 7.6 | 0 | 0 | |

| Tillili | Jan | Feb | Mar | Apr | May | Jun | Jul | Aug | Sep | Oct | Nov | Dec | Sum |
|---|---|---|---|---|---|---|---|---|---|---|---|---|---|
| **1986** | 0 | 0.3 | 5.1 | 16.5 | 9.4 | 225.4 | 400 | 271.1 | 171 | 116 | 0 | 0 | 1214 |
| **1987** | 0 | 0.9 | 0 | 8.3 | 235.3 | 215.1 | 219 | 297.5 | 158 | 57.9 | 0 | 0.1 | 1192 |
| **1988** | 3.9 | 24.1 | 0 | 16.4 | 55.9 | 188 | 444 | 304 | 124 | 120 | 21.6 | 8.8 | 1311 |
| **1989** | 0 | 0 | 7.9 | 9.8 | 123 | 222.6 | 387 | 508.7 | 253 | 86.5 | 1.4 | 3.3 | 1603 |
| **1990** | 4.9 | 6 | 1 | 29 | 6.7 | 97.8 | 575 | 452.4 | 206 | 39.3 | 0 | 0 | 1418 |

| | | | | | | | | | | | | | |
|---|---|---|---|---|---|---|---|---|---|---|---|---|---|
| **1991** | 0 | 0.93 | 7.85 | 19.5 | 74.76 | 277 | 584 | 330.8 | 298 | 106 | 0.9 | 1.8 | 1702 |
| **1992** | 0 | 0 | 4.3 | 63.7 | 49.9 | 122.6 | 291 | 438.3 | 160 | 203 | 65.3 | 0 | 1399 |
| **1993** | 5.5 | 0 | 15.2 | 24.3 | 117.3 | 222.7 | 479 | 362.4 | 235 | 104 | 18.9 | 0 | 1584 |
| **1994** | 0 | 0.8 | 0 | 21.9 | 103.3 | 190.5 | 322 | 272.8 | 136 | 19.2 | 3.7 | 5.6 | 1077 |
| **1995** | 0 | 4.1 | 8.4 | 19.2 | 76.5 | 277 | 402 | 269.9 | 95.8 | 28.9 | 0 | 4.7 | 1186 |
| **1996** | 0 | 0.7 | 29.5 | 47.5 | 100.9 | 284.7 | 302 | 365.2 | 175 | 47.6 | 26.7 | 0 | 1380 |
| **1997** | 0 | 0 | 19.4 | 29.13 | 238.11 | 144.5 | 236 | 200.1 | 174 | 150 | 17.2 | 10.1 | 1218 |
| **1998** | 0 | 0 | 18.8 | 0.8 | 122.73 | 196.5 | 423 | 357.6 | 202 | 115 | 1.1 | 0 | 1438 |
| **1999** | 9 | 0 | 0 | 12.9 | 48.1 | 129 | 415 | 463.8 | 196 | 197 | 3 | 0 | 1474 |
| **2000** | 0 | 0 | 0.3 | 90.3 | 61.2 | 160.4 | 315 | 510 | 239 | 160 | 27.8 | 0 | 1564 |
| **2001** | 0 | 0 | 1 | 22.7 | 55.5 | 249.2 | 398 | 555.3 | 132 | 102 | 2.6 | 16.9 | 1535 |
| **2002** | 0 | 4.1 | 5.3 | 15.9 | 2 | 452.7 | 451 | 423.6 | 135 | 18.3 | 0 | 1 | 1509 |
| **2003** | 0 | 0.4 | 0.9 | 0 | 2 | 193.6 | 380 | | | | | | 196.9 |
| **2004** | 0 | 0 | 4.3 | 63.7 | 49.9 | 122.6 | 400 | 420.3 | 171 | 74.7 | 7.2 | 0 | 673.6 |
| **2005** | 0.7 | 0 | 85.6 | 9.9 | 80.6 | 194 | 528 | 250.6 | 282 | 49.6 | 7.4 | 0 | 1488 |
| **2006** | 3.1 | 0.2 | 0.1 | 6.7 | 151.2 | 226.4 | 571 | 356.3 | 214 | 121 | 0.3 | 4.9 | 1656 |
| **2007** | 0 | 0 | 1.1 | 29.2 | 14.9 | 286.3 | 317 | 326 | 229 | 45.4 | 11.4 | 0 | 1260 |
| **2008** | 1.8 | 0 | 0 | 107 | 86.5 | 174.4 | 483 | 369.1 | 117 | 69.4 | 20.2 | 0 | 1429 |
| **2009** | 0 | 0 | 10.9 | 0.5 | | 87 | 358 | 343.7 | 104 | 56.8 | 3 | 0 | 963.5 |
| **2010** | 13 | 0 | 0 | 42 | 64.1 | 137.7 | | 434.2 | 179 | 45.1 | 1.5 | 0 | 916.9 |
| **2011** | 0 | | 22.7 | 12.9 | 104 | 169 | 405 | 344 | 115 | 29.5 | 26.1 | 0 | 1228 |
| **2012** | 0 | 0 | 0 | 0 | 25.4 | 122 | 501 | 472.1 | 251 | 7.6 | 2 | 11.2 | 1392 |
| **2013** | 0 | 0 | 1.4 | 1.4 | 18 | 172.9 | 590 | 343.2 | 139 | 166 | 16.6 | 0 | 1431 |
| **2014** | 0 | 2.2 | 63.7 | | 20 | 193.2 | 366 | 486.1 | 241 | 117 | 0 | 0.4 | 1469 |
| **2015** | 0 | 0.8 | 0.4 | 0 | 137 | 98.9 | 296 | 268.5 | 201 | 117 | 16.2 | | 1135 |
| **Mean** | 1.5 | 1.63 | 10.72 | 23.48 | 82.55 | 196.9 | 410 | 372.3 | 184 | 88.7 | 10.4 | 2.46 | 1301 |
| **Standard deviation** | 3.2 | 4.65 | 19.63 | 26.22 | 62.43 | 74.85 | 105 | 89.63 | 54.5 | 53.8 | 14.2 | 4.36 | |
| **Variance coefficient** | 2.2 | 2.86 | 1.83 | 1.12 | 0.76 | 0.38 | 0.26 | 0.24 | 0.3 | 0.61 | 1.36 | 1.78 | |
| **Maximum value** | 13 | 24.1 | 85.6 | 107 | 238.11 | 452.7 | 590 | 555.3 | 298 | 203 | 65.3 | 16.9 | |
| **Minimum value** | 0 | 0 | 0 | 0 | 2 | 87 | 219 | 200.1 | 95.8 | 7.6 | 0 | 0 | |

| Zegay | Jan | Feb | Mar | Apr | May | Jun | Jul | Aug | Sep | Oct | Nov | Dec | Sum |
|---|---|---|---|---|---|---|---|---|---|---|---|---|---|
| **1986** | 0 | 0.3 | 5.1 | 16.5 | 9.4 | 225.4 | 400 | 271.1 | 171 | 116 | 0 | 0 | 1214 |
| **1987** | 0 | 0.9 | 0 | 8.3 | 235.3 | 215.1 | 219 | 297.5 | 158 | 57.9 | 0 | 0.1 | 1192 |
| **1988** | 3.9 | 24.1 | 0 | 16.4 | 55.9 | 188 | 444 | 304 | 124 | 120 | 21.6 | 8.8 | 1311 |
| **1989** | 0 | 0 | 7.9 | 9.8 | 123 | 222.6 | 387 | 508.7 | 253 | 86.5 | 1.4 | 3.3 | 1603 |
| **1990** | 4.9 | 6 | 1 | 29 | 6.7 | 97.8 | 575 | 452.4 | 206 | 39.3 | 0 | 0 | 1418 |
| **1991** | 0 | 0.93 | 7.85 | 19.5 | 74.76 | 277 | 584 | 330.8 | 298 | 106 | 0.9 | 1.8 | 1702 |
| **1992** | 0 | 0 | 4.3 | 63.7 | 49.9 | 122.6 | 291 | 438.3 | 160 | 203 | 65.3 | 0 | 1399 |
| **1993** | 5.5 | 0 | 15.2 | 24.3 | 117.3 | 222.7 | 479 | 362.4 | 235 | 104 | 18.9 | 0 | 1584 |
| **1994** | 0 | 0.8 | 0 | 21.9 | 103.3 | 190.5 | 322 | 272.8 | 136 | 19.2 | 3.7 | 5.6 | 1077 |
| **1995** | 0 | 4.1 | 8.4 | 19.2 | 76.5 | 277 | 402 | 269.9 | 95.8 | 28.9 | 0 | 4.7 | 1186 |
| **1996** | 0 | 0.7 | 29.5 | 47.5 | 100.9 | 284.7 | 302 | 365.2 | 175 | 47.6 | 26.7 | 0 | 1380 |
| **1997** | 0 | 0 | 19.4 | 29.13 | 238.11 | 144.5 | 236 | 200.1 | 174 | 150 | 17.2 | 10.1 | 1218 |
| **1998** | 0 | 0 | 18.8 | 0.8 | 122.73 | 196.5 | 423 | 357.6 | 202 | 115 | 1.1 | 0 | 1438 |
| **1999** | 9 | 0 | 0 | 12.9 | 48.1 | 129 | 415 | 463.8 | 196 | 197 | 3 | 0 | 1474 |
| **2000** | 0 | 0 | 0.3 | 90.3 | 61.2 | 160.4 | 315 | 510 | 239 | 160 | 27.8 | 0 | 1564 |
| **2001** | 0 | 0 | 1 | 22.7 | 55.5 | 249.2 | 398 | 555.3 | 132 | 102 | 2.6 | 16.9 | 1535 |
| **2002** | 0 | 4.1 | 5.3 | 15.9 | 2 | 452.7 | 451 | 423.6 | 135 | 18.3 | 0 | 1 | 1509 |
| **2003** | 0 | 0.4 | 0.9 | 0 | 2 | 193.6 | | | | | | | 196.9 |
| **2004** | 0 | 0 | 18.8 | 0.8 | 122.73 | 196.5 | 0 | 420.3 | 171 | 74.7 | 7.2 | 0 | 673.6 |
| **2005** | 0.7 | 0 | 85.6 | 9.9 | 80.6 | 194 | 528 | 250.6 | 282 | 49.6 | 7.4 | 0 | 1488 |
| **2006** | 3.1 | 0.2 | 0.1 | 6.7 | 151.2 | 226.4 | 571 | 356.3 | 214 | 121 | 0.3 | 4.9 | 1656 |
| **2007** | 0 | 0 | 1.1 | 29.2 | 14.9 | 286.3 | 317 | 326 | 229 | 45.4 | 11.4 | 0 | 1260 |
| **2008** | 1.8 | 0 | 0 | 107 | 86.5 | 174.4 | 483 | 369.1 | 117 | 69.4 | 20.2 | 0 | 1429 |
| **2009** | 0 | 0 | 10.9 | 0.5 | | 87 | 358 | 343.7 | 104 | 56.8 | 3 | 0 | 963.5 |
| **2010** | 13 | 0 | 0 | 42 | 64.1 | 137.7 | 380 | 434.2 | 179 | 45.1 | 1.5 | 0 | 916.9 |
| **2011** | 0 | | 22.7 | 12.9 | 104 | 169 | 405 | 344 | 115 | 29.5 | 26.1 | 0 | 1228 |

| Zegay | Jan | Feb | Mar | Apr | May | Jun | Jul | Aug | Sep | Oct | Nov | Dec | Sum |
|---|---|---|---|---|---|---|---|---|---|---|---|---|---|
| **2012** | 0 | 0 | 0 | 0 | 25.4 | 122 | 501 | 472.1 | 251 | 7.6 | 2 | 11.2 | 1392 |
| **2013** | 0 | 0 | 1.4 | 1.4 | 15 | 172.9 | 590 | 343.2 | 139 | 166 | 16.6 | 0 | 1431 |
| **2014** | 0 | 2.2 | 63.7 | | 20 | 193.2 | 366 | 486.1 | 241 | 117 | 0 | 0.4 | 1469 |
| **2015** | 0 | 0.8 | 0.4 | 0 | 137 | 98.9 | 296 | 268.5 | 201 | 117 | 16.2 | | 1135 |
| **Mean** | 1.5 | 1.63 | 10.72 | 23.48 | 82.55 | 196.9 | 410 | 372.3 | 184 | 88.7 | 10.4 | 2.46 | 1301 |
| **Standard deviation** | 3.2 | 4.65 | 19.63 | 26.22 | 62.43 | 74.85 | 105 | 89.63 | 54.5 | 53.8 | 14.2 | 4.36 | |
| **Variance coefficient** | 2.2 | 2.86 | 1.83 | 1.12 | 0.76 | 0.38 | 0.26 | 0.24 | 0.3 | 0.61 | 1.36 | 1.78 | |
| **Maximum value** | 13 | 24.1 | 85.6 | 107 | 238.11 | 452.7 | 590 | 555.3 | 298 | 203 | 65.3 | 16.9 | |
| **Minimum value** | 0 | 0 | 0 | 0 | 2 | 87 | 219 | 200.1 | 95.8 | 7.6 | 0 | 0 | |

| Baher dar | Jan | Feb | Mar | Apr | May | Jun | Jul | Aug | Sep | Oct | Nov | Dec | Sum |
|---|---|---|---|---|---|---|---|---|---|---|---|---|---|
| **1986** | 0 | 0.3 | 5.1 | 16.5 | 9.4 | 225.4 | 400 | 271.1 | 171 | 116 | 0 | 0 | 1214 |
| **1987** | 0 | 0.9 | 0 | 8.3 | 235.3 | 215.1 | 219 | 297.5 | 158 | 57.9 | 0 | 0.1 | 1192 |
| **1988** | 3.9 | 24.1 | 0 | 16.4 | 55.9 | 188 | 444 | 304 | 124 | 120 | 21.6 | 8.8 | 1311 |
| **1989** | 0 | 0 | 7.9 | 9.8 | 123 | 222.6 | 387 | 508.7 | 253 | 86.5 | 1.4 | 3.3 | 1603 |
| **1990** | 4.9 | 6 | 1 | 29 | 6.7 | 97.8 | 575 | 452.4 | 206 | 39.3 | 0 | 0 | 1418 |
| **1991** | 0 | 0.93 | 7.85 | 19.5 | 74.76 | 277 | 584 | 330.8 | 298 | 106 | 0.9 | 1.8 | 1702 |
| **1992** | 0 | 0 | 4.3 | 63.7 | 49.9 | 122.6 | 291 | 438.3 | 160 | 203 | 65.3 | 0 | 1399 |
| **1993** | 5.5 | 0 | 15.2 | 24.3 | 117.3 | 222.7 | 479 | 362.4 | 235 | 104 | 18.9 | 0 | 1584 |
| **1994** | 0 | 0.8 | 0 | 21.9 | 103.3 | 190.5 | 322 | 272.8 | 136 | 19.2 | 3.7 | 5.6 | 1077 |
| **1995** | 0 | 4.1 | 8.4 | 19.2 | 76.5 | 277 | 402 | 269.9 | 95.8 | 28.9 | 0 | 4.7 | 1186 |
| **1996** | 0 | 0.7 | 29.5 | 47.5 | 100.9 | 284.7 | 302 | 365.2 | 175 | 47.6 | 26.7 | 0 | 1380 |
| **1997** | 0 | 0 | 19.4 | 29.13 | 238.11 | 144.5 | 236 | 200.1 | 174 | 150 | 17.2 | 10.1 | 1218 |
| **1998** | 0 | 0 | 18.8 | 0.8 | 122.73 | 196.5 | 423 | 357.6 | 202 | 115 | 1.1 | 0 | 1438 |
| **1999** | 9 | 0 | 0 | 12.9 | 48.1 | 129 | 415 | 463.8 | 196 | 197 | 3 | 0 | 1474 |
| **2000** | 0 | 0 | 0.3 | 90.3 | 61.2 | 160.4 | 315 | 510 | 239 | 160 | 27.8 | 0 | 1564 |
| **2001** | 0 | 0 | 1 | 22.7 | 55.5 | 249.2 | 398 | 555.3 | 132 | 102 | 2.6 | 16.9 | 1535 |
| **2002** | 0 | 4.1 | 5.3 | 15.9 | 2 | 452.7 | 451 | 423.6 | 135 | 18.3 | 0 | 1 | 1509 |
| **2003** | 0 | 0.4 | 0.9 | 0 | 2 | 193.6 | | | | | | | 196.9 |
| **2004** | | | | | | | | 420.3 | 171 | 74.7 | 7.2 | 0 | 673.6 |
| **2005** | 0.7 | 0 | 85.6 | 9.9 | 80.6 | 194 | 528 | 250.6 | 282 | 49.6 | 7.4 | 0 | 1488 |
| **2006** | 3.1 | 0.2 | 0.1 | 6.7 | 151.2 | 226.4 | 571 | 356.3 | 214 | 121 | 0.3 | 4.9 | 1656 |
| **2007** | 0 | 0 | 1.1 | 29.2 | 14.9 | 286.3 | 317 | 326 | 229 | 45.4 | 11.4 | 0 | 1260 |
| **2008** | 1.8 | 0 | 0 | 107 | 86.5 | 174.4 | 483 | 369.1 | 117 | 69.4 | 20.2 | 0 | 1429 |
| **2009** | 0 | 0 | 10.9 | 0.5 | | 87 | 358 | 343.7 | 104 | 56.8 | 3 | 0 | 963.5 |
| **2010** | 13 | 0 | 0 | 42 | 64.1 | 137.7 | | 434.2 | 179 | 45.1 | 1.5 | 0 | 916.9 |
| **2011** | 0 | | 22.7 | 12.9 | 104 | 169 | 405 | 344 | 115 | 29.5 | 26.1 | 0 | 1228 |
| **2012** | 0 | 0 | 0 | 0 | 25.4 | 122 | 501 | 472.1 | 251 | 7.6 | 2 | 11.2 | 1392 |
| **2013** | 0 | 0 | 1.4 | 1.4 | | 172.9 | 590 | 343.2 | 139 | 166 | 16.6 | 0 | 1431 |
| **2014** | 0 | 2.2 | 63.7 | | | 193.2 | 366 | 486.1 | 241 | 117 | 0 | 0.4 | 1469 |
| **2015** | 0 | 0.8 | 0.4 | 0 | 137 | 98.9 | 296 | 268.5 | 201 | 117 | 16.2 | | 1135 |
| **Mean** | 1.5 | 1.63 | 10.72 | 23.48 | 82.55 | 196.9 | 410 | 372.3 | 184 | 88.7 | 10.4 | 2.46 | 1301 |
| **Standard deviation** | 3.2 | 4.65 | 19.63 | 26.22 | 62.43 | 74.85 | 105 | 89.63 | 54.5 | 53.8 | 14.2 | 4.36 | |
| **Variance coefficient** | 2.2 | 2.86 | 1.83 | 1.12 | 0.76 | 0.38 | 0.26 | 0.24 | 0.3 | 0.61 | 1.36 | 1.78 | |

| Dek estifanos | Jan | Feb | Mar | Apr | May | Jun | Jul | Aug | Sep | Oct | Nov | Dec | Sum |
|---|---|---|---|---|---|---|---|---|---|---|---|---|---|
| **1986** | 0 | 0.3 | 5.1 | 16.5 | 9.4 | 225.4 | 400 | 271.1 | 171 | 116 | 0 | 0 | 1214 |
| **1987** | 0 | 0.9 | 0 | 8.3 | 235.3 | 215.1 | 219 | 297.5 | 158 | 57.9 | 0 | 0.1 | 1192 |
| **1988** | 3.9 | 24.1 | 0 | 16.4 | 55.9 | 188 | 444 | 304 | 124 | 120 | 21.6 | 8.8 | 1311 |
| **1989** | 0 | 0 | 7.9 | 9.8 | 123 | 222.6 | 387 | 508.7 | 253 | 86.5 | 1.4 | 3.3 | 1603 |
| **1990** | 4.9 | 6 | 1 | 29 | 6.7 | 97.8 | 575 | 452.4 | 206 | 39.3 | 0 | 0 | 1418 |
| **1991** | 0 | 0.93 | 7.85 | 19.5 | 74.76 | 277 | 584 | 330.8 | 298 | 106 | 0.9 | 1.8 | 1702 |

| Dek estifanos | Jan | Feb | Mar | Apr | May | Jun | Jul | Aug | Sep | Oct | Nov | Dec | Sum |
|---|---|---|---|---|---|---|---|---|---|---|---|---|---|
| **1992** | 0 | 0 | 4.3 | 63.7 | 49.9 | 122.6 | 291 | 438.3 | 160 | 203 | 65.3 | 0 | 1399 |
| **1993** | 5.5 | 0 | 15.2 | 24.3 | 117.3 | 222.7 | 479 | 362.4 | 235 | 104 | 18.9 | 0 | 1584 |
| **1994** | 0 | 0.8 | 0 | 21.9 | 103.3 | 190.5 | 322 | 272.8 | 136 | 19.2 | 3.7 | 5.6 | 1077 |
| **1995** | 0 | 4.1 | 8.4 | 19.2 | 76.5 | 277 | 402 | 269.9 | 95.8 | 28.9 | 0 | 4.7 | 1186 |
| **1996** | 0 | 0.7 | 29.5 | 47.5 | 100.9 | 284.7 | 302 | 365.2 | 175 | 47.6 | 26.7 | 0 | 1380 |
| **1997** | 0 | 0 | 19.4 | 29.13 | 238.11 | 144.5 | 236 | 200.1 | 174 | 150 | 17.2 | 10.1 | 1218 |
| **1998** | 0 | 0 | 18.8 | 0.8 | 122.73 | 196.5 | 423 | 357.6 | 202 | 115 | 1.1 | 0 | 1438 |
| **1999** | 9 | 0 | 0 | 12.9 | 48.1 | 129 | 415 | 463.8 | 196 | 197 | 3 | 0 | 1474 |
| **2000** | 0 | 0 | 0.3 | 90.3 | 61.2 | 160.4 | 315 | 510 | 239 | 160 | 27.8 | 0 | 1564 |
| **2001** | 0 | 0 | 1 | 22.7 | 55.5 | 249.2 | 398 | 555.3 | 132 | 102 | 2.6 | 16.9 | 1535 |
| **2002** | 0 | 4.1 | 5.3 | 15.9 | 2 | 452.7 | 451 | 423.6 | 135 | 18.3 | 0 | 1 | 1509 |
| **2003** | 0 | 0.4 | 0.9 | 0 | 2 | 193.6 |  |  |  |  |  |  | 196.9 |
| **2004** |  |  |  |  |  |  |  | 420.3 | 171 | 74.7 | 7.2 | 0 | 673.6 |
| **2005** | 0.7 | 0 | 85.6 | 9.9 | 80.6 | 194 | 528 | 250.6 | 282 | 49.6 | 7.4 | 0 | 1488 |
| **2006** | 3.1 | 0.2 | 0.1 | 6.7 | 151.2 | 226.4 | 571 | 356.3 | 214 | 121 | 0.3 | 4.9 | 1656 |
| **2007** | 0 | 0 | 1.1 | 29.2 | 14.9 | 286.3 | 317 | 326 | 229 | 45.4 | 11.4 | 0 | 1260 |
| **2008** | 1.8 | 0 | 0 | 107 | 86.5 | 174.4 | 483 | 369.1 | 117 | 69.4 | 20.2 | 0 | 1429 |
| **2009** | 0 | 0 | 10.9 | 0.5 |  | 87 | 358 | 343.7 | 104 | 56.8 | 3 | 0 | 963.5 |
| **2010** | 13 | 0 | 0 | 42 | 64.1 | 137.7 |  | 434.2 | 179 | 45.1 | 1.5 | 0 | 916.9 |
| **2011** | 0 |  | 22.7 | 12.9 | 104 | 169 | 405 | 344 | 115 | 29.5 | 26.1 | 0 | 1228 |
| **2012** | 0 | 0 | 0 | 0 | 25.4 | 122 | 501 | 472.1 | 251 | 7.6 | 2 | 11.2 | 1392 |
| **2013** | 0 | 0 | 1.4 | 1.4 |  | 172.9 | 590 | 343.2 | 139 | 166 | 16.6 | 0 | 1431 |
| **2014** | 0 | 2.2 | 63.7 |  |  | 193.2 | 366 | 486.1 | 241 | 117 | 0 | 0.4 | 1469 |
| **2015** | 0 | 0.8 | 0.4 | 0 | 137 | 98.9 | 296 | 268.5 | 201 | 117 | 16.2 |  | 1135 |
| **Mean** | 1.5 | 1.63 | 10.72 | 23.48 | 82.55 | 196.9 | 410 | 372.3 | 184 | 88.7 | 10.4 | 2.46 | 1301 |
| **Standard deviation** | 3.2 | 4.65 | 19.63 | 26.22 | 62.43 | 74.85 | 105 | 89.63 | 54.5 | 53.8 | 14.2 | 4.36 |  |
| **Variance coefficient** | 2.2 | 2.86 | 1.83 | 1.12 | 0.76 | 0.38 | 0.26 | 0.24 | 0.3 | 0.61 | 1.36 | 1.78 |  |
| **Maximum value** | 13 | 24.1 | 85.6 | 107 | 238.11 | 452.7 | 590 | 555.3 | 298 | 203 | 65.3 | 16.9 |  |
| **Minimum value** | 0 | 0 | 0 | 0 | 2 | 87 | 219 | 200.1 | 95.8 | 7.6 | 0 | 0 |  |

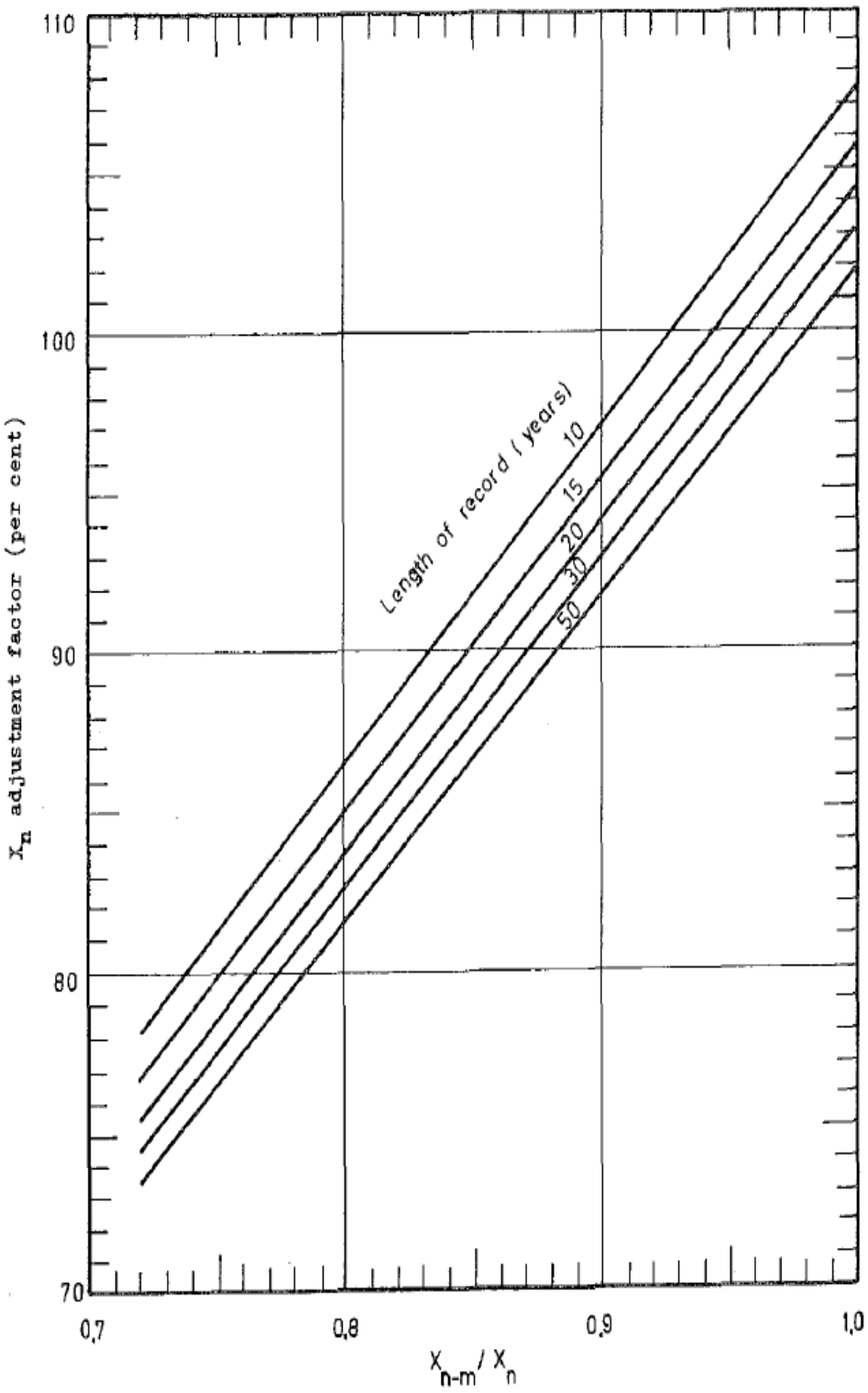
| Askuna | Jan | Feb | Mar | Apr | May | Jun | Jul | Aug | Sep | Oct | Nov | Dec | Sum |
|---|---|---|---|---|---|---|---|---|---|---|---|---|---|
| **1986** | 0 | 0.3 | 5.1 | 16.5 | 9.4 | 225.4 | 400 | 271.1 | 171 | 116 | 0 | 0 | 1214 |
| **1987** | 0 | 0.9 | 0 | 8.3 | 235.3 | 215.1 | 219 | 297.5 | 158 | 57.9 | 0 | 0.1 | 1192 |
| **1988** | 3.9 | 24.1 | 0 | 16.4 | 55.9 | 188 | 444 | 304 | 124 | 120 | 21.6 | 8.8 | 1311 |
| **1989** | 0 | 0 | 7.9 | 9.8 | 123 | 222.6 | 387 | 508.7 | 253 | 86.5 | 1.4 | 3.3 | 1603 |
| **1990** | 4.9 | 6 | 1 | 29 | 6.7 | 97.8 | 575 | 452.4 | 206 | 39.3 | 0 | 0 | 1418 |
| **1991** | 0 | 0.93 | 7.85 | 19.5 | 74.76 | 277 | 584 | 330.8 | 298 | 106 | 0.9 | 1.8 | 1702 |
| **1992** | 0 | 0 | 4.3 | 63.7 | 49.9 | 122.6 | 291 | 438.3 | 160 | 203 | 65.3 | 0 | 1399 |
| **1993** | 5.5 | 0 | 15.2 | 24.3 | 117.3 | 222.7 | 479 | 362.4 | 235 | 104 | 18.9 | 0 | 1584 |
| **1994** | 0 | 0.8 | 0 | 21.9 | 103.3 | 190.5 | 322 | 272.8 | 136 | 19.2 | 3.7 | 5.6 | 1077 |
| **1995** | 0 | 4.1 | 8.4 | 19.2 | 76.5 | 277 | 402 | 269.9 | 95.8 | 28.9 | 0 | 4.7 | 1186 |
| **1996** | 0 | 0.7 | 29.5 | 47.5 | 100.9 | 284.7 | 302 | 365.2 | 175 | 47.6 | 26.7 | 0 | 1380 |
| **1997** | 0 | 0 | 19.4 | 29.13 | 238.11 | 144.5 | 236 | 200.1 | 174 | 150 | 17.2 | 10.1 | 1218 |
| **1998** | 0 | 0 | 18.8 | 0.8 | 122.73 | 196.5 | 423 | 357.6 | 202 | 115 | 1.1 | 0 | 1438 |
| **1999** | 9 | 0 | 0 | 12.9 | 48.1 | 129 | 415 | 463.8 | 196 | 197 | 3 | 0 | 1474 |
| **2000** | 0 | 0 | 0.3 | 90.3 | 61.2 | 160.4 | 315 | 510 | 239 | 160 | 27.8 | 0 | 1564 |
| **2001** | 0 | 0 | 1 | 22.7 | 55.5 | 249.2 | 398 | 555.3 | 132 | 102 | 2.6 | 16.9 | 1535 |
| **2002** | 0 | 4.1 | 5.3 | 15.9 | 2 | 452.7 | 451 | 423.6 | 135 | 18.3 | 0 | 1 | 1509 |
| **2003** | 0 | 0.4 | 0.9 | 0 | 2 | 193.6 | 400 | 430 | 140 | 101 | 2.3 | 0 | 196.9 |
| **2004** | 0 | 0 | 15 | 20 | 15 | 150 | 450 | 420.3 | 171 | 74.7 | 7.2 | 0 | 673.6 |
| **2005** | 0.7 | 0 | 85.6 | 9.9 | 80.6 | 194 | 528 | 250.6 | 282 | 49.6 | 7.4 | 0 | 1488 |
| **2006** | 3.1 | 0.2 | 0.1 | 6.7 | 151.2 | 226.4 | 571 | 356.3 | 214 | 121 | 0.3 | 4.9 | 1656 |
| **2007** | 0 | 0 | 1.1 | 29.2 | 14.9 | 286.3 | 317 | 326 | 229 | 45.4 | 11.4 | 0 | 1260 |
| **2008** | 1.8 | 0 | 0 | 107 | 86.5 | 174.4 | 483 | 369.1 | 117 | 69.4 | 20.2 | 0 | 1429 |
| **2009** | 0 | 0 | 10.9 | 0.5 |  | 87 | 358 | 343.7 | 104 | 56.8 | 3 | 0 | 963.5 |
| **2010** | 13 | 0 | 0 | 42 | 64.1 | 137.7 |  | 434.2 | 179 | 45.1 | 1.5 | 0 | 916.9 |
| **2011** | 0 |  | 22.7 | 12.9 | 104 | 169 | 405 | 344 | 115 | 29.5 | 26.1 | 0 | 1228 |
| **2012** | 0 | 0 | 0 | 0 | 25.4 | 122 | 501 | 472.1 | 251 | 7.6 | 2 | 11.2 | 1392 |

| Askuna | Jan | Feb | Mar | Apr | May | Jun | Jul | Aug | Sep | Oct | Nov | Dec | Sum |
|---|---|---|---|---|---|---|---|---|---|---|---|---|---|
| **2013** | 0 | 0 | 1.4 | 1.4 | | 172.9 | 590 | 343.2 | 139 | 166 | 16.6 | 0 | 1431 |
| **2014** | 0 | 2.2 | 63.7 | 23.48 | 82.55 | 193.2 | 366 | 486.1 | 241 | 117 | 0 | 0.4 | 1469 |
| **2015** | 0 | 0.8 | 0.4 | 0 | 137 | 98.9 | 296 | 268.5 | 201 | 117 | 16.2 | | 1135 |
| **Mean** | 1.5 | 1.63 | 10.72 | 23.48 | 82.55 | 196.9 | 410 | 372.3 | 184 | 88.7 | 10.4 | 2.46 | 1301 |
| **Standard deviation** | 3.2 | 4.65 | 19.63 | 26.22 | 62.43 | 74.85 | 105 | 89.63 | 54.5 | 53.8 | 14.2 | 4.36 | |
| **Variance coefficient** | 2.2 | 2.86 | 1.83 | 1.12 | 0.76 | 0.38 | 0.26 | 0.24 | 0.3 | 0.61 | 1.36 | 1.78 | |
| **Maximum value** | 13 | 24.1 | 85.6 | 107 | 238.11 | 452.7 | 590 | 555.3 | 298 | 203 | 65.3 | 16.9 | |
| **Minimum value** | 0 | 0 | 0 | 0 | 2 | 87 | 219 | 200.1 | 95.8 | 7.6 | 0 | 0 | |

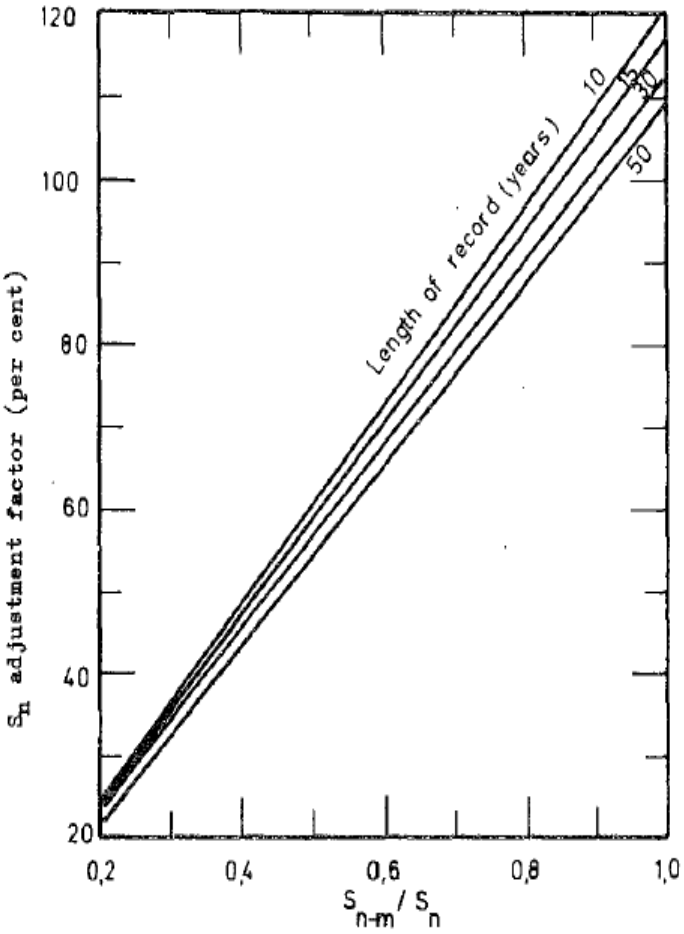
| Enejebara | Jan | Feb | Mar | Apr | May | Jun | Jul | Aug | Sep | Oct | Nov | Dec | Sum |
|---|---|---|---|---|---|---|---|---|---|---|---|---|---|
| **1986** | 0 | 0.3 | 5.1 | 16.5 | 9.4 | 225.4 | 400 | 271.1 | 171 | 116 | 0 | 0 | 1214 |
| **1987** | 0 | 0.9 | 0 | 8.3 | 235.3 | 215.1 | 219 | 297.5 | 158 | 57.9 | 0 | 0.1 | 1192 |
| **1988** | 3.9 | 24.1 | 0 | 16.4 | 55.9 | 188 | 444 | 304 | 124 | 120 | 21.6 | 8.8 | 1311 |
| **1989** | 0 | 0 | 7.9 | 9.8 | 123 | 222.6 | 387 | 508.7 | 253 | 86.5 | 1.4 | 3.3 | 1603 |
| **1990** | 4.9 | 6 | 1 | 29 | 6.7 | 97.8 | 575 | 452.4 | 206 | 39.3 | 0 | 0 | 1418 |
| **1991** | 0 | 0.93 | 7.85 | 19.5 | 74.76 | 277 | 584 | 330.8 | 298 | 106 | 0.9 | 1.8 | 1702 |
| **1992** | 0 | 0 | 4.3 | 63.7 | 49.9 | 122.6 | 291 | 438.3 | 160 | 203 | 65.3 | 0 | 1399 |
| **1993** | 5.5 | 0 | 15.2 | 24.3 | 117.3 | 222.7 | 479 | 362.4 | 235 | 104 | 18.9 | 0 | 1584 |
| **1994** | 0 | 0.8 | 0 | 21.9 | 103.3 | 190.5 | 322 | 272.8 | 136 | 19.2 | 3.7 | 5.6 | 1077 |
| **1995** | 0 | 4.1 | 8.4 | 19.2 | 76.5 | 277 | 402 | 269.9 | 95.8 | 28.9 | 0 | 4.7 | 1186 |
| **1996** | 0 | 0.7 | 29.5 | 47.5 | 100.9 | 284.7 | 302 | 365.2 | 175 | 47.6 | 26.7 | 0 | 1380 |
| **1997** | 0 | 0 | 19.4 | 29.13 | 238.11 | 144.5 | 236 | 200.1 | 174 | 150 | 17.2 | 10.1 | 1218 |
| **1998** | 0 | 0 | 18.8 | 0.8 | 122.73 | 196.5 | 423 | 357.6 | 202 | 115 | 1.1 | 0 | 1438 |
| **1999** | 9 | 0 | 0 | 12.9 | 48.1 | 129 | 415 | 463.8 | 196 | 197 | 3 | 0 | 1474 |
| **2000** | 0 | 0 | 0.3 | 90.3 | 61.2 | 160.4 | 315 | 510 | 239 | 160 | 27.8 | 0 | 1564 |
| **2001** | 0 | 0 | 1 | 22.7 | 55.5 | 249.2 | 398 | 555.3 | 132 | 102 | 2.6 | 16.9 | 1535 |
| **2002** | 0 | 4.1 | 5.3 | 15.9 | 2 | 452.7 | 451 | 423.6 | 135 | 18.3 | 0 | 1 | 1509 |
| **2003** | 0 | 0.4 | 0.9 | 0 | 2 | 193.6 | 410 | 372.3 | 184 | 88.7 | 10.4 | 2.46 | 196.9 |
| **2004** | 0 | 0.5 | 10 | 0.8 | 122.73 | 196.5 | 423 | 420.3 | 171 | 74.7 | 7.2 | 0 | 673.6 |
| **2005** | 0.7 | 0 | 85.6 | 9.9 | 80.6 | 194 | 528 | 250.6 | 282 | 49.6 | 7.4 | 0 | 1488 |
| **2006** | 3.1 | 0.2 | 0.1 | 6.7 | 151.2 | 226.4 | 571 | 356.3 | 214 | 121 | 0.3 | 4.9 | 1656 |
| **2007** | 0 | 0 | 1.1 | 29.2 | 14.9 | 286.3 | 317 | 326 | 229 | 45.4 | 11.4 | 0 | 1260 |
| **2008** | 1.8 | 0 | 0 | 107 | 86.5 | 174.4 | 483 | 369.1 | 117 | 69.4 | 20.2 | 0 | 1429 |
| **2009** | 0 | 0 | 10.9 | 0.5 | 23.48 | 82.55 | 358 | 343.7 | 104 | 56.8 | 3 | 0 | 963.5 |
| **2010** | 13 | 0 | 0 | 42 | 64.1 | 137.7 | | 434.2 | 179 | 45.1 | 1.5 | 0 | 916.9 |
| **2011** | 0 | | 22.7 | 12.9 | 104 | 169 | 405 | 344 | 115 | 29.5 | 26.1 | 0 | 1228 |
| **2012** | 0 | 0 | 0 | 0 | 25.4 | 122 | 501 | 472.1 | 251 | 7.6 | 2 | 11.2 | 1392 |
| **2013** | 0 | 0 | 1.4 | 1.4 | 23.48 | 82.55 | 590 | 343.2 | 139 | 166 | 16.6 | 0 | 1431 |
| **2014** | 0 | 2.2 | 63.7 | 23.48 | 82.55 | 193.2 | 366 | 486.1 | 241 | 117 | 0 | 0.4 | 1469 |
| **2015** | 0 | 0.8 | 0.4 | 0 | 137 | 98.9 | 296 | 268.5 | 201 | 117 | 16.2 | | 1135 |
| **Mean** | 1.5 | 1.63 | 10.72 | 23.48 | 82.55 | 196.9 | 410 | 372.3 | 184 | 88.7 | 10.4 | 2.46 | 1301 |
| **Standard deviation** | 3.2 | 4.65 | 19.63 | 26.22 | 62.43 | 74.85 | 105 | 89.63 | 54.5 | 53.8 | 14.2 | 4.36 | |
| **Variance coefficient** | 2.2 | 2.86 | 1.83 | 1.12 | 0.76 | 0.38 | 0.26 | 0.24 | 0.3 | 0.61 | 1.36 | 1.78 | |
| **Maximum value** | 13 | 24.1 | 85.6 | 107 | 238.11 | 452.7 | 590 | 555.3 | 298 | 203 | 65.3 | 16.9 | |
| **Minimum value** | 0 | 0 | 0 | 0 | 2 | 87 | 219 | 200.1 | 95.8 | 7.6 | 0 | 0 | |

| Finote selam | Jan | Feb | Mar | Apr | May | Jun | Jul | Aug | Sep | Oct | Nov | Dec | Sum |
|---|---|---|---|---|---|---|---|---|---|---|---|---|---|
| **1986** | 0 | 0.3 | 5.1 | 16.5 | 9.4 | 225.4 | 400 | 271.1 | 171 | 116 | 0 | 0 | 1214 |
| **1987** | 0 | 0.9 | 0 | 8.3 | 235.3 | 215.1 | 219 | 297.5 | 158 | 57.9 | 0 | 0.1 | 1192 |
| **1988** | 3.9 | 24.1 | 0 | 16.4 | 55.9 | 188 | 444 | 304 | 124 | 120 | 21.6 | 8.8 | 1311 |
| **1989** | 0 | 0 | 7.9 | 9.8 | 123 | 222.6 | 387 | 508.7 | 253 | 86.5 | 1.4 | 3.3 | 1603 |
| **1990** | 4.9 | 6 | 1 | 29 | 6.7 | 97.8 | 575 | 452.4 | 206 | 39.3 | 0 | 0 | 1418 |

| Finote selam | Jan | Feb | Mar | Apr | May | Jun | Jul | Aug | Sep | Oct | Nov | Dec | Sum |
|---|---|---|---|---|---|---|---|---|---|---|---|---|---|
| **1991** | 0 | 0.93 | 7.85 | 19.5 | 74.76 | 277 | 584 | 330.8 | 298 | 106 | 0.9 | 1.8 | 1702 |
| **1992** | 0 | 0 | 4.3 | 63.7 | 49.9 | 122.6 | 291 | 438.3 | 160 | 203 | 65.3 | 0 | 1399 |
| **1993** | 5.5 | 0 | 15.2 | 24.3 | 117.3 | 222.7 | 479 | 362.4 | 235 | 104 | 18.9 | 0 | 1584 |
| **1994** | 0 | 0.8 | 0 | 21.9 | 103.3 | 190.5 | 322 | 272.8 | 136 | 19.2 | 3.7 | 5.6 | 1077 |
| **1995** | 0 | 4.1 | 8.4 | 19.2 | 76.5 | 277 | 402 | 269.9 | 95.8 | 28.9 | 0 | 4.7 | 1186 |
| **1996** | 0 | 0.7 | 29.5 | 47.5 | 100.9 | 284.7 | 302 | 365.2 | 175 | 47.6 | 26.7 | 0 | 1380 |
| **1997** | 0 | 0 | 19.4 | 29.13 | 238.11 | 144.5 | 236 | 200.1 | 174 | 150 | 17.2 | 10.1 | 1218 |
| **1998** | 0 | 0 | 18.8 | 0.8 | 122.73 | 196.5 | 423 | 357.6 | 202 | 115 | 1.1 | 0 | 1438 |
| **1999** | 9 | 0 | 0 | 12.9 | 48.1 | 129 | 415 | 463.8 | 196 | 197 | 3 | 0 | 1474 |
| **2000** | 0 | 0 | 0.3 | 90.3 | 61.2 | 160.4 | 315 | 510 | 239 | 160 | 27.8 | 0 | 1564 |
| **2001** | 0 | 0 | 1 | 22.7 | 55.5 | 249.2 | 398 | 555.3 | 132 | 102 | 2.6 | 16.9 | 1535 |
| **2002** | 0 | 4.1 | 5.3 | 15.9 | 2 | 452.7 | 451 | 423.6 | 135 | 18.3 | 0 | 1 | 1509 |
| **2003** | 0 | 0.4 | 0.9 | 0 | 2 | 193.6 | 410 | 372.3 | 184 | 88.7 | 10.4 | 2.46 | 196.9 |
| **2004** | 1.5 | 1.63 | 10.72 | 23.48 | 82.55 | 196.9 | 410 | 420.3 | 171 | 74.7 | 7.2 | 0 | 673.6 |
| **2005** | 0.7 | 0 | 85.6 | 9.9 | 80.6 | 194 | 528 | 250.6 | 282 | 49.6 | 7.4 | 0 | 1488 |
| **2006** | 3.1 | 0.2 | 0.1 | 6.7 | 151.2 | 226.4 | 571 | 356.3 | 214 | 121 | 0.3 | 4.9 | 1656 |
| **2007** | 0 | 0 | 1.1 | 29.2 | 14.9 | 286.3 | 317 | 326 | 229 | 45.4 | 11.4 | 0 | 1260 |
| **2008** | 1.8 | 0 | 0 | 107 | 86.5 | 174.4 | 483 | 369.1 | 117 | 69.4 | 20.2 | 0 | 1429 |
| **2009** | 0 | 0 | 10.9 | 0.5 | 50 | 87 | 358 | 343.7 | 104 | 56.8 | 3 | 0 | 963.5 |
| **2010** | 13 | 0 | 0 | 42 | 64.1 | 137.7 |  | 434.2 | 179 | 45.1 | 1.5 | 0 | 916.9 |
| **2011** | 0 |  | 22.7 | 12.9 | 104 | 169 | 405 | 344 | 115 | 29.5 | 26.1 | 0 | 1228 |
| **2012** | 0 | 0 | 0 | 0 | 25.4 | 122 | 501 | 472.1 | 251 | 7.6 | 2 | 11.2 | 1392 |
| **2013** | 0 | 0 | 1.4 | 1.4 | 23 | 172.9 | 590 | 343.2 | 139 | 166 | 16.6 | 0 | 1431 |
| **2014** | 0 | 2.2 | 63.7 | 23.48 | 82.55 | 193.2 | 366 | 486.1 | 241 | 117 | 0 | 0.4 | 1469 |
| **2015** | 0 | 0.8 | 0.4 | 0 | 137 | 98.9 | 296 | 268.5 | 201 | 117 | 16.2 |  | 1135 |
| **Mean** | 1.5 | 1.63 | 10.72 | 23.48 | 82.55 | 196.9 | 410 | 372.3 | 184 | 88.7 | 10.4 | 2.46 | 1301 |
| **Standard deviation** | 3.2 | 4.65 | 19.63 | 26.22 | 62.43 | 74.85 | 105 | 89.63 | 54.5 | 53.8 | 14.2 | 4.36 |  |
| **Variance coefficient** | 2.2 | 2.86 | 1.83 | 1.12 | 0.76 | 0.38 | 0.26 | 0.24 | 0.3 | 0.61 | 1.36 | 1.78 |  |
| **Maximum value** | 13 | 24.1 | 85.6 | 107 | 238.11 | 452.7 | 590 | 555.3 | 298 | 203 | 65.3 | 16.9 |  |
| **Minimum value** | 0 | 0 | 0 | 0 | 2 | 87 | 219 | 200.1 | 95.8 | 7.6 | 0 | 0 |  |




**Annex Figure 7. 5**: Adjustment of mean of annual series for maximum observed rainfall (Hershfield, 1961b)




**Annex Figure 7. 6: Adjustment of Standard deviation of annual series for maximum observed rainfall (Hershfield, 1961b)**

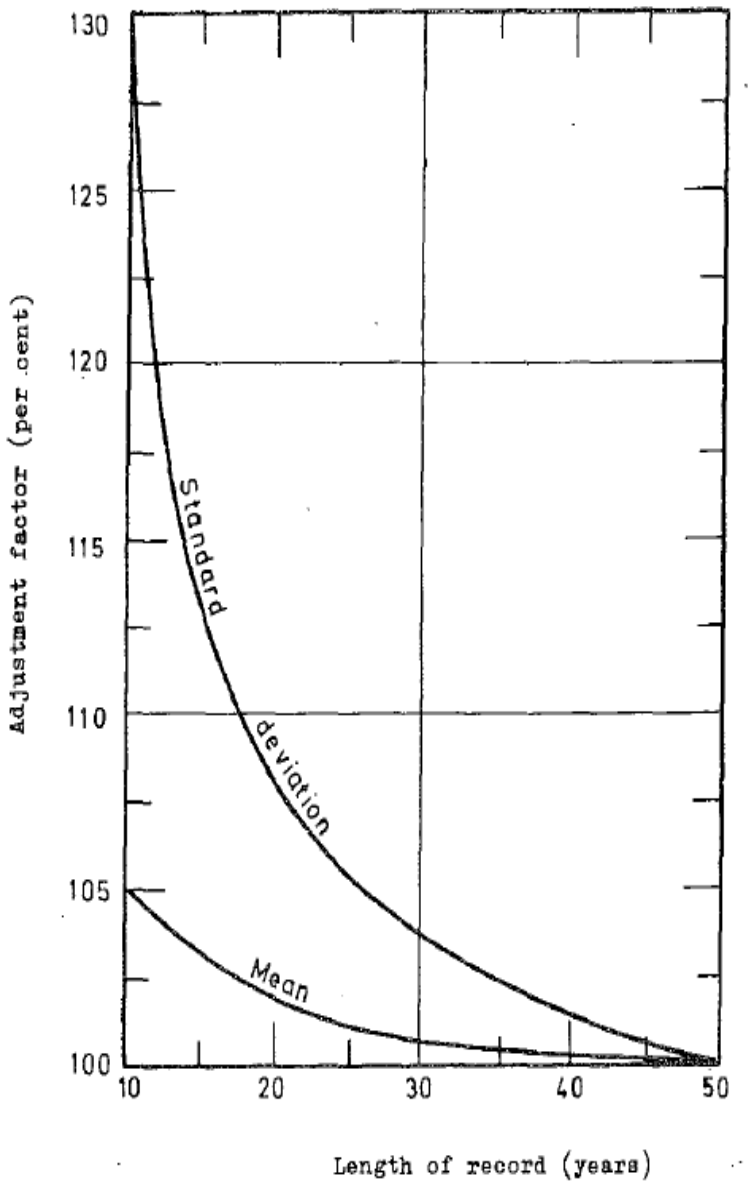
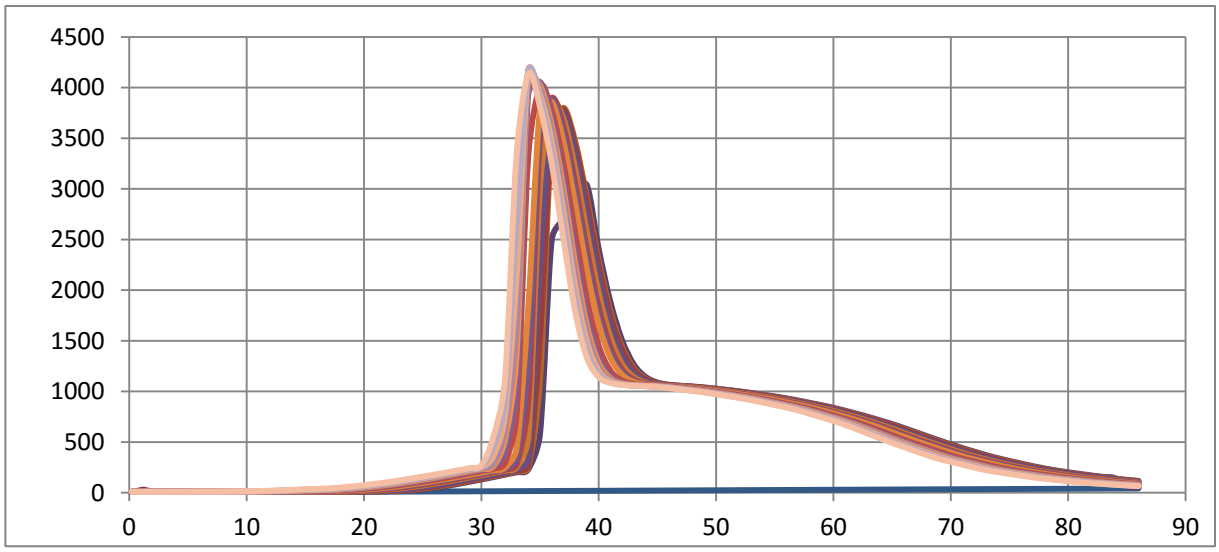


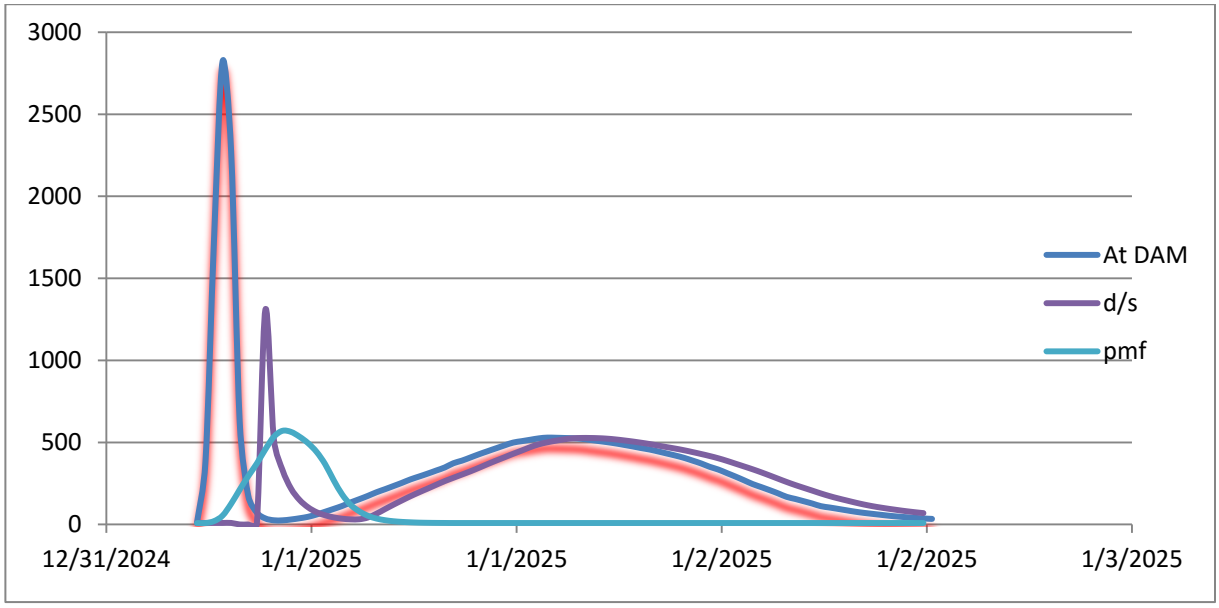

**Figure 7. 1: Adjustment of mean and standard deviation of annual series for length of record (Hershfield, 1961b)**

Annex Table 7. 9: Aerial maximum precipitation of study area.

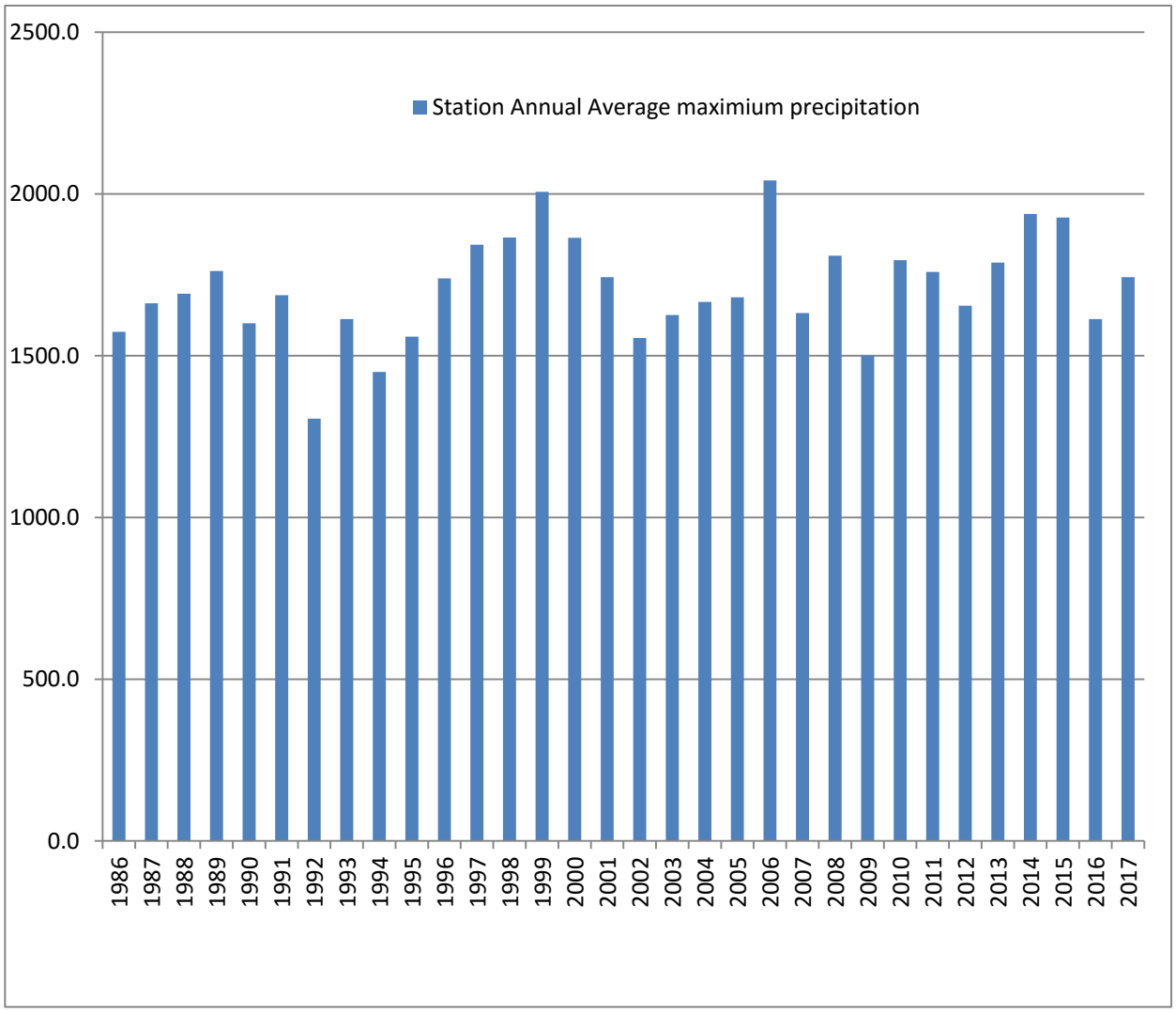
| S.No. | Years | | Max ppn |
|---|---|---|---|
| 1 | 1986 | | 34 |
| 2 | 1987 | | 38 |
| 3 | 1988 | | 55 |
| 4 | 1989 | | 82 |
| 5 | 1990 | | 58 |
| 6 | 1991 | | 59 |
| 7 | 1992 | | 72 |
| 8 | 1993 | | 56 |
| 9 | 1994 | | 49 |
| 10 | 1995 | | 54 |
| 11 | 1996 | | 59 |
| 12 | 1997 | | 71 |
| 13 | 1998 | | 63 |
| 14 | 1999 | | 71 |
| 15 | 2000 | | 47 |
| 16 | 2001 | | 45 |
| 17 | 2002 | | 47 |
| 18 | 2003 | | 59 |
| 19 | 2004 | | 52 |
| 20 | 2005 | | 63 |
| 21 | 2006 | | 64 |
| 22 | 2007 | | 53 |
| 23 | 2008 | | 46 |
| 24 | 2009 | | 41 |
| 25 | 2010 | | 73 |
| 26 | 2011 | | 81 |
| 27 | 2012 | | 82 |
| 28 | 2013 | | 90 |
| 29 | 2014 | | 56 |
| 30 | 2015 | | 75 |
| Total | | | 1796.2 |
| | Mean (n) | | 59.9 |
| | Mean (n-m) | | 61.9 |
| | SD (n) | | 14.1 |
| | SD(n-m) | | 13.9 |
| | CV (n) | | 0.2 |
| | CV(n-m) | | 0.2 |




Annex Figure 7. 7: overtopping Failure at various distance flood hydrograph.




Annex Figure 7. 8: piping Failure at various distance flood hydrograph


2500.0
2000.0
1500.0
1000.0
500.0
0.0
Station Annual Average maximium precipitation
1986
1987
1988
1989
1990
1991
1992
1993
1994
1995
1996
1997
1998
1999
2000
2001
2002
2003
2004
2005
2006
2007
2008
2009
2010
2011
2012
2013
2014
2015
2016
2017